Delft University Of Technology

Faculty of Electrical Engineering, Mathematics and Computer Science

Energy management system for a self-sufficient university campus microgrid

by

Chaturika Chowdhary Kota

to obtain the degree of Master of Science
at the Delft University of Technology,
to be defended publicly on 21st January 2021 at 10:00 AM.

This work was financially supported by
the Netherlands Enterprise Agency (Rijksdienst voor Ondernemend Nederland)
through the TKI Urban Energy grant (Project no. TEUE518021).

Student number:	4847938	
Project duration:	January 15, 2020 – January, 21 2020	
Thesis committee:	Prof. dr. Ad van Wijk,	TU Delft, supervisor
	Prof. dr. ir. Zofia Lukszo,	TU Delft
	Prof. dr. ir. Arno Smets,	TU Delft

TU Delft

Abstract

In a world where electricity demands are progressively growing along with the worsening climate crisis, it is essential to conduct research and build systems that can meet this demand in a sustainable, reliable and cost-effective manner. The building sector accounts for nearly 40% of greenhouse gas emissions in the EU, this is primarily due to the dependence on fossil fuels to provide heat for spaces, heating water and for cooking. Countries have made ambitious goals to reduce these emissions, and one such way is electrification. By electrifying heating, some research suggests that all the Renewable Energy Sources (RES) planned to be deployed in the Netherlands will not be sufficient to meet the demand, even with storage technologies. There are multiple ways to address this problem, one of them is decentralising energy production such that each household or institution accounts for their own production and consumption of energy. While this is in theory a simple solution, in the higher latitudes becomes harder during the colder months to meet the increased electricity demand using only renewable sources. Thus, a combination of them must be used to combat the effects of seasonal RES production. Simultaneously, the wholesale electricity prices in the Netherlands are also projected to increase in the near future, to almost 57€/MWh.

Universities being large load customers, will feel the effects of this increase in electricity prices and the need for heating electrification by 2030. This need could be due to policy implementations or personal choice. It is in the benefit of the university to increase their self-sufficiency, to decrease costs and carbon emissions. Thus, a microgrid is proposed for a university in the Netherlands. This microgrid, utilises on-site Photovoltaics (PV) generation, Fuel Cell Electric Vehicles (FCEVs) in the capacity of back up generation and a flow battery to store any excess energy generated by the PV system. In order to ensure the smooth integration of the components mentioned, an energy management system is designed. Furthermore, a new value proposition is made for the energy storage system where it is utilised during times of high electricity prices.

For the energy management system two control strategies are proposed with different end goals; one based solely on increasing self-sufficiency, while the other is based on decreasing costs. A comparison is made to understand when each control returns the most benefits and what exactly these benefits are. Using a combination of MATLAB and Simulink each of the components mentioned above were modelled using current practices in literature. Scenarios were developed to create a basis for comparison: baseline scenario, Self-sufficiency based (SSB) scenario and Price-based (PB) scenario. The last two are collectively termed the Distributed Energy Resource (DER) scenario.

The electrification of heating has a significant impact on the load profile, the largest loads occur in the winter. It was found that the highest self-sufficiency achieved was 43% utilising the SSB control, whereas with the PB control a maximum self-sufficiency of 41.3% was achieved. These percentages can mainly be attributed to the combination of large load and low PV production during the colder months of the year, indicating a clear need for studies into the impacts of heating electrification for consumers. This fraction can be increased by identifying further combinations of DERs that are sustainable, low cost and also available during the colder months of the year. Furthermore, levelised cost of electricity of the PV system accounted for only 19% of the total system levelised cost of electricity; while the zinc-bromine flow battery and FCEVs accounted for nearly 60% of it. On average the proposed system provides energy at an average (across both controls) cost of 0.304€/kWh. The costs of the proposed system are relatively high, and the largest contributors to this are the FCEV fleet and the chosen battery.

Acknowledgements

The past year has been a roller coaster, with regards to how much I learned and the effects the pandemic has had on my daily life. Looking back to the beginning of this year I am proud of how far I have come, I have learned so much and I am grateful to everyone who played a role in my learning curve this year. Everything I have learned and compiled into my thesis cannot be accredited to me alone, the following are some people that need a mention:

First and foremost Professor Ad van Wijk for his feedback on my report and putting me in touch with Rishabh for a thesis topic that I would find interesting. His advice and supervision was invaluable. Next, I would like to thank Rishabh, his advice from the beginning was on point. I just wish I had listened to him more and did not waste as much time at the beginning of my thesis. To say I have learned how not to fall into the rabbit holes of research thanks to this, is an understatement. He always responded quickly and with amazingly useful insights.

Next I want convey my deepest gratitude to Yiannis, without whose emotional support I am not sure I would have made it through the past year and still meet all my goals. He helped me stay motivated and supported me in any way he could, for which I will always be grateful.

I am also lucky enough to have a good set of people around me who provided me the much needed moral support: Megan, Metin, Amey, Francesco, Tarana, Kristin, Alice, Jamie and Mihika (the list is definitely longer but I am keeping it short). These people kept me sane and entertained during the endless months of quarantine and thesis, so thank you!

Finally, I want to thank my parents and my sister for putting up with my mood swings and for backing me in any way that I asked. Financially the past year has been hell on them, and yet they persevered and continued to do their best for me, for which I will always be in their debt.

Contents

List of Figures

List of Tables

Acronyms

AE	All-electric
AELP	All-electric Load Profile
BAU	Business as Usual
BAULP	Business as Usual Load Profile
BB	Battery Bank
BEV	Battery Electric Vehicle
BoS	Balance of System
CAPEX	Capital Expenditure
CaPP	Car as Power Plant
CCS	Carbon Capture and Storage
CHP	Combined Heat and Power
CoP	Coefficient of Performance
DER	Distributed Energy Resource
DoD	Depth of Discharge
EMS	Energy Management System
ESS	Energy Storage System
ETS	Emissions Trading System
FCEV	Fuel Cell Electric Vehicle
HCS	Hierarchical Control Strategy
HEV	Hybrid Electric Vehicle
KiBaM	Kinetic Battery Model
LCOE	Levelised Cost of Electricity
LCOS	Levelised Cost of Storage
LPG	Load Profile Generator
MC	Micro Source Controller
OCR	Own-consumption Ratio
OPEX	Operation and maintenance costs
P2G	Power-to-Gas
PB	Price-based
PEM	Proton Exchange Membranes
PFCS	Power Flow Control Strategy

PHEV	Plug-in Hybrid Electric Vehicle
PV	Photovoltaics
RES	Renewable Energy Sources
SCR	Self-consumption Ratio
SLCOE	Total System Cost of Energy
SoC	State of Charge
SSB	Self-sufficiency based
SSR	Self-sufficiency Ratio
STC	Standard Testing Conditions
TC	Total Cost
TMY	Typical Meteorological Year
TOU	Time-of-use
TSCoE	Total System Cost of Energy
UCM	University Campus Microgrid
V2G	Vehicle-to-Grid
ZBFB	Zinc-Bromine Flow Battery

1 — Introduction

In 2015 the Paris climate agreement was signed between currently 189 ratified parties, the key aspect of which was to keep global temperature increase well below 2 degrees Celsius from pre-industrial levels [8]. The Dutch government as part of its road map to combat climate change laid down measures to decrease emission intensity for each sector [9]. This includes incentivising the transition for generators and consumers to increase their fraction of renewable energy thereby increasing the share of renewables in the Dutch energy mix [10][11]. Policy instruments to subsidise the usage of electric vehicles, increasing carbon taxes and electrifying heating in all buildings were also part of the measures that were implemented to move towards a higher degree of carbon neutrality [12][13][14]. One main takeaway from these measures is a general trend towards the electrification in the transportation and building sectors. Electrification refers to a shift to direct electricity usage to meet energy demands that are currently being met by fossil fuel based energy carriers [15]. An example of this is building electrification, which implies relying on electricity for heating (space and water) and cooking. This combination of increased reliance on electricity and RES will have significant impacts on the demand profile, electricity prices and load forecasting, while also creating areas for microgrids and energy storage deployment.

One aspect of the impacts of heating electrification in a future with larger quantities of renewables in the energy mix is to address the low renewable energy production during the winter months, the very months during which the heating load increases. An Energy Storage System (ESS) has been shown to be effective in addressing the lack of renewables during these months; in combination with microgrids they play a role in better utilising on-site RES by providing better energy utilisation, stability and security to the consumer and to the distribution grid at large [16] [17]. Current research on microgrids focuses on varying the combinations of DERs, ESS applications and power flow controls, while integrating these elements together. Thus, resulting in differing designs for microgrids. However, in order to meet the needs of the consumers/users while combining high efficiency standards, cost effectiveness, reliability and sustainability, these designs need to be location and application specific.

Furthermore, it has been proven to be beneficial for universities to implement microgrids on their campuses, be it to improving their energy efficiency, reducing the carbon footprint, increasing self-sufficiency, etc [18], [19], [20]. Microgrids deployed on university campuses have been coined university campus microgrids (UCMs). Moreover, interest in UCMs has been gradually increasing and this can be attributed to many factors. One of them being that universities are large-scale energy consumers, thus, relying on RES decreases their energy costs while also enabling them to take a more active role in the transition towards a sustainable future. Sometimes there also exist local policy instruments to increase dependence on RES or to further electrify buildings [9]. Another factor to consider is the rising electricity prices in the Netherlands [21] [22], when large shares of load cannot be deferred, the costs paid to the grid will increase unless other avenues of energy production are explored and implemented. An additional benefit of UCMs is that they also provide a local area of study for the university's researchers.

Combining the effects of the projected increase in Dutch electricity prices and increased electricity consumption (due to electrification) it creates an area of research to explore and assess. The electrification process is especially important for those consumers situated in the higher latitudes, as the benefits reaped from microgrid deployment is dependent on the combination of DERs used. A mix of multiple generation units and energy storage systems are required in such locations given the lower renewable energy production during the winter months [1]. For universities, microgrids, energy management systems and on-site generation can be useful due to their high energy consumption. The critical and non-deferrable nature of portions of their load and their large heating demands are additional points in favour of the need to comprehensively study the benefits of and implement microgrids. University campuses also provide optimal locations where they can act as test-beds for microgrid research, as they fulfil certain technical requirements where microgrids can be implemented and tested furthering

the research needed in this domain [20][23]. This research could be implemented/serve singular entities, like data centres and hospitals, or multiple smaller aggregated loads, like entire neighbourhoods [24].

The main focus of this report is addressing the challenges increased electrification of heating will play in a university campus, for a location in the Netherlands. Projections for 2030 are made, while outlining the techno-economic feasibility of implementing a microgrid in a university campus with PV on-site generation. Understanding the technical viability of the UCM involves analysing the self-sufficiency, self-consumption, grid dependence and quantifying the seasonal patterns observed through the year. While the economic feasibility encompasses detailing the annual costs paid to implement this system, annual costs paid to the grid and the levelised cost of electricity of each physical component and energy carrier (electricity and hydrogen).

First the effects of heating electrification are quantified by extrapolating current electricity and heat consumption patterns, while also accounting for efficiency increases by 2030. Followed by justifying the need for backup generation and an ESS in a UCM whose primary generation comes from a PV system. A flow battery is proposed for the ESS and the car as power plant Car as Power Plant (CaPP) concept is tested (through simulations), to understand the economic benefits, or lack thereof, it provides as backup generation. For the smooth functioning of the microgrid proposed, power flow control strategies need to be developed to coordinate the flows between the generators, storage system and the utility grid.

These control strategies can be centralised, decentralised or hierarchical. This report emphasises on hierarchical control in microgrids, addressing the power flows from the view point of a central controller. It is termed the Energy Management System (EMS) in this report. Two EMS control strategies are developed for separate ESS utility cases; one is a self-sufficiency based control (or the SSB control) and the other is a price-based control (or PB control). The primary goal of the SSB EMS is to increase self-sufficiency while decreasing dependence on the main grid. Additionally, the PB control strategy is proposed to analyse the economic benefits of time-shifting the usage of the ESS based on the electricity prices at any given time. Both these controls are different from one another and are implemented individually in simulations and not in combination. A comparison is made in the discussions to quantify the advantages, disadvantages, utilisation through the year (to understand the seasonal implications) and the economic differences between the two.

1.1 University campus microgrids

Over the years microgrids have been given multiple definitions, one that is noteworthy and relevant to this report is given by Lasseter et al. for the Consortium for Electric Reliability Technology Solutions (CERTS) in 2002; where they state that "the concept of microgrids adopt the aggregation of multiple loads and microsources functioning as a single self-controlled system that provides both power and heat to the consumer" [25]. This system is perceived as a single prosumer by the distribution grid and the majority of the microsources must have the ability to be integrated with power electronics to enhance their flexibility and work in combination with the individual elements of the system; all of which are controlled by a central controller or EMS. An example of the microgrid topology for the proposed UCM with hierarchical control in this report is depicted in figure 1.1.

A UCM in this report is defined as a combination of loads and microsources being controlled by a centralised EMS which balances the demand and supply at all times with the help of an ESS in combination with on-site microsources. Most university campuses host numerous buildings close to one another, each is perceived as an individual load, with existing electrical connections between them. A majority of them could also host rooftop PV generation, signifying multiple microsources providing on-site generation. Universities are usually operated by the same financial and technical facilities throughout campus while also being connected to the main grid

[1]Note that this is not especially true for wind energy, but there do exist days of dunkelflaute where both wind and solar energy is absent for periods of time.

from a single point of common coupling (PCC), this allows for relatively simple switching between autonomous and grid connected modes [23]. Several UCMs have been implemented around the world illustrating the benefits of such systems to the university as well as to the distribution grid[23].

In figure 1.1, the layout of the proposed microgrid is depicted. Note that this figure only indicates the power flows between each element of the system, a detailed description of the complete layout with the data flows and directional power flows can be found in figure 2.1.

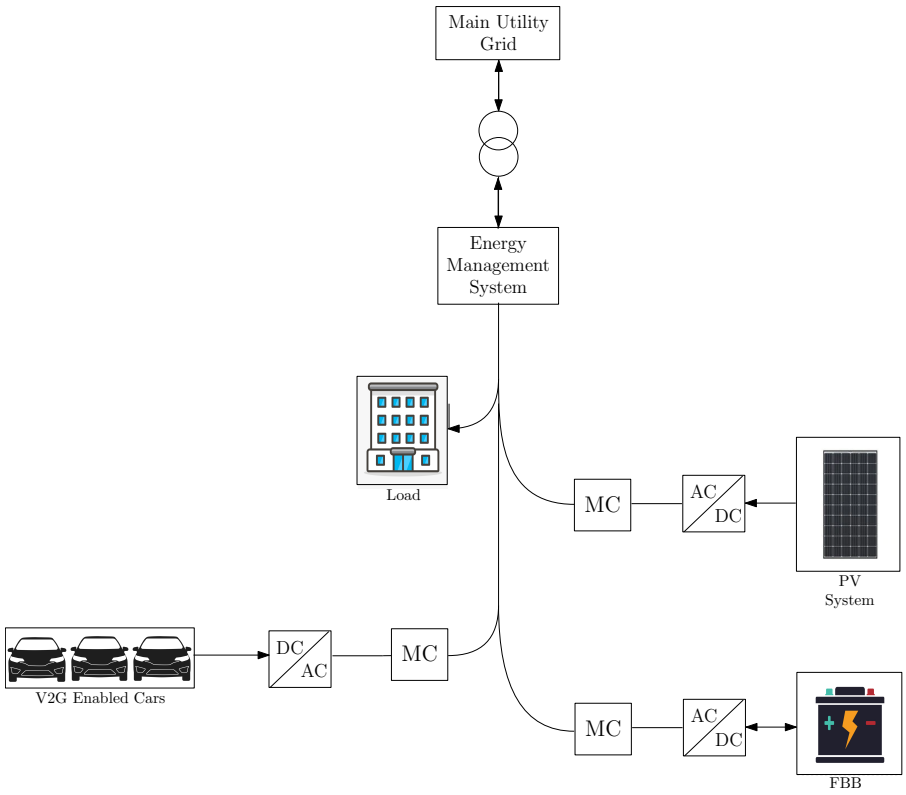

Figure 1.1: General layout of the microgrid and proposed components.

Though numerous UCMs have been implemented, their criteria for implementation are varied and very dependent on local drivers. These could be policy instruments made by governments, economic drivers, the need to stay at the forefront of research, etc. Some of the main applications, or the needs for which current UCMs have been developed, are summarized below:

1. To create a self-sufficient campus using DERs [18].
2. To implement and validate how DERs would work together to reduce electricity costs paid to the main grid, lower operating costs and cut down direct carbon emissions for a campus [18]. In the experimental study completed by Washom et al. [18], control algorithms were designed to economically optimise the utilisation of the on-site DERs of the campus, to primarily decrease costs.
3. To maintain high quality of service for critical load [2] [20]. Microgrids have been shown to provide high security of supply for critical loads as software solutions can be constructed to maintain uninterrupted power supply, by re-regulating power flows, modulating frequency and implementing demand response (to

shed non-critical load during times of low generation).

4. To facilitate peak shaving of load, meet the campus's hourly energy demand and and to increase power quality [26].
5. To analyse forecasting of electricity prices [27].

1.2 Impact of heating electrification

Buildings in the EU account for nearly 36% of CO_2 emissions, to reduce this fraction in a sustainable and cost effective manner the European Commission has stipulated, the increase in energy efficiency, energy performance and decarbonisation in buildings [28]. Microgrids have shown to increase energy efficiency through demand response and more efficiently managing on-site generation resources [25]. Though this report does not focus on the energy efficiency of campus processes, it is a valid point to note when considering the benefits of a microgrid for a university campus. Universities consume large quantities of energy, with increasing average wholesale electricity prices [29], it is essential to understand whether on-site renewable generation would be more cost effective than relying entirely on the grid. Especially given the electrification requirements for all buildings in the near future [9], a lot of the load that occurs during winter months cannot be shifted (i.e.) it is non-deferrable due to the heating requirements that need to be met at that time.

A problem that arises from electrification is the increased load that needs to be met during the colder months of low renewable energy generation [14]. The electrification of heating on a national level will have an impact on wholesale electricity prices, as there will be a need to depend on natural gas turbines to provide the required flexibility, despite the projected increase in renewables in the Dutch energy mix by 2030 [14]. Amongst other factors, this reliance will cause electricity prices to rise due to the carbon taxes that will be included; current projections for the average wholesale electricity price is around 57 €/MWh for 2030 [3] [29]. This increase can be attributed to many factors, some of which is due to the additional infrastructure added to manage increased RES penetration, increased carbon taxes and increased demand projected (due to electrification and economic growth); these factors are further discussed in 2.6. Universities could benefit from implementing UCMs to not only meet their electrified load in the most efficient manner but also in an economical manner.

A major contributor to carbon emissions in university buildings is heating, as can be seen in figure 1.2, based on the quantity of natural gas being used to heat spaces. Currently, the Dutch government stipulates that all new buildings utilise electric heating, while existing buildings slowly phase out fossil fuel based heating [9]. When heating in universities is electrified, it alters a university's load profile drastically in the colder months of the year. In this report building electrification primarily entails shifting to electric space heating, though the author acknowledges that it must also include water heating which is left out of the scope of this report.

[2]Here quality of service refers to uninterrupted power supply. Critical load is one that requires continuous power supply, for universities this could be for laboratories running experiments or equipment that needs constant power input.

[3]Note that a university would incur higher costs per MWh of electricity consumed from the main grid. This due to levied taxes, grid connection costs based on capacity requirements, certificates, transmission and distribution costs, etc. in addition to the production costs.

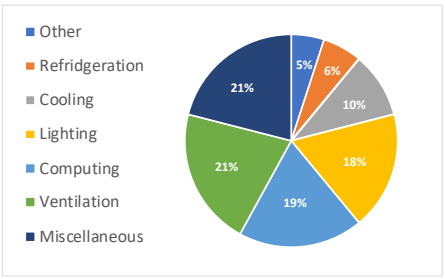

(a) Electricity end usage.

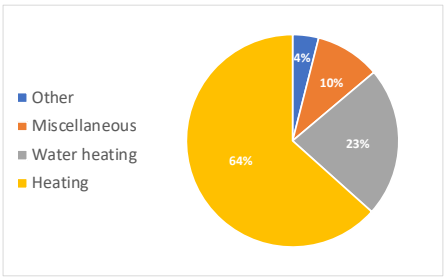

(b) Natural gas end usage.

Figure 1.2: End usage of electricity and natural gas in university buildings in 2012 on average in USA [1].

In figure 1.3, the"heating profile" only represents the extrapolated electrified space heating load, whereas the dashed line represents the extrapolated electric load from 2019, while their sum is shown in the All-electric Load Profile (AELP). This profile was constructed using data obtained from University of Twente, a detailed description of its formulation can be found in subsection 2.1.1. The load profile in the figure is a projection made for 2030, the methodology of generating it is further discussed in detail in section 2.1. As one may note from figure the all-electric load profile has increased relative to the electric load (dashed line). On average it is a factor of approximately 1.38 more than the original electric load. A point to note in the figure, is the consumption during weekends, this can be attributed to lighting, running experiments and equipment that needs constant power supply. When looking closer at the no heating added load profile, one may note that the night load is approximately in the same range as the load during weekends.

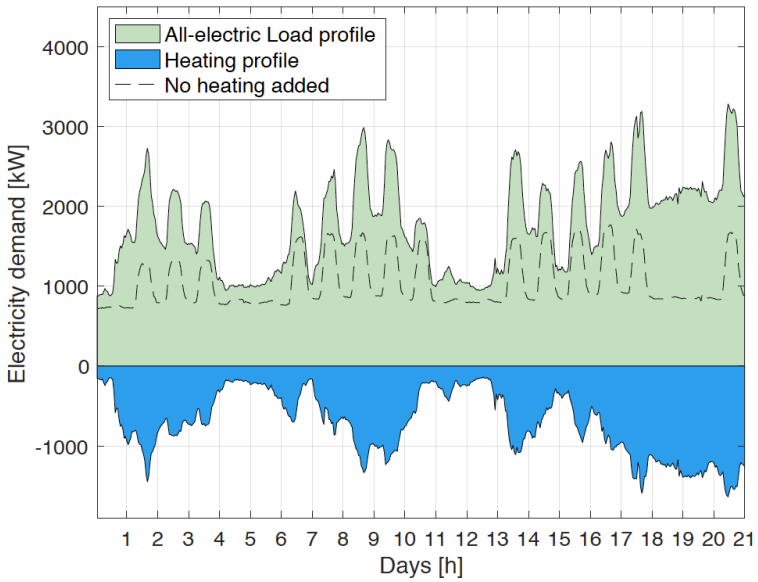

Figure 1.3: Load profile of three example weeks of winter in a university campus with the heating electrified in 2030. Note the original data was obtained from the university of Twente and extrapolated to the required year based on relevant assumptions.

1.3 Energy storage requirements

With the addition of heating to the electric load profile, and integrating a PV system for onsite generation, heating electrification poses a problem due to the low availability of sunlight during the colder months at higher latitudes. This increases the need for flexibility which can be achieved through an ESS and/or utilising another complementary on-site generator. Here flexibility refers to storing any excess generation from the PV system or having a secondary generation which is not intermittent and can be turned ON/OFF when required. The UCM proposed in this study utilises a combination of PV generation and cars as power plant (CaPP) to meet the load directly, while storing the excess PV energy in an ESS to be used during times of low or no generation or high electricity prices depending on the control strategy implemented. Thus, the primary need for the ESS and FCEV fleet is to provide the flexibility and increased self-sufficiency during the colder months of the year. When all these elements are not sufficient to meet the demand, the main grid is utilised to balance the needs of the load.

With a UCM dependent on PV it is essential to either integrate other microsources that can balance the lack of sunlight during winter months, or use a long-term ESS. Various technologies exist in the market that are cost competitive [30], but their utilities vary based on their costs, energy density, power density and durations for which they can store this energy with minimal self discharge. Based on these factors, a flow battery was chosen to meet the requirements of the electricity storage system. ESS have seen various applications from stabilising the voltage and frequency of a distribution system, to balancing power, or enabling a time-shift of the energy produced.

Eyer et al. in 2010 discuss numerous value propositions for different utility cases of energy storage. Three points of interest in their research were the differing roles ESS could play in the electricity grid that have market potential, the challenges to internalizing the benefits of this usage and the infrastructure needed to control and coordinate the applications proposed [31]. Two of the applications in the paper that stand out and are relevant to this report are:

1. **Time-of-use energy cost management:** Consumers charging their ESS during times of low retail electricity prices, and then discharge during times of higher prices, is termed time-of-use (Time-of-use (TOU)) energy cost management[31].
2. **Time shifting of renewable energy:** PV production occurs during times of peak load, but this is not the case with most renewables. When taking into account weekends and holidays, this production coincides with off-peak times. Time shifting of renewable energy refers to charging during times of excess renewable energy production and discharging during times when the load cannot be met directly by the on-site generation[31].

1.4 Problem statement

This master thesis attempts to answer the following research question:

How does a self-sufficiency based control strategy compare economically over project lifetime to a price-based time-shifting control strategy when utilising an electricity storage system and FCEVs with V2G capabilities in a UCM with on-site PV generation?
Given the impacts of heating electrification and increasing electricity prices, it is important to quantify the effects of utilising different DERs in combination with one another to best comprehend their benefits. Furthermore, two of the value propositions made in [31] were combined to develop a new value proposition for ESS utilisation, which is the price-based time shifting of the ESS. The proposition is studied by developing a control strategy to implement this ESS utilisation and assessing its economic benefits (or lack thereof). Thus, this question aims to provide the reader with numbers for costs, advantages and disadvantages of using this particular combination

of RES in a microgrid in the Netherlands. Furthermore, self-sufficiency in this report can be interpreted to a combination of self-sufficiency and decreased grid dependence. The goal is to compare the value this combination will have with respect to the system sizing, reliance on the distribution grid, variation in costs and seasonal dependencies for the two control strategies. The two control systems with differing utilisation schemes for the ESS are proposed and implemented:

1. **Self-sufficiency based control (SSB):** the main goal is to increase self sufficiency. This is achieved by storing any excess PV energy generated on-site, to be used during periods of low or no generation. The priority order of the system is as follows: first the on-site PV generator is used to meet the load, any excess is used to charge the ESS, while if there is a deficit FCEVs are used to meet the load during the day. At night the ESS is discharged and once it is fully discharged, the distribution grid is used to meet the load. Though the dependence on FCEVs cannot be defined as self-sufficiency, it is a means to decrease grid dependence, thus in this report calculations of self-sufficiency include the power provided by the FCEVs as well.
2. **Price-based control (PB):** the primary aim of this control is to decrease cost of electricity. The price-based time shifting involves charging the ESS during excess generation periods of the on-site generator to be discharged during times of "high" electricity prices, it utilises a similar priority order during the day time as the SSB. A combination of the two applications of the ESS mentioned above is the area of interest, wherein the excess renewable energy generated is shifted to be used at a later time period when the wholesale market price of electricity is relatively high. Though the ESS does not charge using the distribution grid, the area of interest from the two cases from [31] is the price-based time-shifted utilisation of the ESS.

The question is answered through the process of modelling, scenario formulation, and analysing the economical impacts of them both with a baseline scenario. The sub-systems are comprised of the PV system, FCEVs and a flow battery modelled in MATLAB and Simulink. PV generation is chosen as it is the most prevalent on-site generation source and the availability of flat roofs in most university campuses; while FCEVs are used as secondary generation to balance the effects of lower solar irradiance during the colder months of the year. Finally, the BB is used in order to store any excess PV generation, thereby increasing self-consumption and self-sufficiency, while also testing the value provided by a price-based time-shifting control.

The research question is divided into sub-questions:

1. How does the total cost of electricity compare in each control strategy when sizing the battery system based on the ideal sizing[4] versus sizing based on highest economically optimum SSR and best battery utilisation?
2. How do the two control strategies compare based on self-sufficiency and own-consumption of on-site PV generation?

Scope and structure of report

The objective of this report is to comprehensively analyse the economic benefits of a new value proposition for the usage of the ESS in a future with electrified heating by integrating it into a microgrid with on-site generation. In this system PV generation is the primary source of power and a flow-battery is utilised as an ESS, along with an FCEV fleet to act as backup generation. It is a complex process to improve the energy processes for the entirety of a university campus, due to the presence of numerous buildings, spread across large areas, along with varying levels of consumption. Due to the complex nature of the loads in varying university campuses it was deemed out of the scope of the project to analyse the entirety of the university in question, but

[4]Ideal sizing in this report is defined as the point at which the highest self-sufficiency is achieved, or the size at which the cost of each additional unit of capacity added after which minimal returns are seen.

rather focus on the majority consumption buildings alone. This not only simplifies the sizing process for the entire system, but also makes it possible to understand on a smaller scale if such a system is techno-economically feasible. If it is, this system can easily be scaled to include more loads (or buildings) easily, as it is designed keeping modularity and scalability in mind.

The modelled sub-systems provide the basic framework of their respective responses as individual units and provide the basis to create an techno-economic analysis of the system as a whole. These models are based on current literature, and in cases where simulations of prices, future load profiles and hydrogen availability is modelled, relevant justifications and assumptions are indicated. Two control strategies were developed and are compared to a baseline scenario, the baseline scenario is used to gain insights into how the system proposed would compare with 100% grid dependence in 2030. The two controls are also compared to one another to understand when each control is most beneficial to be implemented, an analysis of the best way to size the battery bank (BB) and PV system is also discussed and studied based on the goals of this UCM.

The report is structured as follows: **Chapter 2** describes the methodology used to create a load profile for a university campus in 2030 that also includes electrified heating. In addition to this, the modelling methods used to simulate the response of each component of the UCM, justifications for the choices made while building the sub-systems, the relevant cost equations used to create an economic analysis. The chapter concludes with an analysis of future grid electricity prices and how price trends were modelled for 2030 in the Netherlands. Following which **Chapter 3** focuses on the control algorithms designed for the EMS in the UCM, to coordinate and aggregate the PV system, FCEV fleet and the flow battery. The main aim of the chapter is to comprehensively justify the reasoning for the control strategies implemented and describe their functions with graphical representations of their operation. In **Chapter 4** the outcomes of the simulations are discussed, self-consumption, self-sufficiency, Sankey diagrams, PV utilisation for each control and a cost analysis to understand the variations between each control are detailed along with other discussions on system sizing. The chapter concludes with further development ideas for the proposed concept. Finally, **Chapter 5** conclusions are drawn based on results presented in the previous chapter followed by the future work proposed by the author.

2 — System modelling

This chapter details the mathematical models used to simulate the PV generation, battery system response and the equations used to evaluate the economic value of the system proposed. In addition to these, the method of creating the university load profile for 2030 and the pattern of hydrogen fuel available from the FCEV fleet is described. Finally, the chapter concludes with a discussion on how the future electricity prices are projected to evolve based on literature, along with justifications for the electricity price profile developed for 2030.

The microgrid proposed for the university consists of a PV system, a flow battery and an FCEV fleet. Each of these elements' voltage and power output are modulated by their respective local controllers. Meanwhile on a larger scale, an EMS as the central controller directs the power flows within the entire microgrid and initiates communication with the main grid. Figure 2.1 describes this UCM in detail, indicating the communication channels and direction of power within the low voltage (LV) microgrid. The buildings in the illustration represent the loads, where each building has an individual PV system and heat pump. In addition to these components, there is a single flow battery which is housed in a location elsewhere from the load, this is due in part to its large size as well as for safety concerns. Finally, the FCEV fleet is located in a single area close to the consumption, in this case a car park is situated adjacent to the load.

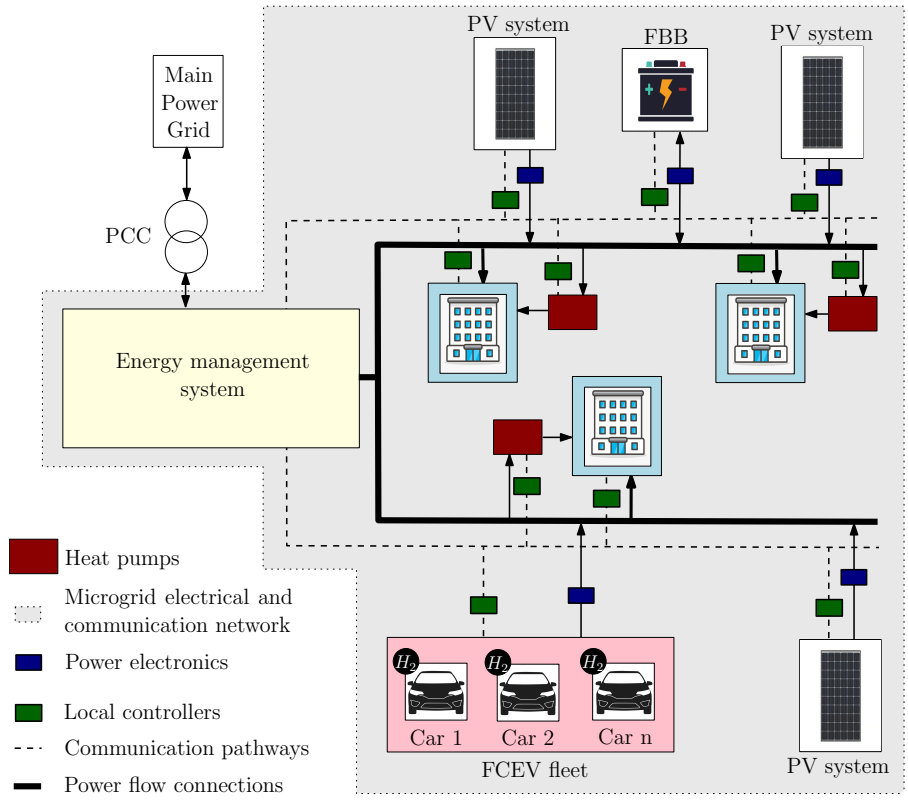

Figure 2.1: Detailed configuration of the UCM proposed. FBB here stands for Flow Battery Bank.

Each of the components of the microgrid is connected to the power and communication channels, as can be seen in the figure. The function of the local controllers is to the operate the voltage and frequency in transient

conditions, based on available data collected at the local points [32]. This type of control is termed primary control, wherein the local controller makes decisions and optimizes the DER for small time-scales. This class of control is extremely important to maintain voltage and frequency stability, the design of which is out of the scope of this report[5]. The local controllers obtain the status of the component they are integrated with and relay this information through the communication pathways to the EMS. The EMS makes the large-scale decisions of when the battery charges or discharges [6], when the FCEV fleet is used as backup generation or when to initiate contact with the main grid to help balance the load that was not met by the microgrid.

For the FCEVs the vehicle-to-grid (V2G) [7] terminals that can be used to charge battery electric vehicles (Battery Electric Vehicles (BEVs)) can be used bidirectionally and thus be used to "discharge" the FCEVs to act as backup generation[8]. A certain restriction needs to be made in order to allow BEV owners to charge their vehicles. Thus a cap is set to how many V2G terminals may be used for the CaPP concept, this along with how the university interacts with the FCEV owners is further elaborated in section 2.5. The interconnection between the FCEV fleet and the LV distribution system is unidirectional as only the discharging of the FCEVs is depicted. The point of common coupling (PCC) acts as the in between for the main grid and the microgrid, with the EMS deciding when to remain in islanded mode or grid-connected mode. The power electronics in the figure refers to the needed power electronic converters, which provide high efficiency switching between one form of electrical power to another (i.e.) DC to AC or vice versa [33]. Some of them have the capacity to be bidirectional, as would be the requirement for the BB system. The battery will henceforth be referred to as the BB due to the modularity of the utilised storage system. Multiple modules of the flow battery are connected in series and parallel to obtain the required voltage and current output, thus signifying a "bank of batteries".

2.1 Load profile

A load profile represents a graph that typically depicts variations in electricity consumption with respect to time. Load profiles vary depending on day night cycles, local weather patterns, seasonal changes and geographic location. Patterns can be seen on a day to day basis, university load profiles typically differ from residential load profiles, not just in scale but also in the occurrence of the peak in the middle of the day, they have non-deferrable loads (load that cannot be shifted to another time) and critical loads. These non-deferrable loads can be seen during the weekends and nighttime, and it typically consists of laboratories in which experimentation is being carried out, lighting on campus, equipment that consumes large quantities of power, etc. Electrified heating cannot be considered entirely of the non-deferrable load category. Though the entirety of the heating load itself cannot be shifted, a certain degree of flexibility is possible. As a certain time period is required between the switching on of the heater and when the space is heated a certain time duration passes before the temperature drops once more. Thereby creating times where the heat pumps may be switched off when they is large electricity consumption that cannot be directly met by on-site generation. This can be achieved by integrating an additional layer of control to optimise the processes for heating. Furthermore, most weekends there is low to no heat requirement, occasionally there are random weekends when there is a heat requirement. This may be attributed to researchers working during the weekend or experiments being carried out, heating

[5]The local controllers are depicted in the figure 2.1 to provide a complete overview to the reader as to how the hierarchical control for this UCM is operates.

[6]This is not to be confused with the battery management system, which is separate and ensures the safe functioning of the battery. These are only the decisions of charging and discharging, while the battery management system can decide locally if there is sufficient capacity to be provided or put into the battery.

[7]V2G is a concept where electric vehicles are used to provide power to the load as backup generation, spinning reserve or even balancing power plants. These use cases have seen experimental applications, the literature of these CaPP applications of FCEVs can be found in [34][35][36][37][38][39][40][41].

[8]Discharging in this context refers to the unloading of hydrogen in the fuel tank to be converted to electricity by the fuel cell in the FCEV.

left on during weekends, etc.

The load (heat and electric) data used in this report was obtained as a timeseries dataset from the University of Twente's (UTwente) data sharing platform [2] and were in the hourly time-scale for the year 2019. The data was first converted to power and then was interpolated to create a dataset with 15 minute time-intervals. This was to provide a finer time-step, in order to analyse the control algorithms designed and compare the economic viability of each control strategy. This time-step is not sufficiently small to analyse transient states (frequency and voltage responses) but it is sufficient to comprehensively understand the techno-economic viability of the controls proposed.

When comparing UTwente with two other universities, its total electricity and gas consumption is relatively low. This information is provided to gain an understanding of how the dataset being used compares to other universities and to shed light on the general energy consumption in universities in the Netherlands. One may also be able to draw conclusions on the scope for UCMs in the Netherlands, of how the electrification of heating will have an impact based on the scale of their current demand. The smaller consumption in UTwente relative to the other universities mentioned can be attributed to the fewer number of buildings, smaller student population and their efforts to decrease their energy consumption [11]. The numbers in table 2.1 are provided as a means to compare the spectrum in which the used data falls under. As can be seen TU Delft, though has a smaller student population than Leiden university, their electricity consumption is almost 1.5 times more. This could be due to more energy intensive research, or another correlation could be drawn wherein the employee population of TU Delft being higher indicates the more number of researchers on campus carrying out experiments. The data obtained in table 2.1 was obtained from each university's websites:

University	**Electricity consumption [MWh]**	**Natural gas consumption [million m3]**	**District heat consumption [MWh]**	**Size of student body**	**Employee population**
University of Twente[2]	14.7	0.40	8.97	11,740	3,105
TU Delft[42]	67.9	1.64	-	24,703	5,421
Lieden university[43]	45	5	-	30,869	3,665

Table 2.1: Comparison of University of Twente's energy consumption with other Dutch universities in 2018 and 2019 (depending on data available).

The load profile comprises of the demand from three buildings (Horst, Carre and the Nanolab) on the UTwente's campus [44], which account for nearly 65% of the total campus load. When analysing the layout of this university's campus, it was noted that these buildings had the highest consumption, a majority of the laboratories and the largest square footage of built space. Each of the buildings excluded individually account for less than 5% of the total electricity consumption of the campus. Another important factor was the proximity of these buildings to one another (as can be seen in figure 2.2), the existence of a large car park with V2G terminals, and the availability of sufficient unused land nearby for the large BB. The study is carried out for these three buildings, and if this proves to be feasible larger areas can be covered or added to the UCM as individual units.

[11] It is possible that there are other factors that contribute to lower consumption, which includes laboratories, the equipment and experimentation carried out, but no comments are made in this regard as it would be speculation without having a concrete basis to draw conclusions from.

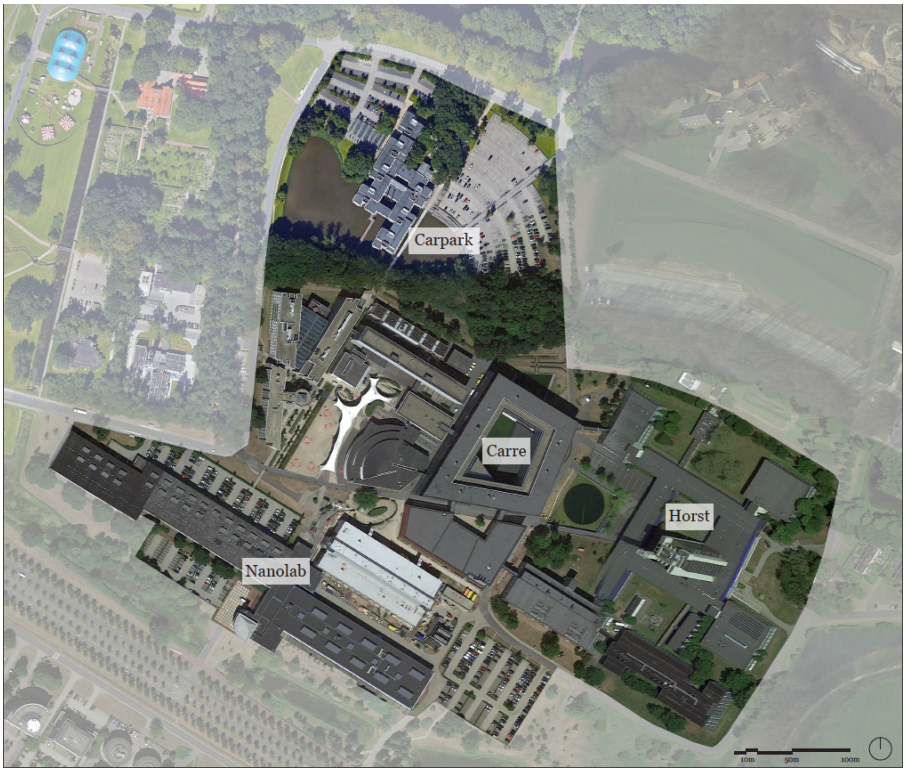

Figure 2.2: Proximity of and roof top area visualisation to gain an overview of distances between buildings, car park and possibility for shading on rooftops.

2.1.1 All-electric load profile

The all-electric load profile (AELP) was built assuming a total of 2% decrease per year in energy consumption, this is due to the university taking active steps to decrease their electricity consumption [45]. One may extrapolate using a trend line utilising the data points available from 2014 to 2019, but there are insufficient number of data points which represent any form of decrease in electricity consumption. When analysing past annual energy demand of the university, a downward trend is noted from 2016 on-wards, these figures can be found in appendix F. This could be attributed to the university increasing the efficiency of the most obvious processes on campus; typically in the early stages of increasing process efficiencies, steep curves can be noted, but as this progresses such drastic changes will be less prevalent and the curves become less steep. So to extrapolate based on these four data points is not realistic. Thus, a generalisation is made, where a certain decrease is assumed for current consumption each year, based on the optimistic goals set by the university. Furthermore, it must be noted that the heating demand is very dependent on weather conditions. Seasonal patterns of heat consumption are unlikely to change by 2030, only the daily patterns of usage might see more changes. As only the seasonal variations bear importance in this report, an assumption is made wherein the heat demand profile is assumed to follow a similar pattern to the original data.

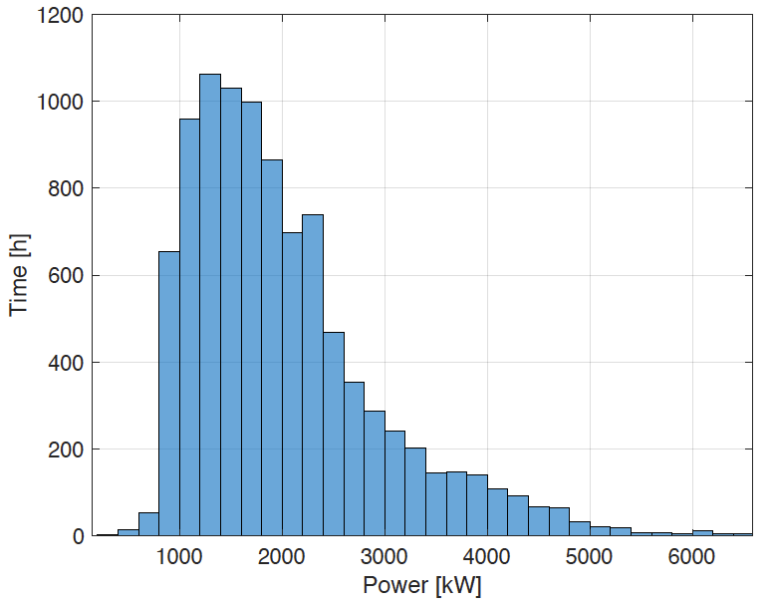

Figure 2.3: Distribution of all-electric university load profile in 2030.

The university obtains the majority of its heat through district heating, from Ennaturlijk [44]. Ennaturlijk produce "heat in as sustainable or low in CO2 as possible" [46]. A part of the university's heat comes from gas consumption, this is used only to heat spaces [2]. Thus the gas consumed by these buildings alone is converted to electricity requirements. Another factor is that since only the gas is a high emission fuel that is being directly consumed and is in the control of the university, it is a possible area to decrease emissions. With increasing carbon taxes and policy instruments to facilitate reduction in SO_2 emissions, there is also the likelihood that the university will either switch their gas consumption to electric heating or move all their heating demand to be met through district heating. Thus, an assumption is made where all the gas consumed and heat procured from the district heating operator is converted into the heating demand for 2030. The gas consumed is converted to MJ/kg using the calorific value of natural gas also taking into account the efficiency of natural gas heating. This heat demanded is then divided by the coefficient of performance (Coefficient of Performance (CoP)) of the air heat pumps.

Figure 2.4 shows the electricity equivalents of the gas consumed and the electricity consumption through the year. It is evident that the the gas consumption is low in the "summer" months [12], while at the same time the electricity consumption goes up relative to the "non-summer" months. This can be attributed to lack of heating but need for cooling loads. When comparing figure 2.4 and figure 2.5, one can note the effect the addition of heating has on the existing electricity profile. The evidence of the effect is apparent when one relates the months when heating is low in figure 2.4 to the same months in figure 2.5.

[12]Summer months here refers to the months between May to August. And the non-summer months refers to the rest of the year.

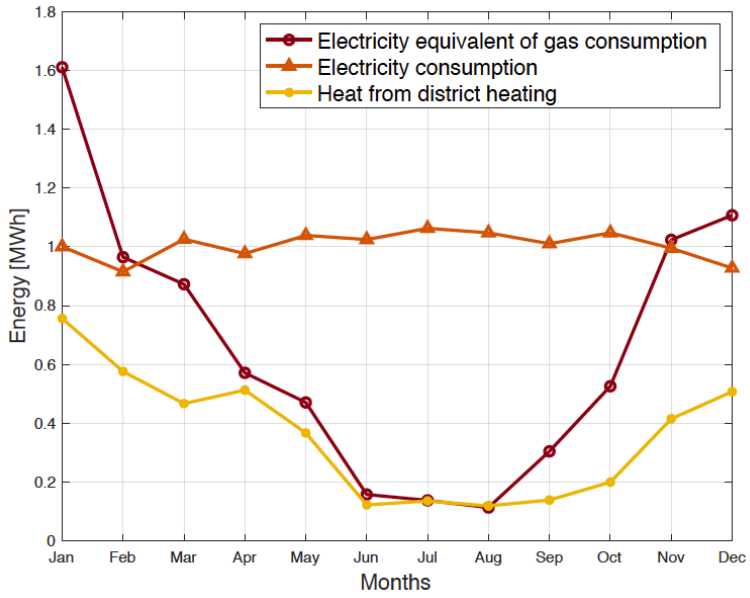

Figure 2.4: Monthly campus load variations seen in UTwente in 2019 [2].

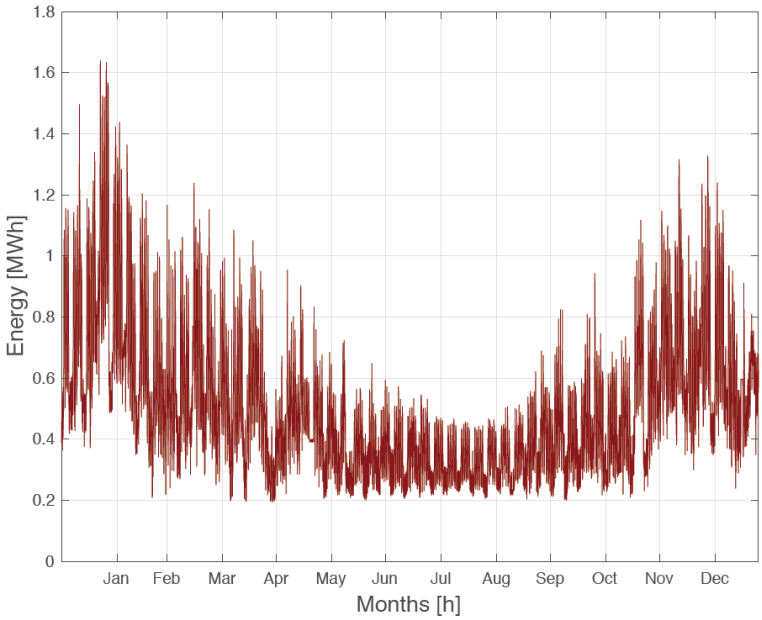

Figure 2.5: Monthly campus load variations seen in 2030 at the UTwente after modifications made to extrapolate data.

University of Twente has indicated that by 2030 they will reduce their energy consumption by 2% annually, this encompasses all energy based processes on their campus. It is difficult to segregate based on this the factor by which the electric load alone will decrease by 2030, but it is possible to approximate the range in which the

decrease will be in. The total energy consumption for 2019 of the university campus was taken and analysed to see on average the fraction electricity contributed to the total energy, this is termed the contribution factor. Once that was established, a decrease of 2% in total energy consumption was implemented per year from 2019 to 2030. This 2% is a valid assumption to make due to technological advances and efficiency increases for many electrical equipment. For example heat pumps, LEDs for lighting, higher efficiency for power electronics leading to lower conversion losses, etc. After which, implementing the contribution factor from earlier, the fraction of electricity was extracted from the totally decreased consumption.

Load component	**Value**	**Unit**
Heating	16.4	GWh
Electricity	9.69	GWh
Total electrical energy consumption	26.09	GWh

Table 2.2: Summary of modelled annual load demand components for 2030.

In figure 2.6, the normalised curve from the beginning of winter, beginning of spring and the end of autumn were plotted to demonstrate the degree of change that can be seen during the relatively colder times of the year. It is evident that when heating is added to the electricity consumption it dramatically changes the annual load profile. This is apparent when one notices that there is a spike in consumption in the morning hours of the colder days, that slowly stabilizes and decreases once again later into the day. When compared to the summer normalised load curve there is a smooth increase and decrease that follows the beginning and end of the workday. These observations imply that an additional underlying consumption pattern exists.

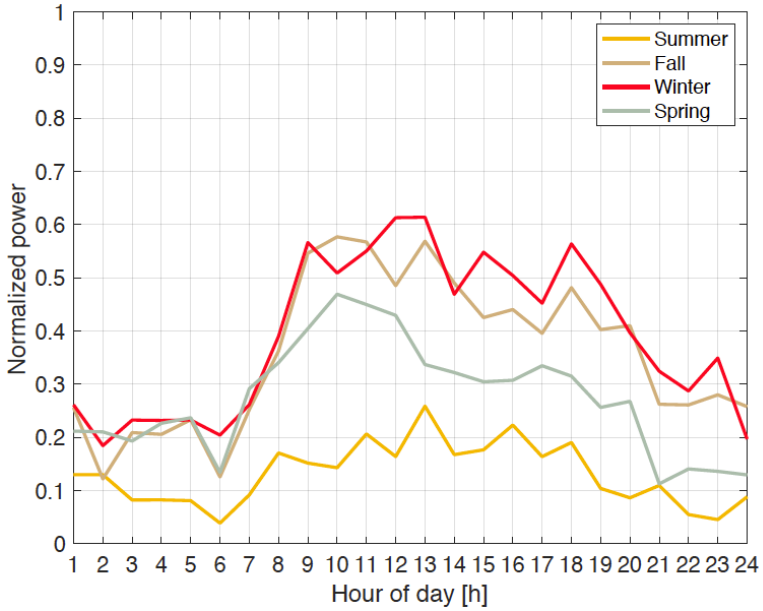

Figure 2.6: Normalised electricity profile of the University of Twente based on seasonal variations for All-electric load profile.

2.2 Heat pump

An air source heat pump is proposed to be used in this system, though they have the lowest efficiency compared to ground and water source heat pumps [47]. These are more economical to be installed in pre-existing buildings with no large water body close by. A major drawback of air source heat pumps is their lowered efficiency in the winter months, when outside temperatures drop below 4.4 °C, the coils of the heat pump are prone to freezing [47]. To defrost the frozen coils, the heat pump needs to be periodically reversed, thereby reducing its CoP. These losses get exacerbated when large quantities of heat are suddenly drawn

The CoP of the heat pump is calculated using:

$$COP = \frac{Q}{W}. \tag{2.1}$$

Where,

- Q is the heat output,
- W is the electric work input.

The CoP of heat pumps currently is in the range of 3 and an increase of 1% is assumed for each year [14], to arrive at an efficiency of 3.38 by 2030, which is exactly the CoP projected by ETRI in 2014 [6]. The economical and technical parameters used in the model to estimate the costs and efficiency of the heat pump used in this system are summarized in the table 2.3.

Parameter	**Value**	**Unit**
Technical		
Type	Air-source	-
COP	3.2	-
Economical		
CAPEX	1780	€/kWth
OPEX	1	%/year
Lifetime	20	years

Table 2.3: Technical and economical inputs for heat pumps projected for 2030 used as inputs to model. The OPEX is a percentage of the CAPEX [6].

2.3 PV system

Amongst all the RES technologies that currently exist, PV technology has shown enormous potential for growth compared to other RES that are more restricted by geographical requirements[15] [48]. Electricity generated from PV panels currently is the most commonly used on-site form of renewable energy generation for primary consumption [49]. Most universities in the Netherlands are situated in densely populated areas, making roof-top PV the best suited RES for on-site deployment and integration into a microgrid. Universities have the added benefit of having large roof areas, which are usually flat [50], this can also be seen in figure 2.2. The Dutch government is also incentivising private individuals and organisations by providing tax exemptions, grants and "crediting electricity supplied to the grid" [51]. Another reason PV was chosen as the primary source of on-site generation is due to the coinciding irradiance profile to the load profile, but in the winter months this not hold entirely true due to the large heating demand. From figure 2.7 it is evident that the PV feed-in occurs

approximately around the same time as the peak in the university's electricity demand during the summer and spring months. Meanwhile, looking at the relatively colder months of the year, the normalised irradiance available is considerably lower, indicating the need for alternative sources of power. Hence, utilisation of FCEVs in the role of back up generation or secondary generation. Furthermore, in the summer the total production is not always completely consumed, therefore to increase the utilisation[16] of the PV system a battery storage system is needed.

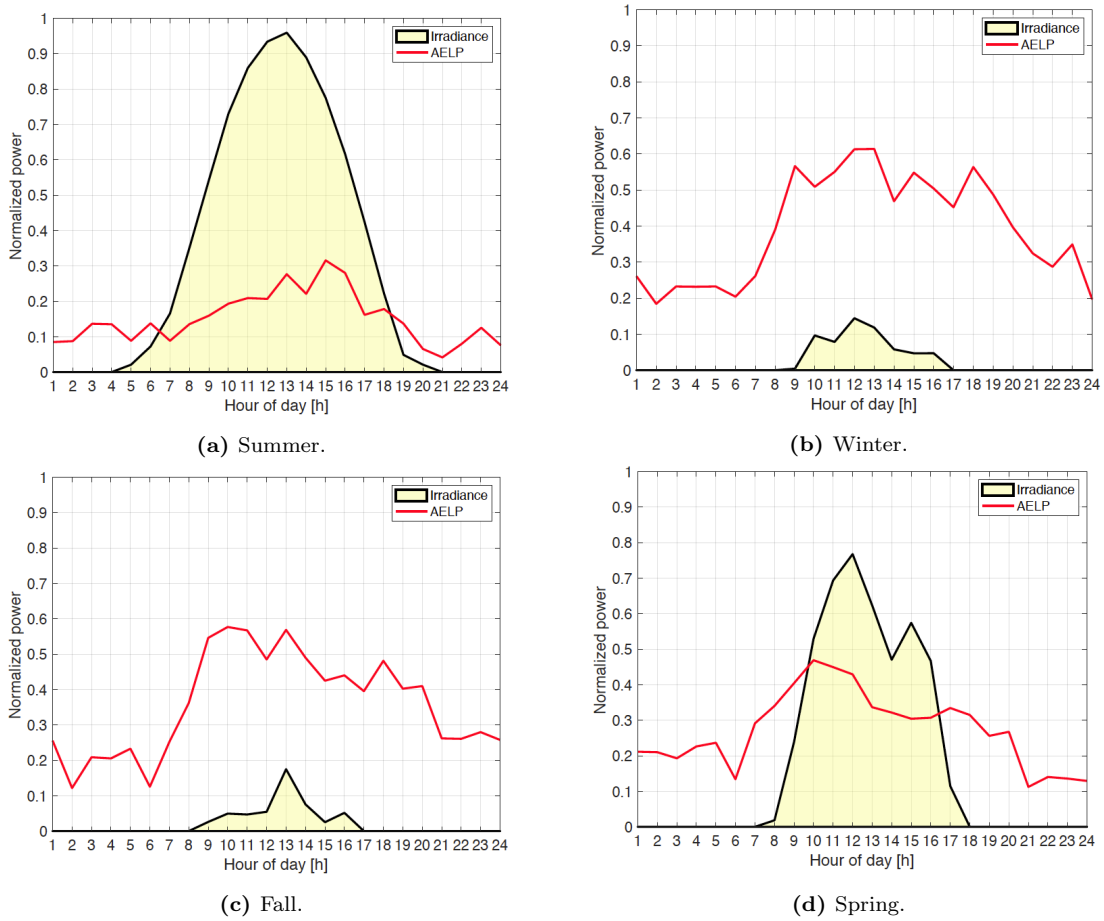

(a) Summer.

(b) Winter.

(c) Fall.

(d) Spring.

Figure 2.7: Normalised irradiance profile for each season vs the university's normalised daily load profile projected for 2030.

2.3.1 System modelling

The data used is of the typical meteorological year (TMY) format obtained from the Photovoltaic Geographical Information System of the EU [52]; this data includes weather data for a particular location. The equations used to simulate the on-site PV generation in Simulink are described below and were collated from Solar Energy: the

[16] When compared with renewable sources like hydropower and wind power, PV technology is not restricted by the local availability of flowing water or the proximity to buildings respectively.

[15] A battery storage system allows to increase the self-sufficiency, reduce amount of energy sold to the grid and reduces curtailment. Thereby lowering the LCOE of the PV system.

physics and engineering of Photovoltaic conversion technologies and systems. The output of the PV modules is heavily dependent on the temperature of the module and surroundings, the amount of solar irradiation incident on the module and the efficiency of the power electronics.

The module temperature is simulated using the Duffie-Beckman (DB) model, that builds on the Nominal Operating Cell Temperature (NOCT) model. The NOCT model only utilises the linear relationship between the difference in the module and ambient temperature and the irradiance incident per m^2 of the module. While the DB model also takes the cooling effect of wind speed into consideration [53].

$$T_m = T_a + \frac{T_{NOCT} - 20}{800} \times G_m \left(\frac{9.5}{5.7 + (3.8 \times w)} \right) \left(1 - \frac{\eta_{cell}}{T \times \alpha} \right). \tag{2.2}$$

Where,

- T_m is the module temperature [°C],
- T_a is the ambient temperature [°C],
- T_{NOCT} is the nominal operating cell temperature,
- w is the measured wind speed [m/s],
- T is the transmittance of the front layers of the module,
- α is the absorptivity of the module,
- G_m is the irradiation incident per unit area obtained for the location through the TMY dataset [W/m^2],
- η_{cell} is the cell level efficiency, which was considered to be the total module efficiency as given in the data sheet.

The effect of irradiance intensity and temperature are taken into consideration to obtain the varying efficiency [53],

$$\eta(T_m, G_m) = \eta(25°C, G_m)[1 + \kappa(T_m - 25°C)]. \tag{2.3}$$

Where,

- $\eta(25°C, G_m)$ is the efficiency at 25°C and varying G_m),
- κ is a constant that is element specific, which signifies the relationship of the efficiency at Standard Testing Conditions (STC) with respect to temperature. It is typically $-0.0035/°C$ [53].

$$\eta(25°C, G_m) = \frac{P_{MPP}(25°C, G_m)}{G_m \times A_m}. \tag{2.4}$$

$$P_{MPP}(25°C, G_m) = FF \times V_{OC}(25°C, G_m) \times I_{SC}(25°C, G_m). \tag{2.5}$$

$$I_{SC}(25°C, G_m) = I_{SC}(STC) \times \frac{G_m}{G_{STC}}. \tag{2.6}$$

$$V_{OC}(25°C, G_m) = V_{OC}(STC) \times \frac{nK_bT}{q} \frac{G_m}{G_{STC}}. \tag{2.7}$$

Where,

- I_{SC} is the short-circuit current [A],
- V_{OC} is the open-circuit voltage [V],
- n is the ideality factor. It was assumed to be 1, which might also cause a slight deviation in results.
- k_b is the Boltzman's constant.

This model does not take into consideration all meteorological parameters, like air pressure, humidity, precipitation, cloud coverage and wind direction [53]. The model was validated using NRELs PV Watt calculator and an average deviation of approximately 5.3% was seen from the PV output of the calculator. The results of this can be found in appendix C.

The optimal tilt angle was assumed to be 10°, for a south facing system [54][55]. The Netherlands has an equivalent sun hours[17] (ESH) of 3.1 hours [53]. A total system loss of 20% was added to account for soiling, shading, mismatch, wiring, snow, connectivity losses and balance of system losses. The efficiency of the modules chosen was 18.9% from Canadian Solar. The final DC output of the panels is found using equation 2.8:

$$P_{DC} = \eta(T_m, G_m) \cdot G_m \cdot A_m. \tag{2.8}$$

Where,

- P_{DC} is the DC power output of the PV panels [W],
- $\eta(T_m, G_m)$ is the module temperature and irradiance dependent efficiency of the panels [-],
- A_m is the area of the module [m^2].

In the future the efficiency of each panel is likely to be higher than it is today. In the past decade an efficiency increase of about 0.4 percentage per annum was seen for c-Si PV modules [56]. Thus, a similar increase in efficiency from 2019 to 2030 is assumed based on literature [57][58]. Thus, with this increase from the current value of 18.9% for Canadian Solar poly-crystalline silicon solar modules, in 2030 they would have an efficiency of approximately 23.1%. The increase is compounded each year to match the efficiency increases observed in literature [59][60][58]. This number can be corroborate by the current state of the best lab modules of c-Si; which have an efficiency of approximately 24.4% [61][62], it is highly probable that these modules will be in the market by 2030.

	Value	**Unit**
Mechanical data		
Module type	Poly-crystalline Si[63]	-
Electrical data		
Maximum power per panel	375[18][63]	W
Current efficiency of panels	18.9[63]	%
Efficiency increase projected	0.4[59][57]	%/year
Optimal tilt	10 [54][55]	°
System losses	20	%

Table 2.4: Mechanical data and system design assumptions made for the PV system summarized.

[17] Equivalent sun hours is the energy available from the sun per m^2 per day [53]. Furthermore, one sun hour is equal to 1000 W/m^2, indicating that on average the Netherlands receives about 3.1 kWh/m^2/day.

[18] With current projects made for the technological advancements and generation from PV technology, it is plausible that the

2.3.2 PV system sizing

The system is sized based on the energy balance paradigm. Where the total load in a year is divided by the product of the area of each module and the sum of a PV module's output through the year. The self-sufficiency ratio (SSR), quantity of energy sold to grid, along with total system costs were the major constraints in system sizing. It is calculated using equation 2.9 [53]:

$$N_{Bal} = \frac{E_L \cdot SF}{A_m \cdot \sum^{year} E_{ac}}. \tag{2.9}$$

Where,

- N_T is the number of modules that area needed [-],
- A_m is the area of one module [m^2],
- E_L is the total load demand in the year [kWh],
- SF is the sizing factor and is assumed to be 1.1[19] [53],
- E_{ac} is the AC power output of one module for an entire year [kWh].

The technical potential can be defined as the product of the power density of the system and the available space for the PV installation [64]. First the technical potential is found for each roof. It represents the maximum PV potential possible on a rooftop, and it depends on the efficiency of the module and the roof area [55]. The PV access factor for a flat roof was found to be 0.65, which accounts for shading, building orientation and structural soundness of the roof [64]. While the ground cover ratio (GCR) was calculated to be 66.4% for module tilt of 10°[55]. Thus, the total roof area available for PV deployment is calculated using [55]:

$$A_{avail} = A_{total} \cdot GCR \cdot \beta. \tag{2.10}$$

Where,

- A_{avail} refers to the roof area available to deploy PV modules [m^2],
- A_{total} refers to the total roof area available [m^2],
- GCR is the ground cover ratio,
- β is the PV access factor, assumed to be 0.65.

Using A_{avail} the maximum number of modules (N_{TP}) that can be installed can then be calculated and is the final technical potential.

2.3.3 DC-AC Inverter

The electricity used in the buildings on campus is generally AC. However in order to utilise the DC power from the PV system inverters are required to facilitate the power conversion from DC to AC. Inverter efficiencies vary based on the input DC power and voltage. Sandia National Laboratory's inverter model has been used in this report to approximate the final AC power output from the inverter [65]. The following equations are used to describe the AC power output:

maximum watt peak of panels will be higher by 2030. Though as legitimate references were unavailable, only an efficiency increase is assumed.

[19]The sizing factor accounts for a 10% loss in power experienced due to conversion, transmission and distribution. The losses are included in order to balance the generation and demand, as the generation has to include the losses incurred.

$$P_{AC} = \left\{ \frac{P_{AC0}}{A-B} - C(A-B) \right\} (P_{DC} - B) + C(P_{DC} - B)^2. \tag{2.11}$$

Where,

$$A = P_{DC0}(1 + C_1(V_{DC} - V_{DC0}), \tag{2.12}$$

$$B = P_{S0}(1 + C_2(V_{DC} - V_{DC0}), \tag{2.13}$$

$$C = C_0(1 + C_3(V_{DC} - V_{DC0}). \tag{2.14}$$

Where,

- V_{DC} is the DC input voltage[20] [V],
- V_{DC0} is the DC voltage level (V) at which the AC power rating is achieved at reference operating conditions.
- P_{AC} AC output power [W],
- P_{AC0} is the maximum AC power rating for the inverter at reference conditions [W],
- P_{DC0} DC power level at which the AC power rating is achieved at reference operating conditions [W],
- P_{S0} DC power required to start the inversion process [W],
- C_0 Parameter defining the curvature of the relationship between AC output power and DC input power,
- C_1 empirical coefficient allowing P_{DC0} to vary linearly with DC-voltage input, default value is zero [1/V],
- C_2 empirical coefficient allowing P_{S0} to vary linearly with DC-voltage input, default value is zero [1/V],
- C_3 empirical coefficient allowing C_0 to vary linearly with dc-voltage input, default value is zero [1/V],

All the parameters described above are very dependent on the inverter chosen, and as many types of inverters exist it is important to understand which one best suits the needs of the installation. For this report, three central inverters are proposed, one for each PV array of the separate buildings. A list of the parameters used as inputs can be found in appendix G.

2.4 Battery system

All the power produced at a given time by the PV system will not be consumed at that given time, supply and demand will not always be matched. This not only decreases the self-sufficiency but also decreases the utilisation of the PV system. In order to make the most efficient use of the power produced, it can be stored in batteries to be consumed at later times. This also provides the much needed flexibility to such an intermittent resource. In this report the storage system is designed to provide back-up during night time. It must be noted that during winter months the PV power production will be much lower relative to the summer months, this implies there will not always be excess generation to charge the batteries. During such periods the load will be met by the main grid.

For the smooth functioning of the UCM and to ensure security of supply, with minimal losses[21] in PV generation, it is crucial to size the energy production and the storage system complementary to one another. If the systems

[20] Typically it is assumed to be the solar array's maximum power voltage. Here array refers to the group of solar panels arranged in series and parallel to obtain the required power output.

are oversized there is the problem of not recovering costs whereas if the system is undersized, the benefits of integrating an electricity storage system will not be felt[66].

Figure 2.8 gives an overview of the current electricity storage technologies used, their periods of discharge and potential power output. Due to their ability to be used for either high power applications or long durations of discharge, flow batteries were chosen as the electricity storage technology of choice. A disadvantage of this choice is the higher cost of flow batteries relative to other mature battery storage technologies in the market today. This technology is still chosen due to its long cycle life and ability to stay in the discharged state for extended periods due to decoupled electrolyte and electrodes [30]. Due to the low availability of sunlight during the winter months, it is highly likely that the battery cannot be charged for a consecutive days. Despite a safety threshold being set to maintain a certain minimum capacity in the batteries, most technologies have self-discharge rates higher than those of flow batteries. Thus, integrating them into this microgrid ensures a layer of safety in the case the battery encounters extended periods of time during the winter without being charged.

Flow-batteries come in two types, hybrid flow batteries and redox-flow batteries. Of the two of the most commercially promising flow batteries, Vanadium redox flow and zinc-bromine flow batteries (ZBFB) [67], the technical specifications of a ZBFB was used as an input to the battery model in the UCM[22]. Currently, flow batteries (ZBFB and vanadium redox flow batteries alone) account for 0.03% share of grid-connected utility scale storage, and approximately 46 MW of total global installed capacity [68].

ZBFB fall under the hybrid classification of flow batteries, as the zinc in the system plates itself on the negative electrode during the charge cycle [30]. Though ZBFB have the disadvantage of releasing toxic bromine gas, this problem has been solved by the usage of amine compounds in the anolyte to facilitate bromine gas absorption [30]. Another point of safety is the release of hydrogen gas if the ZBFB is overcharged [30]. This occurs in situations when the electrolyte is favourable for this type of gas evolution and the zinc ions in the electrode are completely depleted. Thus, it is important not to over charge ZBFB and ensure sufficient safety measures are incorporated when utilising this technology.

On the other hand ZBFB have the advantage of having the largest cell potentials, in the range of 1.38V per cell [30]. Meanwhile, to combat degradation of the electrolyte over long periods of usage, the electrolyte in the tanks can be also be replaced with new solutions [31]. Flow batteries have an advantage over regular batteries, wherein their active material is decoupled during stationary condition, thus they have lower capacity for mechanical breakdown [30]. This reduces the breakdown of active material as they are not in constant contact. The fluids in the tanks can be replenished, thereby providing an additional advantage to closed battery systems. They also have high flexibility in terms of power to energy rating [30]. The ability of the flow batteries to store their active materials in separated tanks also means that the electrodes do not constantly form/reform during each charge/discharge cycles (though this is not true for hybrid flow batteries). Some studies even state that deep discharges of the zinc-bromine batteries extend the lifetime of the battery, rather than decrease it [69].

[21] Losses here refers to incomplete utilisation of the produced PV power on-site, meaning any excess generation is curtailed or sold to the grid.

[22] The reason ZBFB was chosen over vanadium redox flow batteries in this project to model the battery response is due to the lack of complete charge and discharge information for vanadium redox flow batteries. Detailed charge and discharge curves, along with voltage and capacity removed curves are required to be input for the KiBaM model.

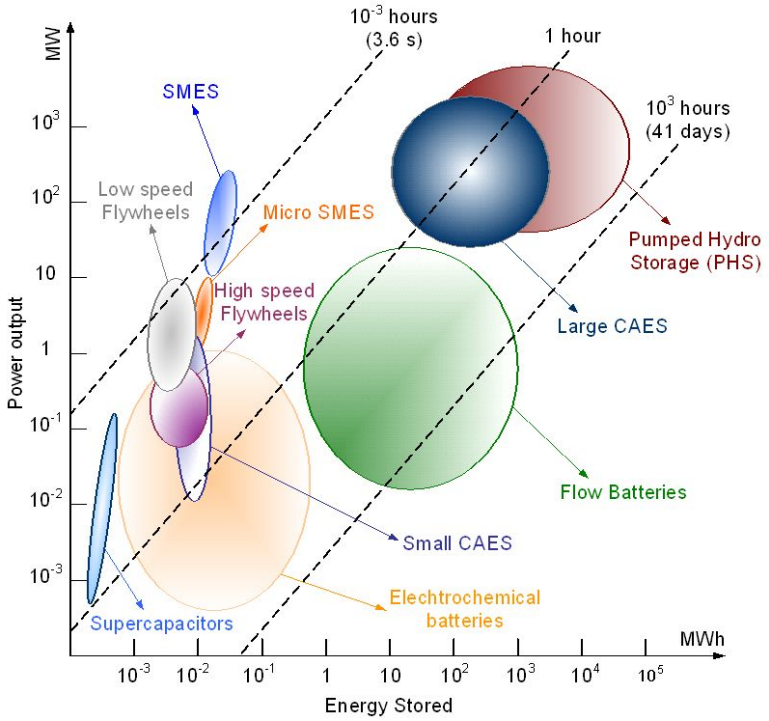

Figure 2.8: Different electricity storage systems based on their discharge durations versus their power output [3].

2.4.1 Kinetic Battery Model

The most detailed battery models would use electrochemical models, these models can depict the transient effects occurring within the battery. These models (low-level or microscopic models) are usually used by battery designers to better understand and improve the battery [70]. But when using the battery in a larger system, a high-level model provides a macroscopic view of the intricacies of integrating that specific battery into the system. Thus a high-level of precision was deemed unnecessary and so the Kinetic Battery Model (KiBaM) has been used to model the battery.

The KiBaM was initially designed to represent the response of the lead acid batteries, these batteries have relatively flat discharge curves and sharp knees just before they are completely discharged. ZBFB at low c-rates have almost flat discharge curves as well, these curves can be seen in appendix A. Though this does not hold at higher c-rates, as was noticed when analysing the validity of the model's response when compared to its data sheet voltage depictions. Thus, the BB c-rate was limited to a maximum of 5 hours or 0.2C, at which point the model responded similarly to the response depicted in the data sheet. Furthermore, at charge currents higher than 8 mA/cm^2, the likelihood of forming zinc dendrites is increased [30], which is also a reason for limiting the maximum charge current of the battery. Thus, i this model was deemed sufficient for the current study.

The KiBaM is an analytical model, which uses the chemical kinetics of the battery to model it as a voltage source [71][4] and can be utilized in timeseries simulations [72]. The model accounts for the dependence of capacity on the c-rate being used by implementing the discharge data provided by the battery manufacturers [4]. The c-rate is a measure of the rate of charge or discharge of a battery. The model reflects the voltage variation due to change in current and state of charge (SoC) but does not include the sharp increase/decrease in voltage at the end of charging/discharging cycle respectively [72].

The model assumes that the charge in a battery exists in two tanks, the available charge and bound charge. The rate at which the charge is transferred to the available tank, is the rate constant. Two sets of constants are found, capacity constants and voltage constant, using which the response of the battery can be simulated.

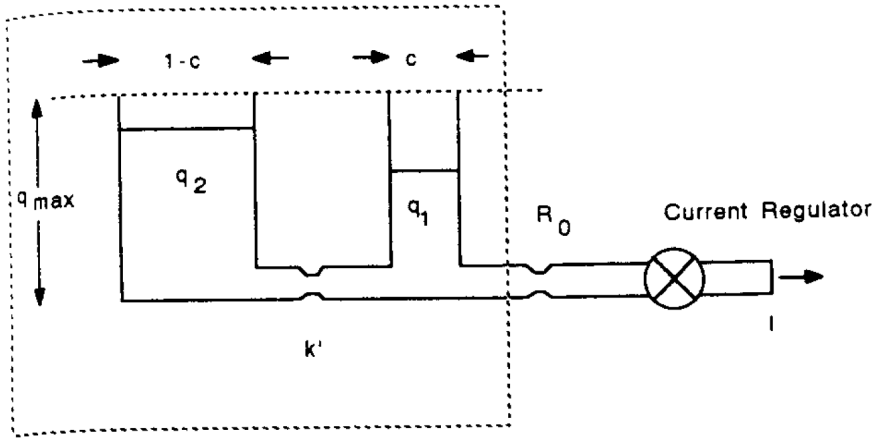

Figure 2.9: An illustration representing the visualisation required to understand the rationale and working of the KiBaM model as depicted by Manwell et al [4].

$$q_{1,t} = q_{1,0}e^{-kt} + \frac{(q_0kc - I)(1 - e^{-kt})}{k} - \frac{Ic(kt - 1 + e^{-kt})}{k}. \tag{2.15}$$

$$q_{2,t} = q_{2,0}e^{-kt} + q_0(1 - c)(1 - e^{-kt}) - \frac{I(1 - c)(kt - 1 + e^{-kt})}{k}. \tag{2.16}$$

$$q_0 = q_{1,0} + q_{2,0}. \tag{2.17}$$

Where,

- $q_{1,t}$ and $q_{2,t}$ are the available and bound charges respectively at time t
- $q_{1,0}$ and $q_{2,0}$ are the amount of available and bound charge at the beginning of the cycle
- k is the rate constant
- c is the width of the tank q_1
- I is the charge or discharge current
- q_{max} is the total maximum capacity of the battery

$$I = \frac{kcq_{max}}{1 - e^{-kt} + c(kt - 1 + e^{-kt})}. \tag{2.18}$$

c,k and q_{max} are the capacity constants and are found using the voltage vs charge removed curves available in the data sheet of the battery. These curves can be found in A. The constants were found using a non-linear least squares curve fitting method based on the Levenberg-Marquardt algorithm. The voltage constants are also

found using the same method, the charge removed at each C-rate is first normalized to obtain internal voltage (E) vs normalized charge removed (X) curves. These curves depict the internal voltage of the battery for the corresponding normalized charge removed from the battery. Equation 2.19 describes the internal voltage of the battery, the equation correlates the charge removed from the battery to the internal voltage. It is important to note that when there is no charge removed, E and the fully charged internal voltage have a linear relationship. This equation allows at higher charge or discharge rates for the voltage to vary non-linearly, to account for larger losses at higher voltages or larger charge removed. The voltage constants are found in a similar manner to the capacity constants, wherein curve fitting was used. Implementing the equation 2.19 [4], where E and X are obtained through experimentation[23]:

$$E = E_0 + AX + CX/(D - X). \tag{2.19}$$

Where,

- E_0 is the fully charged internal battery voltage,
- A is the parameter reflecting the initial linear variation of internal battery voltage with SoC,
- C,D is the parameters reflecting the decrease of battery voltage when the battery is progressively discharged,
- X is the normalized charge removed from the battery at the given discharge current.

Some assumptions made for the BB modelling:

1. Constant internal resistance, R_0.
2. The discharge and charge constants are the same. This was done due to the lack of available charge specific data for the battery chosen.
3. The maximum current is set depending on the maximum current allowed by the battery power electronics and the cabling combined.
4. A minimum and maximum SoC is set, where the range is between 0.5% to 95%, using the voltage of the battery.

Model specific points to note:

1. To discharge: the current demanded by the load is found, by quantifying the power needed [kW] and dividing it by the nominal battery voltage [V].
2. The charge and discharge currents change as a function of the SoC, the maximum current possible at a given time-step is found using equations 2.21 and 2.21 respectively. These currents are also dependent on the maximum current allowed by the battery power electronics and the cabling combined, and the maximum c-rate.

$$I_{d,max} = \frac{kq_{1,0}e^{-kt} + q_0kc(1 - e^{-kt})}{1 - e^{-kt} + c(kt - 1 + e^{kt})}. \tag{2.20}$$

$$I_{c,max} = \frac{-kcq_{max} + kq_{1,0}e^{-kt} + q_0kc(1 - e^{-kt})}{1 - e^{-kt} + c(kt - 1 + e^{-kt})}. \tag{2.21}$$

Where,

[23]Fact sheets obtained from Redlow [73], provided the required experimental data.

- $I_{d,max}$ is the maximum possible discharge current at time t,
- $I_{c,max}$ is the maximum possible charge current at time t.

Parameter	Value	Unit
Technical		
Capacity	10	kWh
Voltage (nominal)	48	V
Maximum current	125	A
Round-trip efficiency	80	%
Maximum c-rate	0.2	-

Table 2.5: Summary of technical input parameters to the KiBaM and the economical parameters used to account for BB costs. The economical parameters are projections made for 2030. The CAPEX accounts for power electronics and stack cost and the OPEX is a percentage of the CAPEX.

2.5 Hydrogen Car

The FCEVs may be used to provide stability to the UCM during hours of peak consumption. The storage unit provides security of supply for the night load and the FCEVs provide backup during hours or minutes of low PV generation, to enable a certain amount of independence from the grid. For an FCEV to be able to provide electricity to the UCM it needs to be connected to a V2G terminal. FCEVs have been tested in experimental setups in the Green Village at TU Delft by Oldenbroek et al. in 2017. They modified a Hyundai ix35 FCEV to have a power output with a three phase AC 9.5 kW connection [36]. This experimental setup was also viewed by the author during the process of understanding how the FCEV was controlled to provide V2G services. After studies had shown that high load cycles, repeated start up and shut downs reduce the durability of the fuel cell. Furthermore, at powers higher than 9.5kW, the heat produced by the fuel cell cannot be dissipated while the car is in stand-by. Thus, the limitation of the power output to 9.5kW, which is 10% of the rated power of the fuel cells in FCEVs. They verified experimentally that that FCEVs can be used for mobility and backup power while they are parked, and found that ambient conditions played a role in the cooling of the fuel cell. They came to the conclusion that the FCEVs could respond to very high load gradients and if integrated into virtual power plants they could execute higher gradients than existing fast reacting thermal plants, with a mean maximum downward gradient of -47kW/s and a mean maximum upward gradient of +73kW/s. A consumption of 0.55 kg/h of hydrogen was noted when the FCEVs were connected to the grid with an efficiency of 44%.

The model was built to simulate the collective amount of hydrogen available in the fuel tanks of the "connected cars". Thereby depicting the amount of available hydrogen that can be used by the microgrid. The amount of hydrogen in the fuel tanks can be measured by the density of hydrogen in the tank, but in order to simulate the amount remaining it is important to understand how the state of charge works. ISO has formulated a definition for state of charge of hydrogen: "state of charge (SOX) ratio of hydrogen density to the density at the maximum operating pressure rated at the standard temperature 15°C in a compressed hydrogen storage system (CHSS)"[74].

$$SOX(\%) = \frac{\rho(P,T)}{\rho(NWP, 15°C)} \times 100\%. \tag{2.22}$$

[5]These costs include power electronics and stack costs.

Where,

- $\rho(P, T)$ is the density of hydrogen at that particular temperature and pressure,
- $\rho(NWP, 15°C)$ is the density of hydrogen at nominal working pressure (NWP). It is in the range of 700 bar.

Typically polymer electrolyte membrane fuel cells (PEMFCs) used in FCEVs have efficiencies (% HHV) in the range of 60%. The FCEV fleet modelled have a 5.3 kg fuel tank size with a power output of 100kW and a driving range approximately 594 km, with a fuel consumption of around 0.89 kg/100km [75]. In the model only cars that have an SOX of minimum 10% are allowed to connect to the microgrid, while the hydrogen consumption from cars is restricted to allow a minimum threshold of hydrogen is kept in the tanks of the cars so they may be used to make a trip to the nearest refueling station. This threshold would be very location specific. For the University of Twente for example, a minimum threshold of 17% of the total tank capacity would need to be unconsumed,based on existing hydrogen re-fuelling stations. Whereas for TU Delft, this threshold could be lower at 10%. Given the interest in the EU in a hydrogen economy and its role in decarbonising the transportation sector, about 3700 refuelling stations are currently planned for across Europe [76]. Though, as no current plans exist for a refuelling station closer to the University of Twente, 17% is assumed as the threshold. The number of FCEVs in the fleet is determined as a total percentage of the employees owning FCEVs.

2.5.1 System modelling

The hydrogen in the tanks of the FCEVs is modelled as a combined aggregate, henceforth termed FCEV fleet. The fuel was aggregated to simplify the modelling process, as only the total quantity of hydrogen is required to be known in order to determine whether there is sufficient power to meet the load or not.

As no data was available for the probability distribution of the quantity of hydrogen available in the tanks of the cars that park at a place of work in the Netherlands. A simplification was made, where measurements were taken from a study done by the Idaho National Laboratory on the statistics of the probability distribution of the SoC BEVs have when they are plugged in at work[77].

The model assumes that:

1. There will be no FCEVs available over the weekend and over holidays.
2. Cars will be available between an 8AM to 6PM window, increasing gradually (in a randomized manner) at the beginning of the day and decreasing post 1PM.
3. All V2G spots will be full if the number of FCEVs with the minimum required SOX are available.
4. When an FCEV is connected to a V2G point, it stays connected for a minimum of four hours.
5. The SOX of FCEVs on arrival when plugged into a V2G terminal are assumed to be similar to the SoC of BEVs, disregarding the factors of difference between the FCEVs and BEVs. In reality the SOX in FCEVs when compared to the SoC in BEVs will vary due to the larger driving range that FCEVs are capable of and the shorter re-fuelling periods they offer [78]. Another factor is the larger distances that Americans generally travel, relative to the Dutch in the Netherlands, and the effect this has on the quantity of fuel in the tank that is available for use [13][79]. As this is to only simulate how hydrogen could be used in a UCM, and to analyse the economic feasibility, the simplification made is sufficient for this study. In reality, Furthermore, the quantity of hydrogen available might actually be larger if all other assumptions hold.

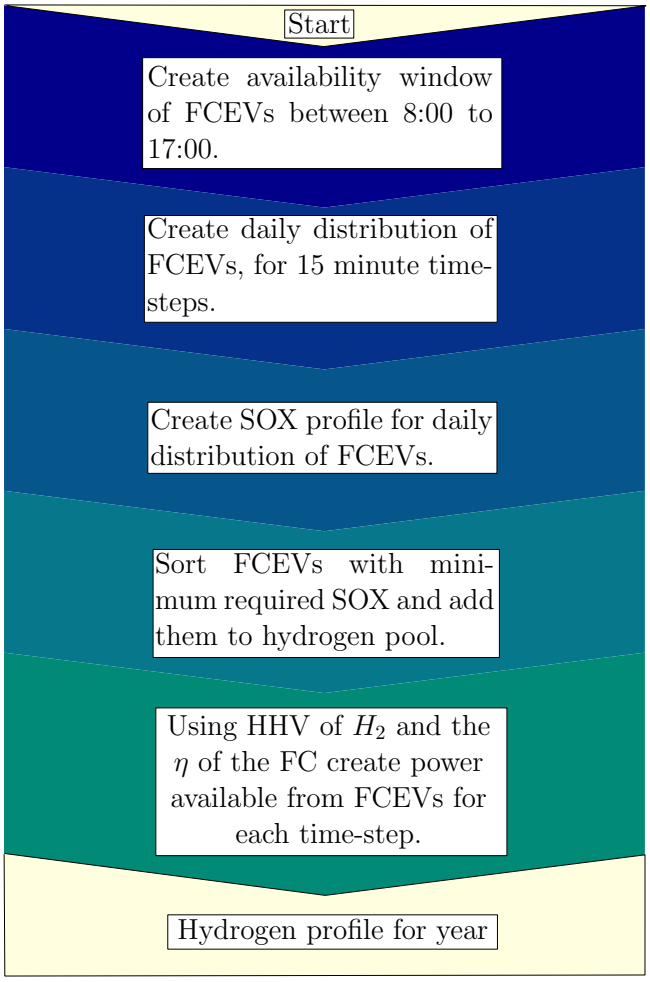

Figure 2.10: Model step by step method to create a hydrogen pool of fuel availability profile for one year.

The power output from the FCEVs was limited to a maximum of 9.5kW per terminal, this is based on studies using FCEVs as backup generators carried out. They suggest that partial loads provide higher efficiency and longer lifetime for the fuel cell in the vehicle when used in the V2G capacity [36]. This was found to be due to the larger amount of heat generated at higher loads that would require additional infrastructure to cool the fuel cells when they are stationary.

Most universities own car fleets, these car fleets would have to become "green" in order to keep cost of the vehicles low. Amongst other drivers current EU regulations and green initiatives to curb carbon emissions from transportation [80]. These effects in the Netherlands have resulted in tax levies on cars based on their quantity of emissions. Furthermore, about 20% of the cost of a car in a fleet accounts for fuel costs, 15% for O&M of the vehicles and about 2% is accounted for by taxes[24]; while the remaining fractions are interest, insurance and management fees[80]. Meanwhile studies by Delloite show that FCEVs are set to become cheaper than internal combustion engine (ICEs) vehicles and BEVs by 2030 [76]. When taking these two aspects into account, it is beneficial for the university to slowly phase out from ICEs and switch to BEVs or FCEVs. An alternative to this would be to also lease an FCEV fleet for fixed prices from car fleet managers, these cars would not only be utilised by the university for transportation but for backup generation as well. Some FCEV manufacturers, like

Daimler AG also own car fleet managements organisation in the Netherlands. Contracts could be made with such organisations[24]. An addition to the university's vehicle fleet, the university's employees who own FCEVs can also be allowed to participate in the CaPP concept. In such instances valid contracts must be drawn in order to compensate for the discomfort experiences by the car owner. Such contractual agreements between institutions and individual car owners were proposed and studied by Park Lee et al. [81].

In order to calculate the price of energy from the FCEVs, it is important to understand all the costs that are involved in such a system. V2G terminals are bi-directional,with projections for increased BEVs more charging points will be made available to provide charging infrastructure. These terminals may also be used to "discharge" the FCEVs to provide backup generation when needed if they are plugged in. Thus, no installation cost for the terminals is assumed. The hydrogen fuel used on the other hand will be paid for directly by the university at the time of each re-fuelling, this is an integral cost to include when analysing the economic viability of using FCEVs to provide backup generation for a university. The EU has made price projections for hydrogen based on the source of hydrogen, these can be found in table 2.6:

Type of hydrogen fuel[25]	**Price (€/kg)**
Fossil-fuel based	1.5
Fossil-fuel based with CCS	2
Renewable based	2.5 - 5.5

Table 2.6: Current projections for hydrogen fuel prices in the EU by 2030 [7] (CCS - Carbon Capture and Storage).

It must be noted that the cost of purchasing the FCEVs by the university or the contract mechanisms suggested between car fleet managers and the university are not explored. Though these costs are important to understand the actual impact of integrating FCEVs in a UCM, they have not been included in the cost analysis.

Parameter	**Value**	**Unit**
Technical		
Fuel cell power output	100	kW
V2G limiting power output	9.5 [36]	kW
Efficiency	60	%
Tank maximum capacity	5.63 [75]	kg
Nominal working pressure	70 [82]	MPa

Table 2.7: Technical and economical input parameters of the V2G components of the UCM.

[24]These percentages are averages taken for the whole of Europe. The levied taxes are very country specific. As of 2016 beginning from an emission range of 0-50 grams of SO_2 there are 15% additional tax liabilities, ending at 25% additional taxes for over 106 grams of SO_2 [13].

[24]Such contracts are deemed out of the scope of this report though this provides an avenue of research that could be carried out. Studies that have been carried out analysing the different contract mechanisms between car owners and institutions can be used as a reference point to build from [81]. Though many focal points would differ between individual car owners and organisations that own car fleets.

[25]Depending on the source of hydrogen the prices vary, note that for the fossil-fuel based cost of hydrogen, the price of carbon was not included.

2.6 Grid electricity prices

As the penetration of renewables increases Mulder et al in 2013 studied that electricity markets become more sensitive to weather conditions [83]. They noted that there was a slight increase in prices which could be correlated as a consequence of wind speeds, but in general the Dutch electricity prices have a stronger correlation to the marginal costs of conventional gas fired power plants than the increasing share of renewable generation in the Dutch energy mix. But it is important to remember that since 2013 the share of PV has almost since doubled, and yet the Dutch electricity prices still see a high correlation to gas fuel prices [26] [84]. As the German and Dutch electricity markets are interlinked, some effects from the German market are felt in the Netherlands [85]. Another point to note is the higher degree of convergence in the day-ahead market prices between Germany and the Netherlands.

It is hard to predict how prices will vary, or how volatile they will be in the span of a decade, as this is very location specific [86], and also highly correlated to fossil fuel prices depending on the level of dependence and also the level of interaction between cross-border markets. Rintamaki et. al compare the cases of Denmark and Germany, both leaders in the fraction of renewables they use to generate electricity. They find that in Denmark though 50% of electricity is generated from wind, electricity production from wind during peak hours brings down the electricity price and thereby decreases volatility. At the same time in Germany, where almost 50% of electricity is generated from a variety of renewables, the off-peak electricity prices are driven even further down by electricity production from solar during those times. This suggests that price volatility is highly dependent on the share of each type of RES, cross-border electricity exchange and the electricity markets of neighbouring countries. According to PBL, the Netherlands environmental agency, the average wholesale market electricity price by 2030 will be 57€/MWh [29], with a maximum minimum range of of 162.4 €/MWh and - 12.1[27] €/MWh. Meanwhile, in 2019 it was at approximately 41.2[28] €/MWh [84]. Between 2018 and 2019 there was a decrease seen in electricity prices that can be attributed to lower natural gas and coal prices and stabilisation of CO_2 prices. But this future projected increase can be due to various reasons, some of them are increased dependence on distributed generation causing an increasing need to build infrastructure to integrate them into the existing grid, increasing carbon prices, volatility in prices due to policy and regulatory changes which causes a certain level of uncertainty for an investor in the liberalised electricity market [21][22][29]. Furthermore, in figure 2.11, natural gas prices and wholesale electricity projections were made by [5] which also corroborate the findings made. Note that is said figure CHF stands for Swiss Franc; as the difference between the euro and CHF are minimal this graph is still relevant to understand.

[26] In 2030 the share of renewables in electricity production will be at 70% [9]. Thus, they will probably have a larger effect on the prices in the Netherlands than they currently do today. Wherein, the average price of electricity during the day might actually be lower than the average at night. The availability of renewables at night time is relatively lower than during the day (based on the current share of solar and wind in the energy mix). This implies that in order to meet any demand at night, plants that can be ramped up or down will need to be deployed. Typically these plants use fuels, that by 2030, will be more expensive than they are now. But the author assumes that the current price trends will follow and no such increase in average nighttime electricity prices will be seen.

[27] The price range is a result of a simulation and not obtained from PBL. The method of generating the price profile is discussed below.

[28] The corresponding price range for 2019 based on data is 121.5 €/MWh to -9 €/MWh [29].

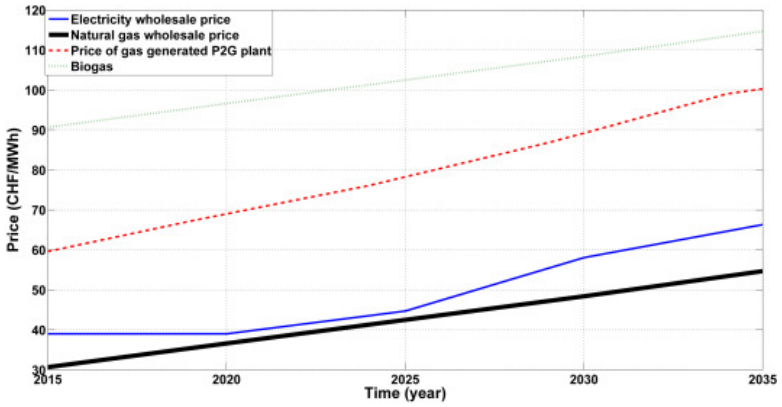

Figure 2.11: Projections of wholesale electricity and natural gas prices [5].

One of the drivers causing an increase in electricity prices is the the market stability reserve, that the emissions trading system (ETS) introduced in 2020 [87] [88]. The price of emission allowances which have been in surplus since the economic crises of 2008 will decrease. ETS is a market instrument used by the EU to reduce greenhouse gases in a cost-effective manner, in order to achieve its climate targets. The market stability reserve is a part of the EU ETS's long-term solutions to address the excess emissions allowances and to constantly adjust their numbers to improve system resilience. That along with financial speculation will cause an increase in carbon prices [66], the Netherlands having such a large dependence on gas, coal and oil [89] will see this reflected in the electricity prices. Currently the Netherlands procures approximately 20% of their power from renewable resources (wind, solar, waste, biofuels, hydro), while the remaining 80% comes from fossil based fuels as of 2019 [89]. The dependence on gas-fired power plants is only projected to grow, given the independent increase in electricity demand due to economic progress, electrification of various sectors, the planned decommissioning of coal, oil and nuclear power plants and the insufficient planned increase in renewable power generation [14].

Universities, as other consumers, currently obtain their electricity through the retail market. Retail prices are generally higher than wholesale prices, where wholesale prices only account for the cost of generation, the former also includes transmission, distribution supply costs, commodity prices, taxes and levies [22]. Typically universities being large energy consumers, they enter into contracts with energy retailers. These contracts set price caps or a fixed price to be paid on a yearly basis. These contracts are in general confidential and not much information could be found on them, as they are also very specific between the agents involved in the contract, thus they are also bound to vary by large degrees. The retail price stipulated in contracts also varies based on location, grid connection charges, distribution and transportation charges, certificates, etc. As these contracts are private, it is assumed that in 2019 the maximum and minimum prices paid for by the university to the retail electricity supplier is 0.0535 €/kWh and 0.0408 €/kWh, for times of high and low wholesale prices respectively. This assumption is made after consultation, therefore no reference is provided. It must be noted that these prices are subject to change based on the supplier and contract type between the members involved. Currently, platforms are emerging where aggregated consumers participate in the wholesale electricity market [90].

Equigy is one such platform, where consumers are allowed to buy and sell electricity. Equigy is a collaboration between Germany, the Netherlands, Italy and Sweden [91][90]. More countries are expected to join this platform to allow for the trade of electricity and utilisation of small kW storage systems to solutions for grid stabilisation. The platform utilises blockchain technology with no fees required to participate in exchanges. Sophisticated software solutions can be devised to create a collaboration with the EMS of the UCM with the Equigy platform, current technology is sufficient to predict demand and supply with reasonable accuracy 24 hours ahead of time.

This report proposes the UCM participate in the wholesale market due to the higher costs incurred for electricity in the retail market.

In 2011, the energy costs in the post-tax total price of electricity in Amsterdam accounted for approximately 44%, while network charges and taxes accounted for the remaining portion, but a general increasing trend is noted in total retail electricity prices [22]. The network component of the prices has remained relatively stable in the period 2008 to 2015 [92]. Thus, an assumption is made that the network component shares in the post-tax prices do not change drastically till 2019 and will remain in the range of . But with the projected increase in shares of renewables in the electricity mix, the network component of retail prices is bound to increase [92]. Though the effect of this on large energy consumers like universities will be minimal. The taxes and levies, along with inclusion of certificates will also cause an increase in retail prices. To include these affects in the retail prices, a 0.5% increase is assumed for each year to account for the increased share of taxes and network costs by 2030. This results in a a maximum and minimum of 72 €/MWh and 55 €/MWh. Based on this price increase, it is beneficial to create systems that can participate in wholesale markets.

2.6.1 Creating price profile for 2030

By 2030 about 70% of the electricity generated in the Nethelands will come from renewable resources according to the klimaat akkoord signed by the Dutch government [9]. This results in a 3.5 times increase in renewables in the generation mix, the effects of these will likely be felt on the electricity prices. Currently though, about 20% of the electricity generated in the Netherlands comes from renewable sources [89], and thus far no drastic implications have been seen. Bearing in mind the varying effects increased penetration of renewables has on price fluctuations between countries, it is difficult to comprehensively understand how the wholesale market prices in the Netherlands will behave by 2030. A more in depth study would need to be carried out

A simplification is made in creating a price profile where the electricity prices in 2030 are assumed to increase by a factor of difference between the current and projected prices. Taking the aforementioned factor into consideration along with a price profile is build assuming a linear relationship between the 2030 and 2019 prices [29]. Based on data collected from Entso-e's transparency platform the mean wholesale electricity prices in 2019 differs from the average wholesale electricity price projected by PBL for 2030, by a factor of 1.38 (termed γ for ease of reference) [93]. This ratio is multiplied with the 2019 price trends obtained to create the wholesale electricity price profile for 2030. This profile is depicted in figure 2.12.

[29] This is an oversimplification, where daily weather changes, increased cross border effects on the prices and increased renewable penetration are not taken into account.

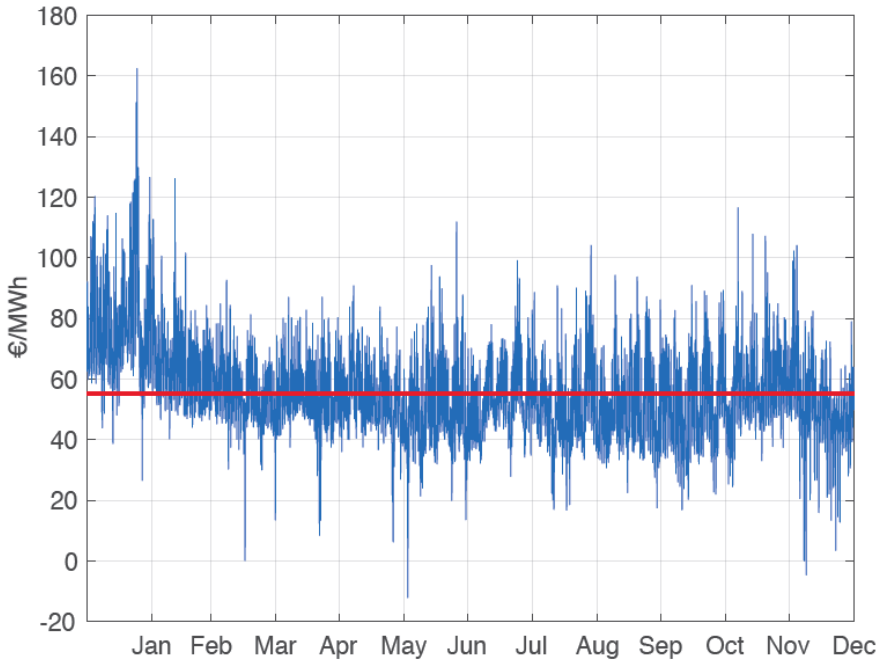

Figure 2.12: Wholesale electricity price profile for 2030 simulated using the 2019 wholesale electricity price as a base.

Electricity market	Year	Value			Unit
		Max	Mean	Min	
Wholesale	2019	121.5	42.6	-9	€/MWh
	2030	162.4	57	-12.1	€/MWh
Retail	2019	53.5	47.2	40.8	€/MWh
	2030	71.5	63	54.54	€/MWh

Table 2.8: Electricity price spread in the wholesale and retail markets in 2019 and 2030. The 2019 values are obtained from data while the 2030 numbers are based on simulation results.

2.7 Scenario development

There are two scenarios developed in this section that will be used to test and compare the economic viability of both control strategies of the UCM with. These scenarios are reference scenarios that provide the means and establish a method to compare the controls developed, one is the baseline scenario and the other is the DER scenario.

2.7.1 Baseline scenario

The baseline scenario described is used to create a basis to compare the benefits or lack thereof in the control strategies devised. The scenario assumes 100% of the electricity demand (electrified heating included) is met by the main utility grid. This is done to understand what a complete dependence on the grid would look like in 2030, economically speaking.

2.7.2 DER scenarios

The Distributed Energy Resources scenario involves the university developing a UCM that uses PV generation as its primary source of electricity. The electricity generated from the PV system is used to meet the load's demands during the day and store the excess to be used at night. In order to meet the large quantity of load during the day, the PV system will try to meet the majority and the residual load still remaining after PV feed-in would be met using the FCEVs. If there is still more load to be met, it is met by the main distribution grid. The PB and SSB control implementation, all economic and technical assumptions and projections made pertain this scenario.

2.8 Economic model

The economic model comprises of the cost calculations that are used to analyse the economic viability of the proposed system. The analysis is performed for each control strategy and the total cost of the system is one of the factors used to size system components in the UCM.

2.8.1 Total System Cost of Energy

The TSCoE gives a complete overview of the costs incurred by the system proposed each year, the formulation was obtained from [39]. The TSCoE is a combination of the total cost of each individual component of the system where the capital cost is discounted with an annuity factor. It is the present value of a cash flow that produces one unit of monetary value in income over t period of time. The annuity factor allows to split the cost of the investment over the n years of the project to estimate the cost of said project in terms of the annual price to be paid divided over those years.

$$TSCoE[€/year] = \sum_{i=1}^{n} TC_i. \tag{2.23}$$

$$TC_i[€/year] = CC_i + OMC_i. \tag{2.24}$$

$$CC_i[€/year] = AF_i \cdot Q_i \cdot IC_i. \tag{2.25}$$

$$AF_i[\%] = \frac{r(1+r)^{LT_i}}{(1+r)^{LT_i} - 1}. \tag{2.26}$$

Where,

- i a component of the system [-],
- TC_i is the annual total cost of that component of the system (in €/year),
- LT_i is the economic lifetime of that component (in years),
- CC_i is the capital cost or CAPEX per annum for that component (in €/year),
- OMC_i (€/year) is the OPEX costs per year for that component,
- n is the different components of the system, namely the PV system, BB and FCEV fleet,
- AF_i is the annuity factor (%),

- Q_i is the installed capacity of that component (unit is component specific),
- IC_i is the investment cost per specific energy component (€/component specific capacity),
- r is the real discount rate.

$$OMC_i[€/year] = OM_i \cdot Q_i \cdot IC_i. \tag{2.27}$$

2.8.2 Total cost of energy

The sum of the TSCoE with the annual price paid to the distribution grid, in the wholesale market utilising the Equigy platform.

$$TCE[€/year] = TSCoE + C_{grid}. \tag{2.28}$$

$$C_{grid}[€/year] = \sum_{t=1}^{year} (V_{grid}(t) \times W_{grid}(t)). \tag{2.29}$$

Where,

- C_{grid} is the annual cost of electricity paid to the grid [€/year],
- $W_{grid}(t)$ is the electricity price for each time-step [€/MWh],
- $V_{grid}(t)$ is the volume of energy procured from the grid at that time-step [MWh].

2.8.3 System levelised cost of electricity

The system levelised cost of energy (SLCOE) is calculated for electricity and hydrogen consumption. The individual share of TSCoE for electricity and hydrogen are found and then divided by their respective amounts consumed. Equation 2.30 is obtained from [39]:

$$SLCoE_e[€/kWh] = \frac{TSCoE_e}{EC_e}. \tag{2.30}$$

Where,

- EC_e is the electricity consumed [kWh],
- $TSCoE_e$ is the electricity share of TSCoE [€],

2.8.4 LCOE

The levelised cost of electricity (LCOE) offers a basis to compare different electricity generation sources. It is the present value of electricity that is generated over the lifetime of the energy source[8]. It is the sum of the investment cost, split into annual payments with the annuity factor, and the O&M costs, divided by the sum of generated energy. This method of formulation assumes that the O&M costs and the generation output will remain constant throughout the project lifetime. For both the PV and BB systems the energy generated (or throughput in the case of the BB) reduces over its lifetime, this is not considered in this formulation. Equation 2.31 gives the LCOE formulation for this report [8]:

$$LCOE_i(€/kWh) = \frac{TC_i}{Q_i}. \tag{2.31}$$

The capital, operation and maintenance costs were calculated for 2030 using prices from 2019. According to [62] the c-Si market of PV technology currently has 95% of the market share and these shares are not projected to change considerably in the coming years. The main components of the CAPEX are the costs of the PV modules and the balance of system (Balance of System (BoS)). Up until 2014 the cost of the modules bore the majority of the capital costs, but due to developments in PV technology since 2014 the share of PV module costs have gone down in the total CAPEX [57] [94]. The PV module prices have followed their respective technology learning curves, corresponding drops in prices have occurred when the global cumulative production was seen to double. A learning curve of 20% is found for PV modules based on the average learning curves seen in the past years. The learning curve of the BoS components is harder to estimate as only the inverter prices follow learning curves while the cabling, land costs, labour costs, permits, etc. are all more geographically linked [57]. Due to cross border influences in the EU similar costs can be assumed for the BoS components, though labour costs are likely to be different. Thus, a turnkey cost is directly obtained from Fraunhofer to be used for the LCOE calculations of the PV system [62]. Furthermore, the following are assumptions made for PV system LCOE calculation:

1. Market prices will converge by 2030 in Europe, especially the Netherlands and Germany, so similar rooftop PV CAPEX is assumed [57]. The same assumption is made for the PV modules and the BoS components.
2. A 25 year lifetime is assumed, though the lifetime might actually be slightly higher by 2030 due to technological advancements.
3. As an initial figure, PV system CAPEX of approximately 1300$€/kW_p$ was assumed for 2019 [62]. This cost includes cost of BoS and installation.
4. A 40% decrease in CAPEX costs from 2015 to 2019 [59], thus arriving at a 2.6% decrease per year.
5. The OPEX is assumed to be 2% of the total capital investment. In general a commercial rooftop PV system's OPEX is 1-2% of the system CAPEX [57].
6. An overall 30% decrease will be seen between 2014 to 2030 OPEX prices [57].
7. A discount rate (real) of 4% is assumed, which is the average between a high and low discount rate assumed for commercial systems [59].

Due to the experimental nature of most of the ZBFB applications currently, their costs are relatively high when compared to more mature battery storage technologies, these costs are projected to decrease by almost 66% by 2030 [95]. The inputs of capital cost and O&M costs were obtained from TNO's technology factsheet, with projections made for 2030 [68], and can be found in table along with a summary of the costs for the PV system 2.9:

	Value	Unit
Discount rate[13]	2 [59]	%
PV system		
Decrease in CAPEX	2.6[59]	%/year
$CAPEX_{(2019)}$[14]	320[96]	€/kW_p
$CAPEX_{(2030)}$	239.5	€/kW_p
OPEX	2[57]	%
System lifetime	25[59]	years
BB system		
CAPEX	338[68]	€/kWh
OPEX	2[68]	%
Lifetime	10[68]	years

Table 2.9: Summary of assumptions made for PV system LCOE calculations, the starting values from 2019 to the inputs used for 2030. The OPEX is a percentage of the CAPEX, and is paid per year.

[14]This CAPEX is turnkey costs, and thus includes BoS and installation costs.
[13]As the investment is made by the university, a low discount rate can be assumed due to their public nature in the Netherlands.

3 — Control algorithm designed

Two distinctive types of control approaches exist for the control of a microgrid: centralised and decentralised. Completely centralised control involves collection and processing of data from all system units, identifying the actions needed to be performed by each unit and communicating the actions to be executed by the units it is controlling. This requires extensive and quick communication relays between all participating members for the smooth and robust functioning of the microgrid. On the other hand, a completely decentralised microgrid is where each unit acts of its own accord, collecting, processing and interpreting the local data and executing actions based only on local conditions (i.e.) without system-wide awareness of what or how the other units are performing. Hierarchical control lies between centralised and decentralised control; where there exist local controllers and centralised controllers. The former enable the smooth functioning of the individual components where decisions need to be made in the span of seconds, while the latter receives information from the local controllers and coordinates all units at a larger scale. This relay of information occurs in larger time scales, spanning up to a few minutes. Tsikalakis et. al note that in order to experience the benefits of a microgrid like enhanced reliability, reduced emissions, improved power quality, reduced energy costs, it can only be provided by a more decentralised system that can make decisions locally to manage supply and demand; especially in cases where there are multiple sources, loads and interaction with the utility grid. A hierarchical control strategy (HCS) also contributes to the ideal operation and interaction between low voltage (LV) and medium voltage (MV) networks [32].

As the UCM is designed to rely on the utility grid at certain times but also be self-reliant at other times, it is beneficial to implement an Hierarchical Control Strategy (HCS). It is assumed that each of the microsources will have a controller that ensures the optimal operation. An HCS is necessary for a university campus where each unit is at a distance from one another, and sometimes local decisions need to be made and quick response times is important to ensure security of supply. Within hierarchical control there are three crucial levels, namely primary, secondary and tertiary control.

Energy Management System

Secondary control, or in other words, an Energy Management System (EMS), is the topic of interest in this report. The EMS is the control strategy that ensures the safe, reliable and robust overall operation of this UCM by regulating the power flows between different sources and loads. Each DER is equipped with a microsource controller (Micro Source Controller (MC)); their function is to the control the voltage and frequency in transient conditions, based on available data collected at the local point [32]. This type of control is termed primary control, wherein the local controller makes decisions and optimizes the DER for transient states. This class of control is extremely important to maintain voltage and frequency stability, it is also out of the scope of this report.

The fundamental concept of the UCM is as follows: deploy the PV system and FCEV fleet during the day to meet demanded electrical load, while utilising the battery and the main utility grid to meet demand at night. This combination of the battery and utility grid is adopted as the author was curious to understand whether a balance could be found between battery costs and grid dependence while still providing high security of supply for the load at night. A factor to consider is that due to electrification, there are higher electrical loads during the colder months of the year when there is low solar insolation in the Netherlands (as seen in figure F.3. This implies two things: one that the PV generation during winter might not be sufficient to meet the load during the day and two, the occurrence of excess generation is rare in those months, so that battery will not be sufficiently charged to meet the full load at night. Hence using the FCEV fleet to balance the supply and demand during the day complementary to the PV generation, while the BB and the distribution grid are utilised at night to meet the load.

Two control strategies were formulated for the EMS with one major variant between them, how the BB is utilised at night:

1. **SSB:** it is based purely on the demand of the load and battery SoC available (at night). Its primary goal is to increase self-sufficiency at all times.
2. **PB:** is based on decreasing the price for the electricity bought from the wholesale market. It shifts the BB utilisation based on grid prices, meaning if the control deems the electricity price at a given time to be too expensive, it discharges the BB, else it uses the grid. To understand if the price at a given time is "too high", the daily average price is calculated at the beginning of each day based on the day-ahead market prices. The main goal of this control is to decrease cost of energy when compared to the reference baseline amounts paid to the distribution grid in 2030.

Both controls fall under dynamic power flow control strategies, as defined by Muhlbauer et al. [97], due to the fact that the amount of power made available to be used by the UCM is a combination of the BB power output which is dependent on the SoC, the available energy of the FCEVs and the constantly changing PV generation.

The EMS with its power flows was designed, simulated and analysed in Simulink and Matlab respectively. Some of the simulation attributes to be noted are listed below:

1. The simulations are run for an entire year for 15-minute time-steps.
2. The SoC of the ESS is set to 100% at the beginning of the year.
3. The average price of electricity from the utility grid in 2030 will be 57 €/MWh. Price fluctuations are modelled based on the method described in section 2.6.
4. Dynamic security issues were not considered, though they are an important and integral part of switching between islanded and grid connected mode.
5. The order of deployment of the PV and CaPP in both strategies is the same in both cases during the day.

3.1 Self-sufficiency based

As the name suggests, this control algorithm's main goal is to meet the demand at any given time and to increase self-sufficiency. There are various reasons to increase self-sufficiency, the ones that pertain to this report are summarized below:

1. Reduced CO_2 emissions from electricity consumption.
2. Self-sufficiency and self-consumption have been shown to contribute to general trends in efficient energy usage as consumers take responsibility for their energy consumption and production [98].
3. Creating areas for self-sufficiency relieves the strain on the distribution grid that is slowly arising due to the increasing feed-in of renewable energy [98]. Studies have shown that by using demand response and storage, integration costs could be decreased by almost 20%.

Own-consumption (or self-consumption) ratio (Own-consumption Ratio (OCR)) in this report is defined as the quantity of electricity that is produced on-site that is consumed directly by the load and not injected into the distribution grid or curtailed. In equation 3.3, the power produced and consumed from the FCEV fleet is also included despite the hydrogen not being produced on-site. To fully comprehend the effects of using an FCEV fleet the results from equations 3.2 and 3.3 need to be compared. The self-sufficiency ratio (SSR) gives insights into the energy flows in the UCM, with regards to the quantity of the total load that is supplied by the PV system, BB and the FCEV fleet.

Self-sufficiency ratio of the PV system (SSR_{PV}) and own-consumption (OC_{PV}) are calculated using equations 3.1 and 3.2. SSR_{PV} is different from the total SSR of the UCM as the former does not include the utilisation of the FCEV fleet.

$$SSR_{PV}[\%] = \sum^{year} \frac{E_{PV,direct} + E_{PV,indirect}}{E_{L,year}} \times 100. \tag{3.1}$$

$$OC_{PV}[\%] = \sum^{year} \frac{E_{PV,direct} + E_{PV,indirect}}{E_{prod,PV}} \times 100. \tag{3.2}$$

Where,

- SSR_{PV} is the self-sufficiency ratio only considering the on-site PV generation [%],
- $E_{PV,direct}$ is the sum of the total annual PV electricity that is used directly to meet the load, without feeding into the grid [kWh/year],
- $E_{PV,indirect}$ is the sum of the total annual PV electricity that is used indirectly (i.e.) via the BB system [kWh/year],
- $E_{prod,PV}$ is the sum of the total annual electricity produced by the PV system [kWh/year],
- $E_{L,year}$ is the sum of the total annual electricity demanded (including heating) [kWh/year].

The OCR and SSR maybe be written mathematically as follows:

$$OCR(\%) = \sum^{year} \frac{E_{PV,direct} + E_{PV,indirect} + E_{cons,FCEV}}{E_{prod,PV} + E_{prod,FCEV}} \times 100. \tag{3.3}$$

$$SSR(\%) = SSR_{PV} + \sum^{year} \frac{E_{cons,FCEV}}{E_{L,year}} \times 100. \tag{3.4}$$

Where,

- $E_{prod,FCEV}$ is the total annual electricity produced on-site by the FCEV fleet [kWh/year],
- $E_{cons,FCEV}$ is the total annual electricity consumed from the FCEV fleet [kWh/year],
- $E_{PV,direct}$is the sum of the total annual PV electricity that is used directly by the load [kWh/year],
- $E_{PV,indirect}$ is the sum of the total annual PV electricity that is used indirectly (i.e.) via the BB system [kWh/year],
- SSR_{PV} is the self-sufficiency ratio of the direct and indirect PV annual energy to the annual load demanded [%],
- OCR
- $E_{L,year}$ is the total annual electricity demanded [kWh/year].

A point to note in equation 3.4 and 3.3 is the inclusion of the FCEV energy. Though in order to calculate the contribution of the UCM system components, it is necessary to assume that despite the hydrogen being consumed has been produced off campus, the power used is produced on-site.

Current demand forecasting models are able to predict energy demands based on weekly, seasonal and annual time scales, a prediction model can be used based on the time scale required; though never with 100% accuracy. Thus, it is safe to assume that the EMS would be able to predict the demand for up to at least a week and a year but the closer to the time period the predictions become more accurate. Contracts can be made with the energy retailer for the demand that will need to be met in the future between the parties in question, with the predicted demand that is going to occur that the UCM will not be able to satisfy through on-site generation.

The sizing of system components was based on increasing self-sufficiency to its maximum degree while also taking economical parameters into consideration. This sizing approach is discussed in detail in section 4.1, and is based on the equations 3.1 - 3.4. The control of the EMS is built to maximise self-sufficiency at all times, wherein the on-site generators and storage are prioritised over buying from or selling to the grid. Each time-step the EMS re-calibrates whether the on-site generators are being used in the best possible way, by calculating P_{Diff} and P_{res} (the residual load). If the power output of the PV system is greater than zero, then depending on the status of P_{Diff} either the BB is charged or the FCEV fleet is utilised. In figure 3.1, each block leads to individual sub-blocks for charging/discharging the BB or utilising the FCEV fleet. The charging and discharging blocks are not the battery management system (BMS) but rather the EMS's method of communicating with the BMS.

The basic working of the control is described in the flowchart in figure 3.1, where,

- $P_{pv}(t)$ is the AC power output of the PV system (after losses) at time-step t [kWh/15 mins],
- $P_{load}(t)$ is the load demanded at t [kWh/15 mins],
- $P_{res}(t)$ is the residual load in at t [kWh/15 mins], where it is any load remaining after all the PV energy generated in that time period is consumed.
- $G_m(t)$ is the irradiance on the solar module at t [W/m^2],
- $Q(t)$ is the available capacity of the BB at t [kWh/15 mins],
- $W_{avail,FCEV}(t)$ indicated the availability of FCEVs each day within a given time window. It is either 0 or 1,
- $Q_{max}(t)$ is the maximum possible capacity of the BB at t [kWh/15 mins].

Each of the blocks described are colour coded, and the same colour scheme is followed through the rest of the report whenever their respective components are referred to. The night block is only colour coded to clarify the distinction in times of day between the processes that are carried out. Figure 3.1 represents the algorithm for the SSB control, while the following figures 3.2-3.3 are common for both controls.

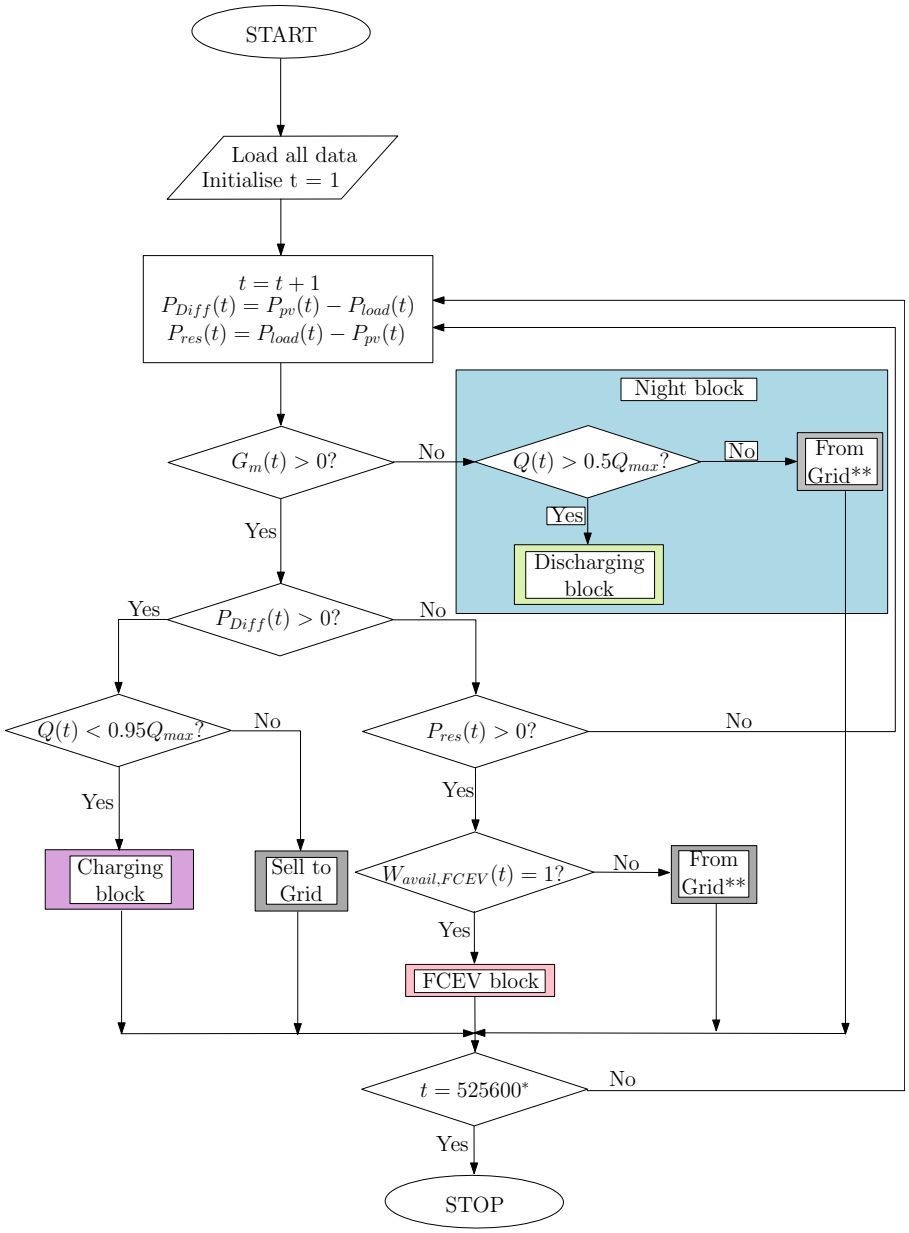

Figure 3.1: Flowchart depicting the SSB control strategy implemented. The outputs of each block (FCEV block, charging block, etc.) are elaborated on below and all have their outputs of their block following the arrows depicted here.(* - 525600 signifies the number of minutes in the year.

3.1.1 Charging block

This block is enabled by the incoming charge power, that is the excess of the PV generated, and may also be identified as the positive P_{Diff}. Thus this block identifies the charge current that will be input into the KiBaM simulate the response of the BB. In figure 3.2,

- $P_{BB}(t)$ is the BB power/available charge at t [kWh/15 mins],
- $P_{sold}(t)$ is the power sold to the distribution grid at t [kWh/15 mins],
- P_{max} is the the maximum capacity of the BB [kWh],
- P_C is the charging power at that given t [kWh/15 mins].

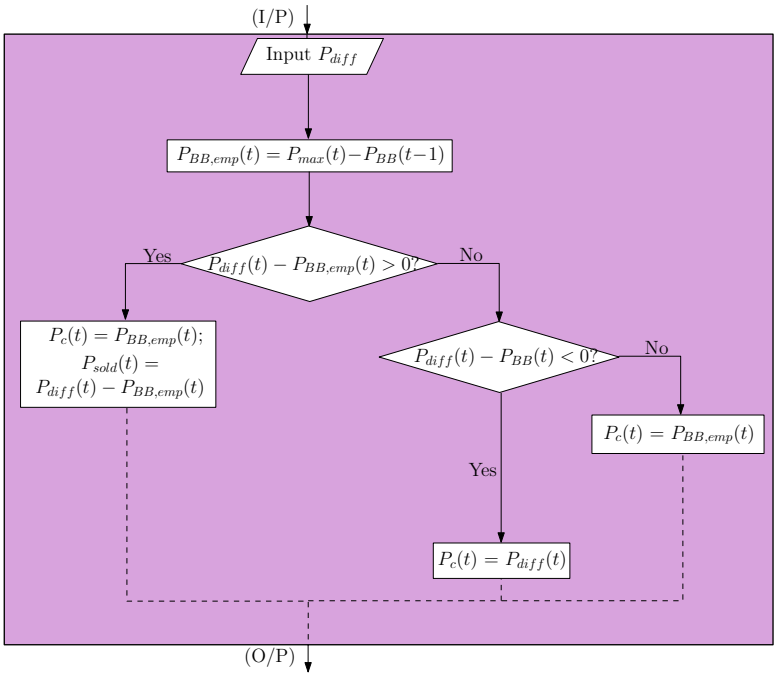

Figure 3.2: The internal workings of the charging block. The dotted lines represent the outputs that flow out of this block, but not all outputs are ON at the same time; at a given time t, only one of the outputs are passed on to outside of this block. I/P and O/P signify the input and output respectively.

3.1.2 FCEV block

The FCEV block of the UCM utilises the hydrogen pool created using the steps in figure 2.10. The hydrogen pool was created independent of the EMS in order to simulate a realistic hydrogen profile for a year. It is assumed that every four hours the FCEVs will be changed, (i.e.) FCEVs whose fuel was used are switched with those FCEVs that were not yet used in that day. This is done as a safety to maintain a minimum SOX and to replenish the hydrogen pool in case of days of high FCEV fleet utilisation. A point to note is that due to the distribution of the SOX created through the day, and to maintain the validity of this distribution used, this resetting of the hydrogen pool was necessary. Thus, an internal time counter, k, is created as a signal to enable the "switch" of FCEVs (or resetting the hydrogen pool). In figure 3.3,

- $P_{H_2,tot}(t)$ is the total hydrogen power available in the hydrogen pool after power limitations at the V2G terminals are accounted for at t [kWh/15 min],
- k is an internal time counter. It increments at the same t is incremented in every iteration, and is reset when 4 hours have passed. Due to the nature of the H_2 profile, such a mechanism was necessary to simulate new car arrivals.

- $P_{H_2,rem}(t)$ is the remaining hydrogen in the pool at t [kWh/15 mins].

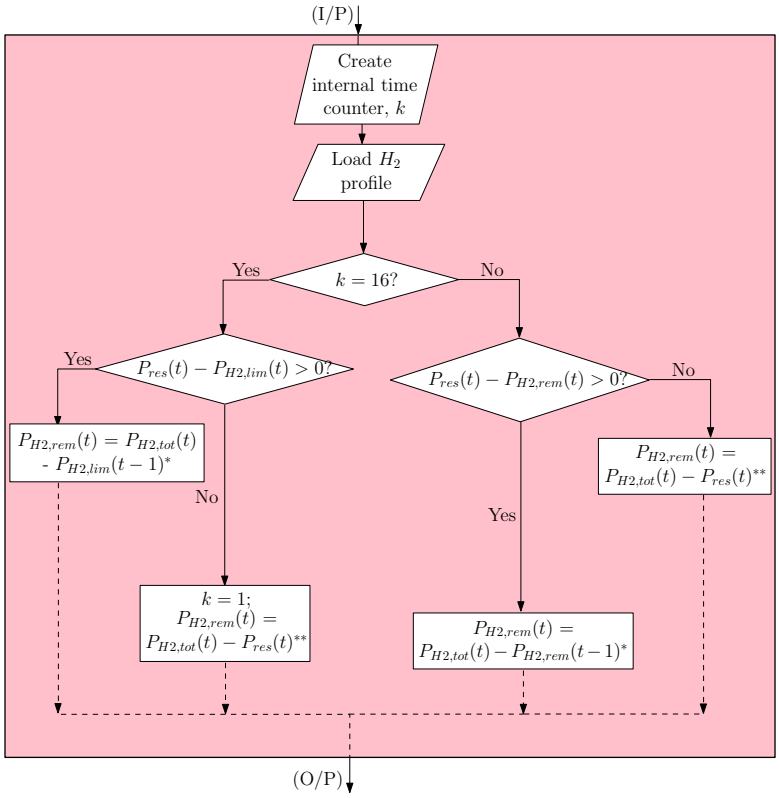

Figure 3.3: The internal working of the FCEV block. There is only one input and output to and from this block, the dotted lines represent that either one of those outputs could be passed out of the block. (* - P_{res} met partially by grid; ** - P_{res} met fully/partially met by the FCEV fleet.

3.1.3 Discharging block

In a similar manner to the charging block, the discharging block defines the discharge current. For the input, the P_{res}, to be enabled to enter the block the irradiance should be equal to zero. Another output of this block is the amount of power needed to be provided by the utility grid. This could either be due to the c-rate of the battery or the lack of available capacity to meet the load.

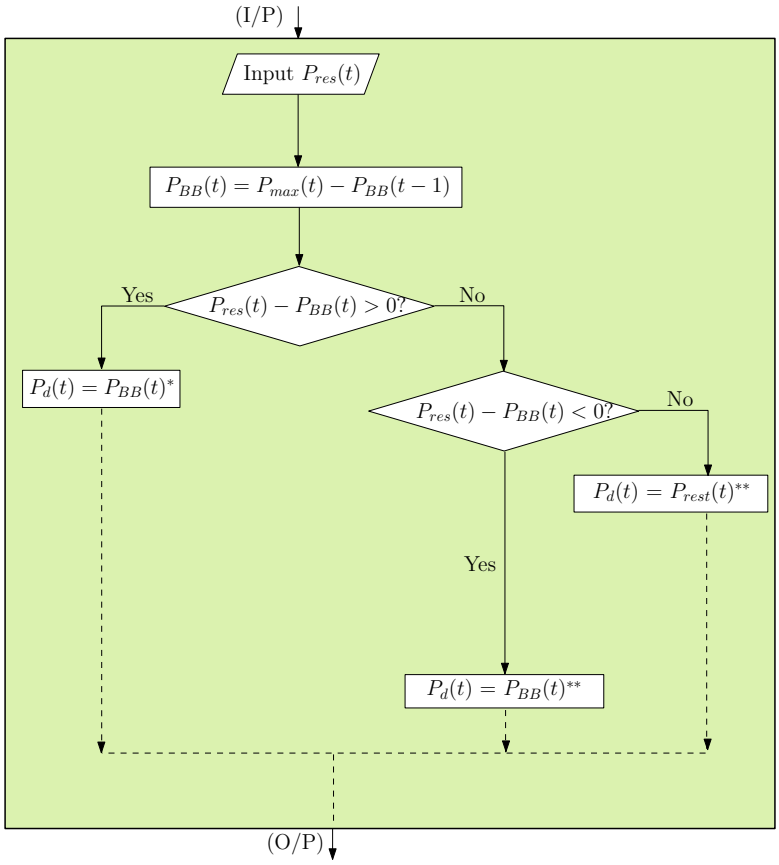

Figure 3.4: Internal mechanism of the discharging block. $(^{(}*)$ - P_{res} met partially by BB; $^{(}*)$ - P_{res} met by grid.

The control in this strategy prioritises meeting the load using the UCM before relying on the grid, this can be seen in figures 3.5 and 3.6. In both figures, the consumption of power depicted is using the negative y-axis, while the production is depicted using the positive y-axis. One must also note that, P_{load} is the original load that is needed to be met, while P_{res} is the residual load after the share that is met by the PV system is removed. This is to give clarity as to the quantity of load yet to be met by either the other components of the microgrid or the main grid. Furthermore, one can differentiate between day and night time loads easily by looking for a peak, typically one week's load curve would depict five peaks two days of relatively constant consumption (indicating the weekend).

Figure 3.5 depicts a example day in winter, as there is a slight excess in PV generation, the BB is charged. The components sizing is discussed in the following chapter, and this depiction is to give the reader a visual representation of the working EMS. Furthermore, the BB charging is depicted in purple and on the negative y-axis, while the corresponding increase in BB SoC can be seen in figure 3.5b. As can be noted, the BB does not reach 100% SoC, this is to be expected for most of the winter months (with some exceptions). Furthermore the BB is discharged during night time, which is triggered by the lack of solar irradiance, this is clearly visible when one looks closely between 17h to 18h in the figure. Meanwhile, the FCEVs are primarily used during the late afternoon and early morning times, when there is low PV production, but there are days when they are used through the day if PV generation is exceptionally low. In the figure 3.5 there is no hydrogen power illustrated, due to the day depicted being a holiday. This can also be corroborated by the relatively low peak

in load during daytime for winter time.

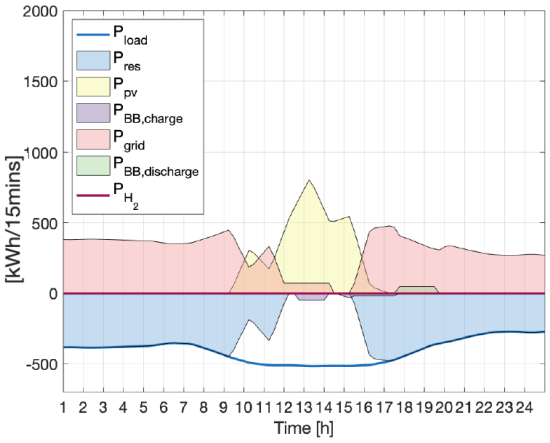

(a) Demonstration of control implementation for a example day during winter.

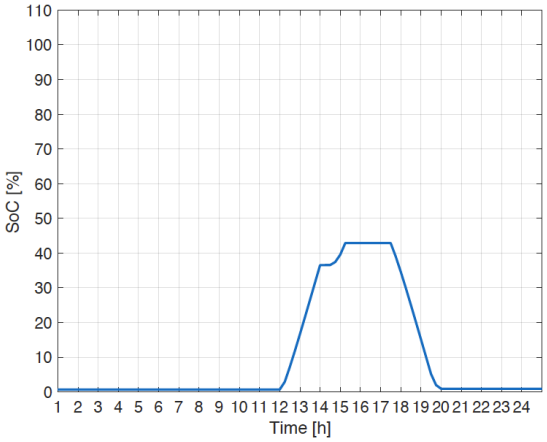

(b) Corresponding BB SoC response.

Figure 3.5: Example winter day's demonstration of the SSB control. The minimum set for BB SoC is $0.05Q_{max}$, hence the SoC not reaching 0%. All labels used in this plot can be correlated to power values deocribed in the SSB control flowchart depicted in figure 3.1.

When comparing figures 3.5 and 3.6, it is evident that the quantity of available PV energy is relatively larger in the latter figure. The BB reaches 100% SoC during the day, there is FCEV usage seen during early morning and evening hours. Following which, after sunset, the BB can be seen to have a longer discharge duration than in the winter depiction. Though it discharges through the night, dependence on the grid is also required due to the c-rate limitation that was applied.

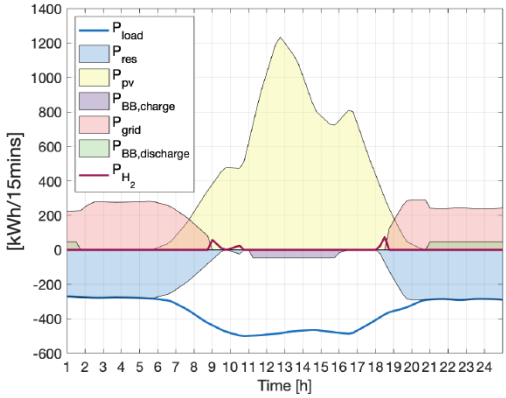

(a) Demonstration of control implementation for a example day during summer.

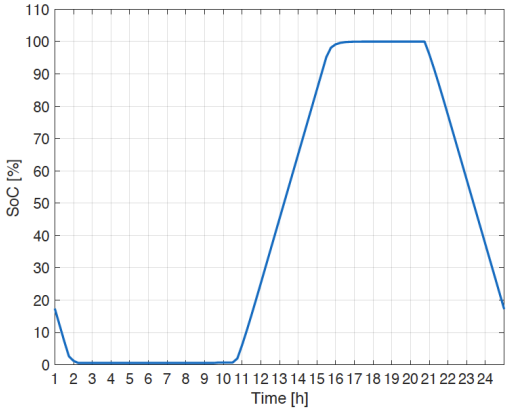

(b) Corresponding BB SoC response.

Figure 3.6: Example summer day's demonstration of the SSB control.

3.1.4 Grid utilisation

Through the year the dependence on the main grid sees a seasonal variation, where in the summer months grid dependence is relatively lower than in the winter months. One could argue that since the consumption is also lower in the summer when compared to winter, the grid dependence is thereby automatically lower. But when comparing figures 3.7a and 3.7b power taken from the grid during the day is considerably lower. This can be mainly attributed due to the increased PV generation and the lower load during the warmer months of the year. In addition to these observations, in figure 3.7 one may note the rapid fluctuations in the power extracted from the grid, this is due to the portions of the load being met by the FCEV fleet. If a low quantity of hydrogen is available during that day, such sporadic fluctuations become more evident when they correspond to low PV generation times.

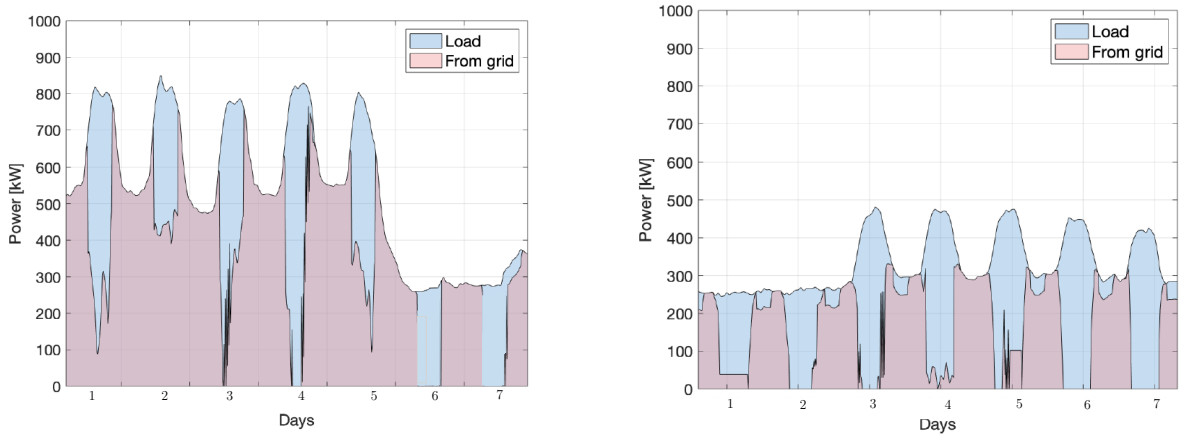

(a) Winter.

(b) Summer.

Figure 3.7: A week's demonstration of grid utilisation in the winter and the summer.

3.1.5 PV and FCEV fleet utilisation

In figure 3.8, a seasonal comparison is made between the availability of PV energy, BB charge and discharge and the FCEV fleet utilisation for example weeks chosen in winter and summer [30]. A clear indication that FCEVs are used majorly in the winter months in depicted in figure 3.8a. Furthermore, one can infer from the flat curve of the P_{h_2} on the fifth day, that a large quantity of hydrogen is available and used. The flatness is due to the limitation set by the V2G terminals at 9.5kW per terminal. Meanwhile during the warmer months, the FCEV usage is lower, while the charging and discharging of the BB is higher.

[30]It must be noted that the weeks for grid utilisation and PV, FCEV utilisation are not the same.

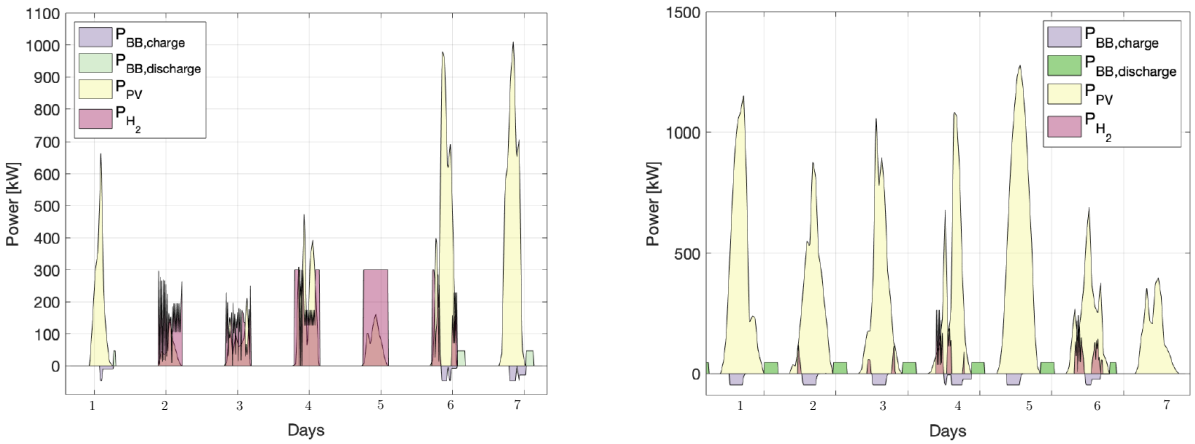

(a) Winter.

(b) Summer.

Figure 3.8: A week's demonstration of variations in the PV, BB and FCEV fleet utilisation in the winter and the summer.

3.2 Price-based

The difference between the non-price-based and price-based control is that the latter utilises the battery based on the market price of electricity at that point in time of night. This is highlighted in red in figure 3.9. This control uses the price profile built as described in section 2.6 and correlates it to the day-ahead market prices to decide whether the utility grid can be relied upon or not. A certain threshold is set by the system for each day, based on the mean electricity price of that day, so when the utility price of electricity is higher than this threshold the EMS deems the electricity from the main grid too "expensive" and uses the BB to meet the load instead. Another advantage to this method apart from cost reduction on the side of the prosumer, is that at times of high prices one may assume one of two things: a) the high price is an indication of a shortage of electricity in the distribution grid or b) that there is high demand and thus the demand cuts the supply curve at a point in the higher priority order range. Thus it is beneficial also from the distribution grid side where the UCM could be relieving possible network congestion [32].

The primary goals of the PB control strategy listed in order of relevance to the control:

1. Create a cost-effective balance between using the BB and the utility grid at night.
2. Minimize cost paid to grid as much as possible.
3. Increase self-sufficiency.

With the presence of the Day-ahead in the Netherlands the price of electricity for the coming day is released 24 hours ahead of time. The Day ahead market gives a good overview of what the prices on that day will be 24 hours ahead of time, so the EMS can calculate the mean for the day before-hand and avoid the grid electricity if it deems it too expensive. The grid is not used to charge the BB during low price times so as to keep the SSR only inclusive of energy produced on-site.

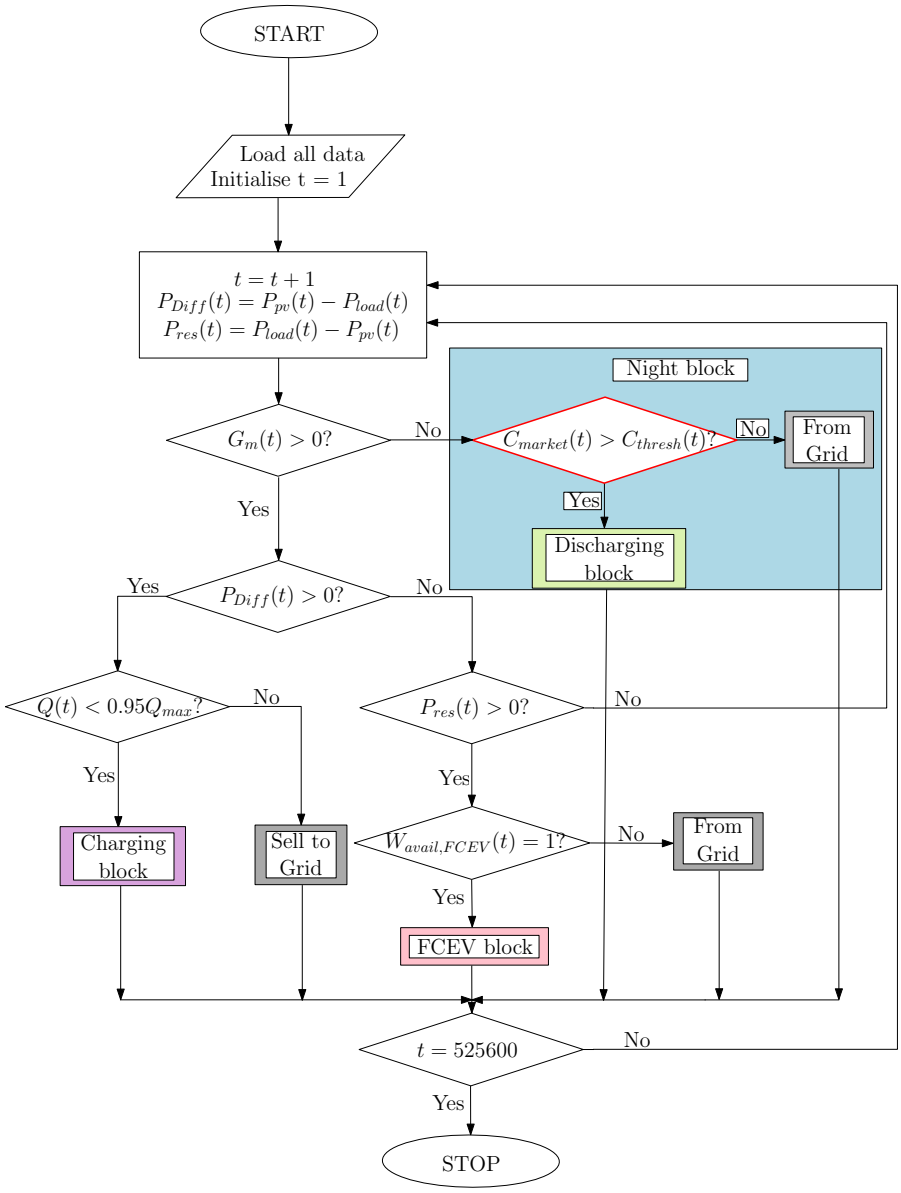

Figure 3.9: Flowchart depicting the non-price based control strategy implemented. C_{market} and $C_{threshold}$ refer to the wholesale market electricity price and the price threshold for that day respectively. The internal workings of the charging, discharging and FCEV blocks remain the same as in the price-based control.

- $C_{market}(t)$ is the market price of electricity at given time t [€/kWh],
- $C_{threshold}$ is the daily price threshold set by the EMS [€/kWh],

Figures 3.10 and 3.11 give an overview of the working of the PB control, the price signals needed to discharge the battery are also shown [31]. When C_{market} exceeds $C_{threshold}$ it indicates to the EMS that the price is too "high" and thereby it discharges the energy stored in the BB instead. This control does not aim to decrease dependence on the grid, but rather the cost of electricity paid to the grid, thus an almost sporadic BB utilisation

can be seen in later figures.

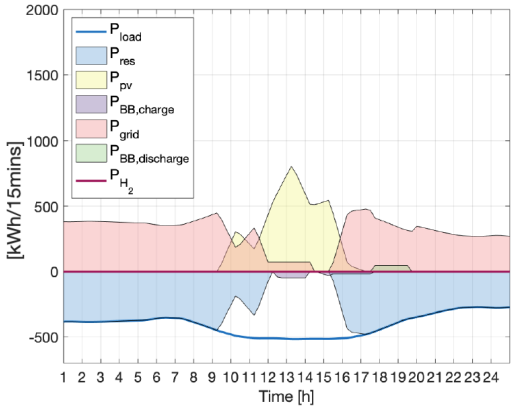

(a) Demonstration of control implementation for a example day in winter.

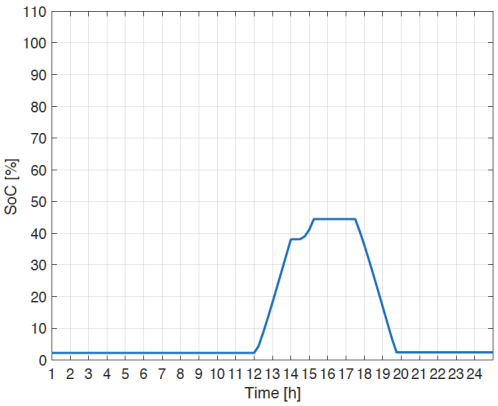

(b) Corresponding BB SoC response.

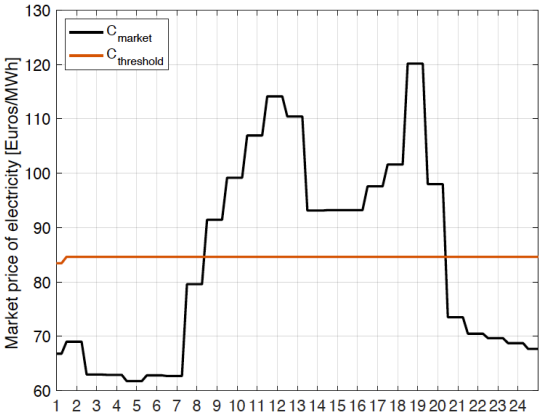

(c) Corresponding wholesale electricity prices.

Figure 3.10: Example winter day's demonstration of the PB control, one may note that the BB is used sporadically, coinciding with the spikes in prices that go higher than the threshold.

The summer utilisation of the control is depicted in figure 3.11, it is interesting to note that for the same summer day of both controls in SSB and PB, the SoC of the BB behaves differently. The price signals needed for the BB to discharge do not allow the BB to discharge completely at all times, whereas in the figure 3.6 the BB was charged and discharged to its full capacity [32].

[31] Both figures are plotted for the same days as in SSB to give the reader a basis to compare the controls.

[32] The inability of the BB to be discharged completely may be viewed as a drawback of the PB control in a way. As some battery technologies have the tendency to create a memory effect, which inadvertently decreases the capacity available. Thus, for this control to be beneficial, care must be taken to choose the right battery technology.

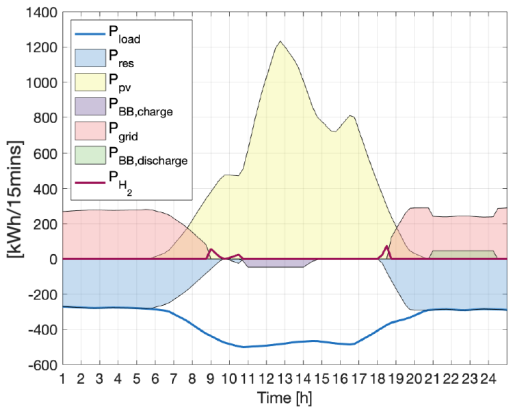

(a) Demonstration of control implementation for a example day during summer.

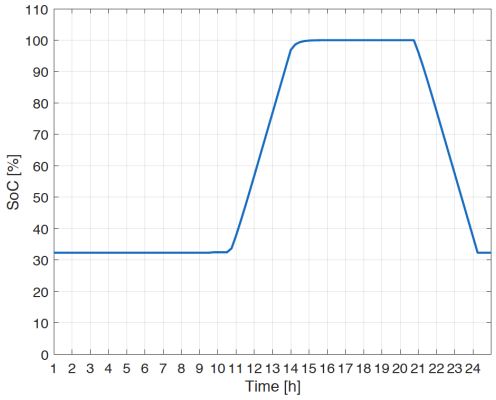

(b) Corresponding BB SoC response.

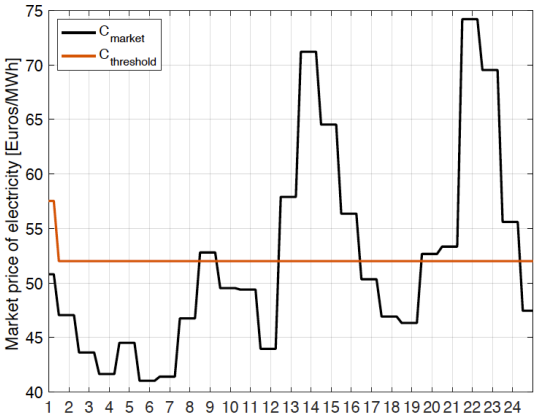

(c) Corresponding wholesale electricity prices.

Figure 3.11: Example summer day's demonstration of the PB control.

3.2.1 Grid utilisation

In the figures below, one can see the comparison in grid reliance based on seasonal variations [33]. It is evident from figure 3.12a that the BB usage at night time in winter is almost non-existent. This can be inferred from the complete grid dependence seen during the night time. When one compares this to the figure 3.12b, small portions of the power taken from the grid can be seen to be missing. This is the energy that is supplied by the battery, due to price signals that indicate "high prices" to the EMS.

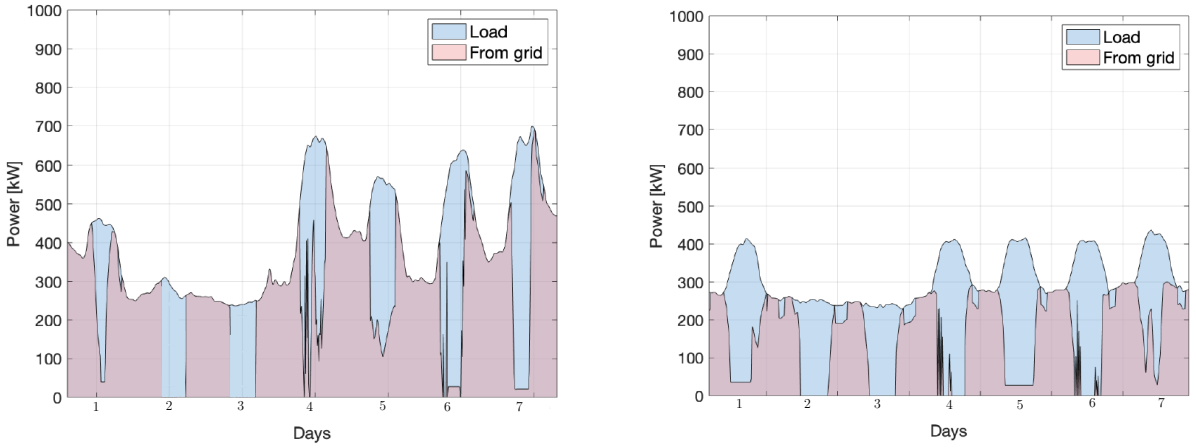

(a) Winter.

(b) Summer.

Figure 3.12: A week's demonstration of grid utilisation in the winter and the summer.

3.2.2 PV and FCEV fleet utilisation

In figure 3.13, a seasonal comparison is made for PV generation, BB and FCEV utilisation correlating them to the price signals for the EMS. The points to note are the durations of discharge of the BB that correspond to the times of "high prices". The discharge durations a relatively and distinctly smaller when compared to the SSB control. The difference in the winter months between SSB and PB are minor due to the lack of excess PV energy to discharge. So the major differences can be viewed in the summer months. On the other hand, FCEV utilisation remains unchanged between the two controls.

[33]Note that the weeks plotted here are not the same as in the grid utilisation of the SSB section.

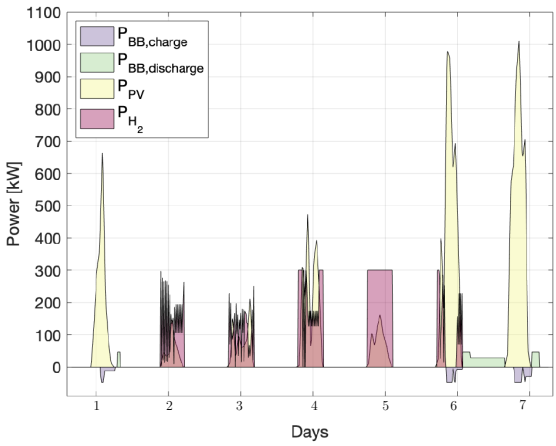

(a) Winter.

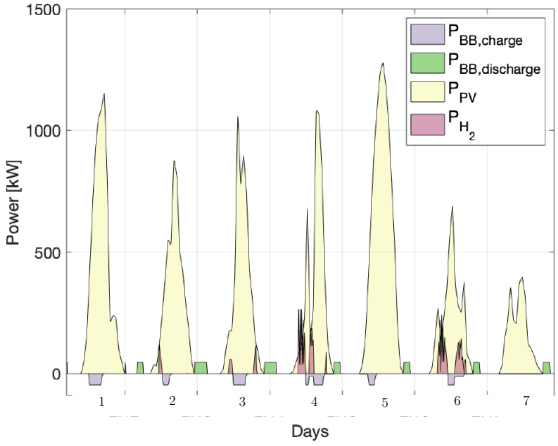

(b) Summer.

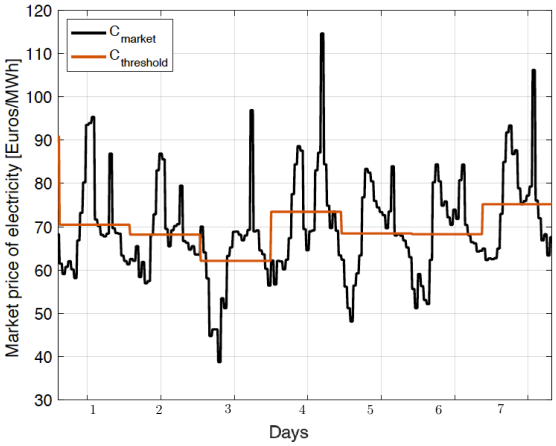

(c) Corresponding price profile in the winter week.

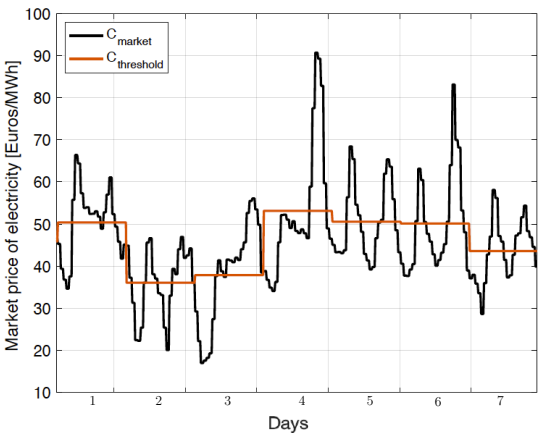

(d) Corresponding price profile in the summer week.

Figure 3.13: A week's demonstration of variations in the PV, BB and FCEV fleet utilisation in the winter and the summer and the price signals that the trigger the BB discharge at night.

4 — Simulation Results and Discussion

The results of the simulations, metric formulation and analysis, comparison of the different scenarios outlined in the previous chapters are delved into this chapter. The first part of this chapter details the analysis of the DER indices followed by an assessment of the economic indices, how do the baseline scenarios compare to the scenarios where the control is being used and what is the levelized cost of electricity for each of the elements proposed to be used in the UCM. Parallels are drawn from graphical analysis of the simulated results.

4.1 System sizing results

A common objective between both controls is to increase the self-sufficiency. Due to the PB control's goal is to decrease the costs paid to the grid as well. This entails different sizing approaches for the BB for each of the controls, while the PV and FCEV fleet size remain constant. Furthermore, if the BB utilisation changes, the indirect utilisation of the PV energy by the load also changes accordingly. Thus, it is important to understand the effects of varying BB and PV system sizing. This section details the method of sizing the PV and BB system, while also providing justifications for the size of the FCEV fleet. The size of the FCEV fleet refers to the number of FCEVs used to provide backup generation.

4.1.1 PV system

The sizing of the PV system is based on the energy balance paradigm and this size is cross-checked using the technical potential to ensure sufficient roof area is available, as was discussed in subsection 2.3.2. The balancing of the demand and production can be done in multiple ways, three approaches were simulated using the paradigm to understand the full extent to which the additional heating load impacts system sizing. First, as the winter load is relatively higher than the summer load, only the winter demand with the power output of the array during winter were balanced, to arrive at an PV array size A1. The second approach was to balance the entire year's load with the annual PV generation, resulting in an array size A2. Due to insufficient roof area, A1 and A2 were too large to be technically feasible. The third approach was to create a basis of understanding of the impact of heating, and so only the original annual electric profile was used to balance for the whole year, termed A3. A3 is only meant to offer a comparison and is not a true sizing at all. As the results of the energy balance paradigm resulted in array sizes too large for the roofs to host, the final sizing is based on the technical potential area available using equation 2.9, arriving at the final array size of A4. A summary of each sizing approach are summarized in table 4.1. Furthermore, in order to understand the fraction of TSCoE, SSR and OCR for varying PV array sizes, the array size was iteratively increased from $375kW_P$ to $3MW_P$ for both control strategies. While running these simulations, the size of the BB and FCEV fleet were kept constant, at 100kWh and 30 V2G terminals respectively, to understand the effects of only changing the size of the PV system.

	A1	**A2**	**A3**	**A4**
Rated power [MWp]	11.2	2.9	1.5	2.1
Number of panels	31,932	7,823	3,958	5,503

Table 4.1: The resulting PV system sizes for the two balances proposed (based on annual load and winter load).

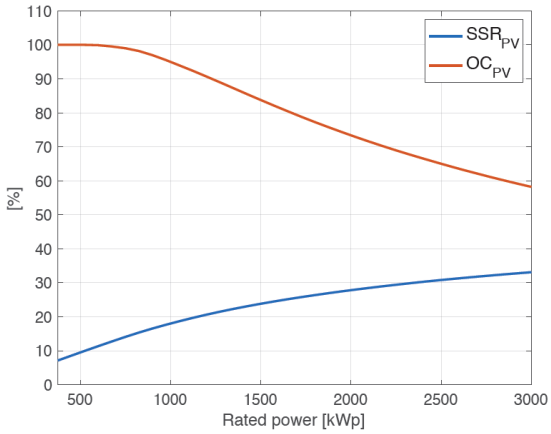

(a) Comparing the SSR_{PV} and OC_{PV} for SSB control.

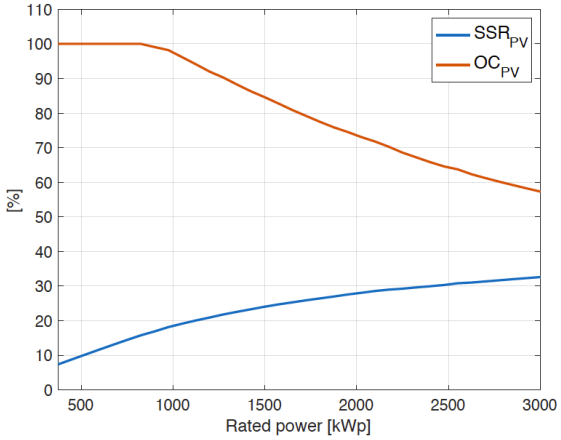

(b) Comparing the SSR_{PV} and OC_{PV} for PB control.

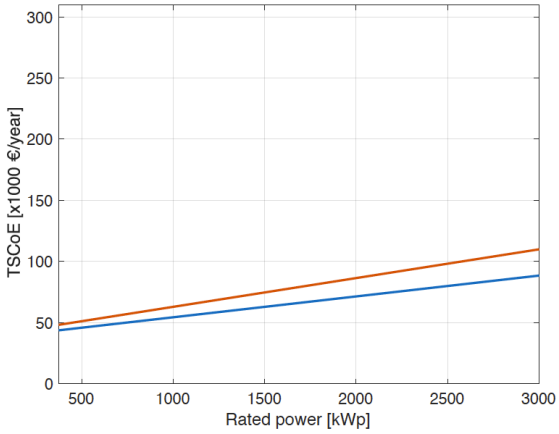

(c) Corresponding total system cost of electricity for PB control.

Figure 4.1: Comparing self-sufficiency ratio (SSR_{PV}) and own-consumption ratio (OC_{PV}) calculated for increasing rated power of the PV system for both controls. Note that the ratios and the total system cost of electricity (TSCoE) are calculated using equations 3.1, 3.2 and 2.23 respectively.

When analysing figure 4.1, one may note the gradual decrease in OCR, the slope of the SSR, all while the TSCoE increases linearly. It is evident that at smaller rated power of the PV system the OCR of the system decreases from 100%, this is to be expected as the smaller amount of energy produced from the system, the more likely it is that it will all be consumed (directly or indirectly) by the load. As this is a ratio of the total PV energy consumed by the total PV energy produced, at higher rated powers the likelihood of all the PV generation coinciding with the consumption is less and less likely; especially given the larger loads are consumed during the colder months. Simultaneously, the SSR increases linearly with the increase in rated power of the system, this is a consequence of the consumption increasing but the annual load summed remaining the same. Meanwhile the slope of the SSR is not steep, indicating that large changes in the rated power will not see enormous impacts in the self-reliance of the university campus, but will result in higher costs. Furthermore, in order to increase the SSR_{PV}, other areas would need to be harnessed. For example, utilising the nearby car parking areas to install PV modules. The TSCoE does not change between the two controls as it is calculated

using the rated power of the system.

4.1.2 Battery sizing

The sizing of the BB was implemented using the SSR, where the number of modules in the BB was iteratively increased while calibrating the SSR at each instance. Figure 4.2 depicts this iterative increase and corresponding SSR and OCR.

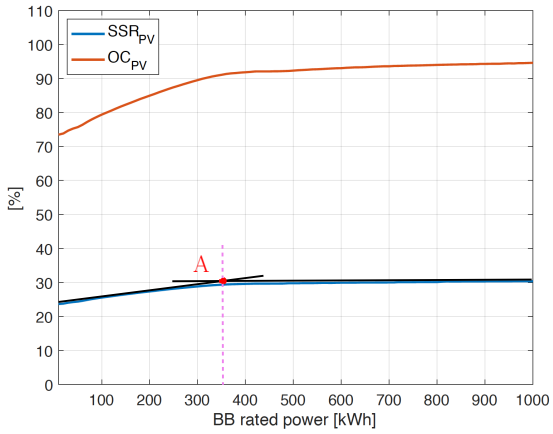

(a) Comparing the SSR_{PV} and OC_{PV} for SSB control.

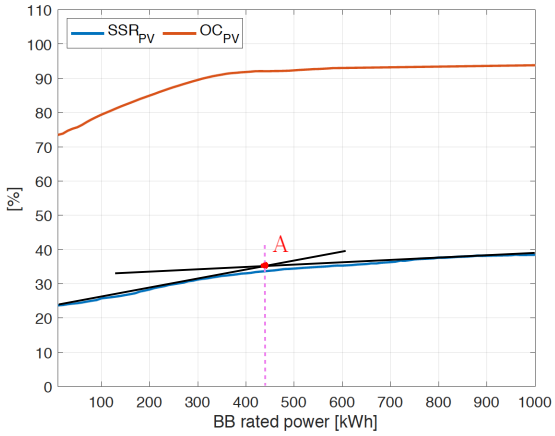

(b) Comparing the SSR_{PV} and OC_{PV} for PB control.

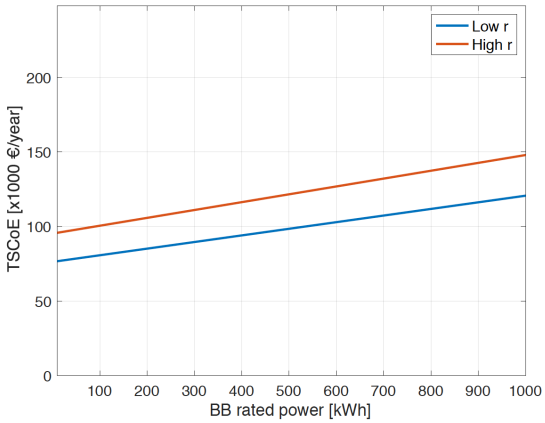

(c) Corresponding total system cost of energy for PB control. Note that this is the sum of the TSCoE and cost paid to the grid, calculated using 2.28.

Figure 4.2: Comparing self-sufficiency ratio (SSR_{PV}) and own-consumption ratio (OC_{PV}) calculated for increasing rated capacity of the BB system for both controls.

One important point noted while sizing the BB system were that if the BB size was increased past a certain rated capacity, its full capacity was not utilised through the whole year. Meaning that it did not reach 100% DoD during the summer months and did not charge to 100% SoC during the winter and some fall months,

[22]High and low r in both TSCoE plots are the high and low discount rates of 2% and 6% respectively.

thereby not utilising its full capacity for storage. Thus, two sizes are chosen for the BB system, one based on the best capacity utilisation of the BB (termed S1), and the other based on the best[33] SSR (termed S2) based on figures 4.2a and 4.2b. For S2, the optimum[33] is indicated by the point A, at the intersection of the tangents to the SSR curves. Two sizes are chosen to indicate how the system responds to these extreme sizing approaches. Detailed comparisons are made in subsequent sections to analyse the costs and the PV utilisation for both sizes.

In both figures, 4.2a and 4.2b after a certain point the increase in SSR and OCR is negligible. This implies that the marginal utility of each additional unit of capacity added does not increase by a large factor. Indicating that after point A, any additional capacity added will not provide the benefit for the increasing costs paid. Further information of such effects can be found in other papers, where the diminishing returns with increasing battery capacity is studied [99] and [50]. A summary of the final BB sizing results is given in table 4.2.

	S1	**S2**
ssb control [kWh]	50	350
PB control [kWh]	50	430

Table 4.2: Final BB system rated capacities for each control.

4.1.3 V2G system sizing

The main factor to consider while deciding on the number of V2G terminals to be made available for the FCEV fleet is the cost of hydrogen the university is willing to pay and the inconvenience caused to the BEV owners due to lower availability of vehicle charging points. The V2G terminals being bidirectional signifies that the same terminals that are used to charge the BEVs can be used to "discharge" the FCEVs to participate in FCEV fleet. The number of V2G terminals were iteratively increased from 0 to understand by how much the self-sufficiency would increase/change. As the utilisation of the FCEV fleet does not change between controls, there was no variation seen in the SSR during the sizing process. Figure 4.3 depicts the iterative increase in V2G terminals. In the figure, after a certain point the SSR does not increase by much. This is due to the PV system[34] and the unavailability of cars when there is low to no PV (weekends and holidays). Indicating that after a certain value, increasing the FCEV fleet does not see large returns. Furthermore, in the figure point A denotes the final size of the FCEV fleet. The costs in this case were not analysed as only the cost of hydrogen as a fuel is considered, and that is entirely dependent on the quantity of hydrogen being consumed, therefor it is a function of the load and the number of FCEVs. Thus, the final FCEV fleet size is set to 30. Furthermore, it must be noted that these results are very dependent on the assumptions made.

[33]Here this point is defined as the optimum in this report, as with every unit increase in rated capacity from that point on-ward one does not see any significant increases in the OCR and SSR. But the TSCoE still increases linearly.

[34]It was noted that as the size of the PV system increased the V2G contribution to the load decreased, this implication is simple and obvious; the larger the size of the PV system the lesser the dependence on the FCEV fleet.

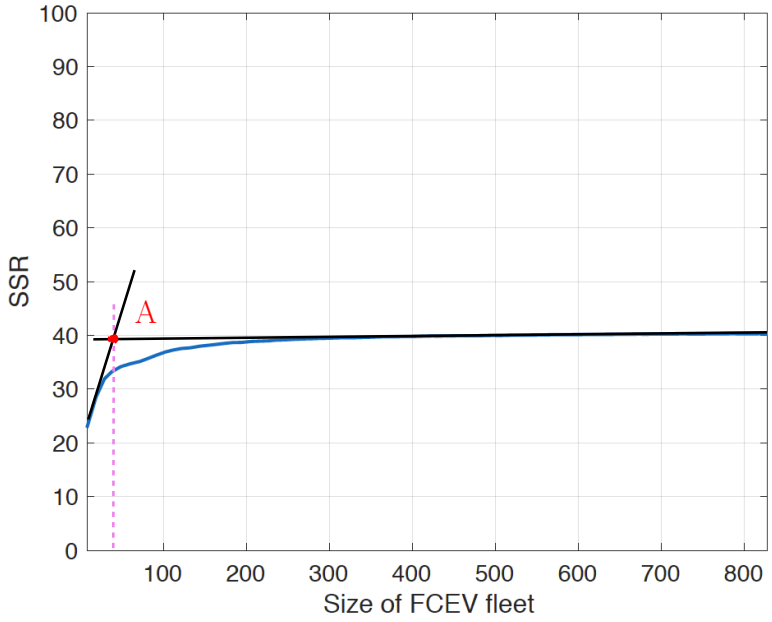

Figure 4.3: Increasing the number of V2G terminals while

4.2 SCB control analysis

This section compares the two sizing approaches of the BB and the power flows when implementing the SSB control. The SSB control when analysed is most useful in a scenario when more self-sufficiency is required than 100% grid dependence in 2030. This section gives an overview of the important results observed in SSB control analysis. First, the SoC variations through the year for both sizing methods are compared to understand the impacts of each, followed by analysing the power flows for both methods using sankey diagrams.

4.2.1 SoC comparison of the two sizing approaches

As mentioned in previous sections, two approaches to size the BB were considered. Considering the fact that the main goal of this control is to increase self-sufficiency, the BB was oversized to understand the benefits such a sizing could offer. Factors taken into consideration were costs, capacity utilisation of the BB through the year and the SSR.

Figure 4.4 depicts the SoC variation of the BB for both sizing approaches, S1 and S2. From figure 4.4b it is evident that the battery only reaches it's full capacity during the warmer months (also the months with higher irradiance). While during months of lower irradiation, the BB reaches 50% on occasion. If the main goal is to increase self-sufficiency, decrease grid dependence and not the BB utilisation, this sizing approach is sufficient. Meanwhile, figure 4.4b clearly indicates a fuller capacity utilisation through the year.

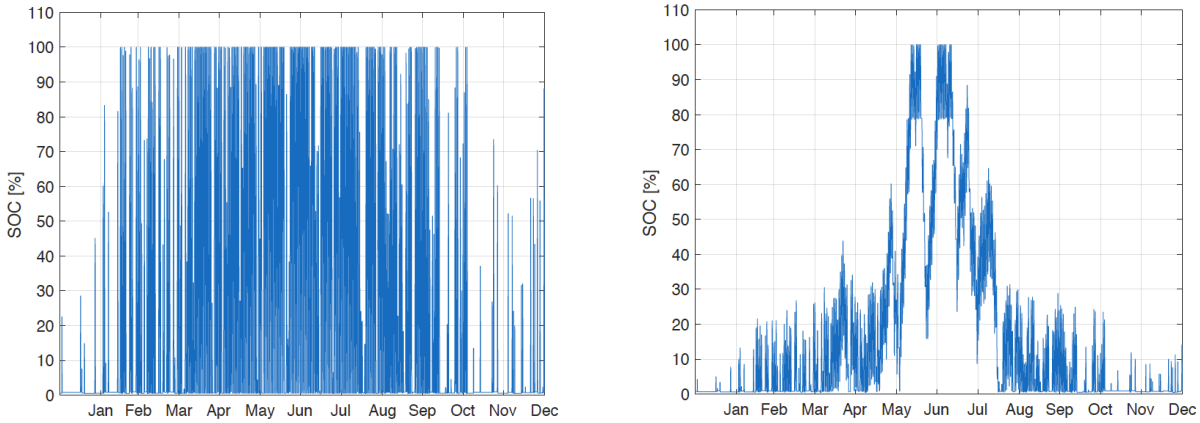

(a) SoC of the BB for S1 sizing approach.

(b) SoC of the BB for S1 sizing approach..

Figure 4.4: Depiction of the BB SoC for both the sizing approaches, S1 and S2, through the year for SSB control. This depiction is to graphically portray the capacity utilisation of the BB to the reader.

	Winter months [h]	**Summer months [h]**
S1	1360.9	3335.60
S2	1114	4523

Table 4.3: Hours of utilisation through the year for both sizing approaches for SSB control.

It is interesting to note that despite increasing the capacity of the BB, its utilisation time in the winter months [35] has in fact reduced. This was already evident from the figure 4.4a. It indicates that increasing the size is not sufficient, but how the BB is charged and discharged also plays a role in its utilisation. Here, a reference is not made to the amount of energy put in or taken out of the battery, but rather the durations and depths to which charge/discharge is done.

4.2.2 Power flow split

The power flows within this system are detailed in the sankey diagram[36], for both sizing approaches of the battery, in figure 4.5. For both approaches since the PV system and number of allowed V2G terminals remain constant no change is seen in their direct contribution to the load. Any variation between them is due to the energy passing through the BB. With the smaller sizing approach, the BB contributes to 1.1% of the total load, meanwhile for the alternative method its fraction increases to 8.99%. These are relatively low contributions when considering the size of the BB system. This can be attributed to the high winter load occurring at times of low PV production, thereby resulting in insufficient excess production to charge the BB. Correspondingly, 2.69% (S1) and 18.43% (S2) of the PV output go into charging the battery for each sizing approach.

A detailed summary of the SSR, grid contribution and the percentage of PV energy sold can be found in table

[35] Here winter months refers to the months from September to the end of February, while summer months refers to the months between February and September.

[36] As the heating is also electric, no distinction was made when analysing the flows, as all the electricity consumed goes is either indirectly for space heating or directly for electricity consumption.

4.4. It must be noted that the percentage of power sold does not contribute to the SSR PV or the total SSR. It is a fraction of the PV output that is unused and thus sold to the grid.

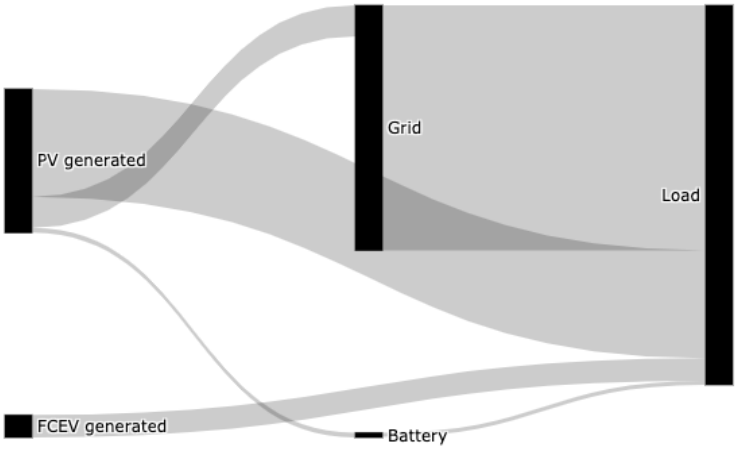

(a) Power flow analysis for the S1 sizing.

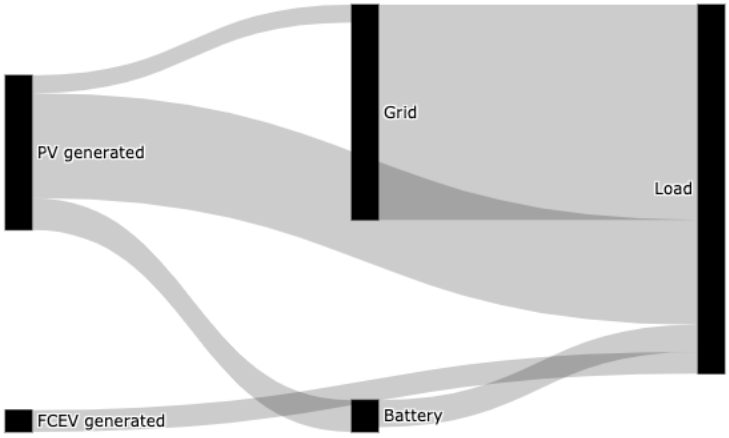

(b) Power flow analysis within the system for the S2 sizing.

Figure 4.5: Sankey diagrams for SSB scenario depicting all the power flows into and out of the system. All values are in MWh/year.

Sizing	SSR_{PV} [%]	SSR_{FCEV} [%]	Grid [%]	Sold [%]
S1	29.50	5.92	64.58	19.45
S2	37.42	5.92	56.66	10.26

Table 4.4: A summary of each components' role in meeting the load in the SSB control. The SSR_{FCEV} refers to the self-sufficiency ratio in equation 3.4, without the PV component.

The BB it has been shown is not utilised to its fullest capacity in the S2 sizing. The combination of low of solar irradiation and limiting c-rate play a role in its inability to charge fully for the whole year. This can be combated, by either charging the BB using electricity from the grid or by increasing the maximum c-rate possible. In the former case, it would become hard to define the SSR due to the higher integration of grid electricity. While for the latter, a ZBFB cannot have too large charge currents due to the formation of dendrites at large current densities [30]. Alternative battery technologies could be employed to test for the best possible combination, the vanadium redox flow batteries for example or even lithium-ion batteries.

For this control the maximum SSR (sum of SSR_{PV} and SSR_{FCEV}) comes up to about 43.34% approximately for approach based S2 sizing of the BB. As the main goal of the SSB control is to increase the self-sufficiency, this number is important to bear in mind. This fraction accounts for the direct PV feed-in, FCEV power and BB contribution (indirect PV usage). The SSR may be further increased by increasing the size of the FCEV fleet, but in that case a larger number of V2G terminals would not be available to charge BEVs on-site. The number of PV panels may also be increased, for example by integrating them into the car park available.

Alternatively to increase the SSR, an electrolyser could be utilised to convert any excess PV generation left over after charging the BB. Instead of selling it to the distribution grid or curtailing the power, hydrogen could be produced on-site and stored for later usage; which has potential to be used to directly provide heating or produce electricity[37].

4.3 PB control analysis

The PB control was designed to analyse if a price-based time shifting of the BB utilizing is capable of reducing costs, both as investment to the designed system and the costs paid to the grid. It was noted that despite reducing costs considerably (when compared to the baseline scenario), it did not reduce costs anymore than the SSB already had. This is primarily due to the insufficient on-site power production during the colder months of the year.

4.3.1 SoC comparison of the two sizing approaches

It is evident from figure 4.6 that the method of utilisation of the BB in the PB is drastically different from the SSB control. The BB sees a fuller utilisation in the S1 sizing, though it is evident that the BB is not fully discharging in the warmer months of the year. Meanwhile, in the S2 sizing approach the SoC sees more deviation from perfect utilisation in the summer, where it is not allowed to discharge completely at any given time. As it is to be expected, the number of hours of utilisation through the year increase with the size of the BB, even in the winter. This is primarily due to the sporadic utilisation seen in this control, which allows the

[37]Though, it must be mentioned that in order to put to use an electrolyser's capacity, and decrease the levelised cost of hydrogen produced from the system, it would need to have a load of at least 30% its nominal capacity [100]. The levelised cost of hydrogen (LCOH) when using electrolyser for at least 2900 hours of the year is less than 10 €/kg [100], thus increasing the number of hours of utilisation decreases the LCOH.

BB to charge (adding to existing capacity already stored) and discharge for smaller time durations making it available for use for larger durations when needed. Meaning that, the fact the BB is not fully discharged each time it is used, is a benefit that increases its winter utilisation in the larger sizing approach.

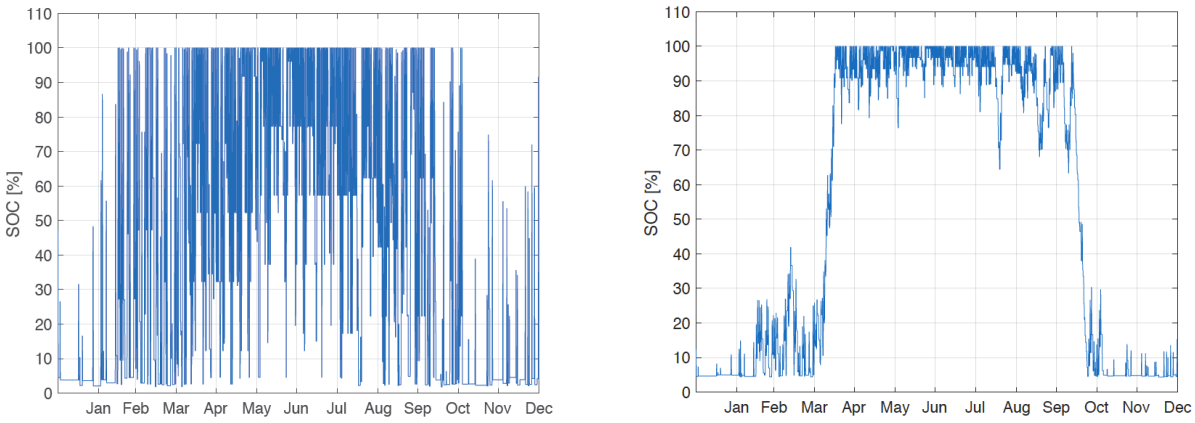

(a) Sizing S1.

(b) Sizing S2.

Figure 4.6: SoC variation through the year of the two sizing approaches, S1 and S2, of the BB for PB control.

	Winter months [h]	**Summer months [h]**
S1	1229.80	2218
S2	1436.5	2116.80

Table 4.5: Hours of utilisation through the year for both sizing approaches for PB control.

4.3.2 Power flow split

The power flows between controls do not differ drastically, except in the reliance on the distribution grid and BB utilisation. The PB control causes an increase in grid reliance and decrease in BB dependence. Which translates to a lower amount of PV energy stored for self-sufficiency and thus an overall lower SSR relative to the SSB.

The SSR has decreased in this scenario, when compared to the SSB scenario, by almost 2% for the S2 sizing of the BB. This can be attributed to the method the PB control employs the BB, where it is not allowed to discharge if the EMS deems the price of electricity from the grid to be below its daily threshold. This in turn causes any excess PV generation to be either sold to the grid or curtailed if the BB has sufficient charge. The direct PV feed-in and FCEV contribution remain constant due to their method of utilisation remaining constant across controls, while the BB contribution to the load has decreased by 26% and 22.5% for the S1 and S2 sizing respectively.

Sizing	SSR (PV) [%]	SSR (FCEV) [%]	Grid [%]	Sold [%]
S1	34.04	6.83	59.13	19.09
S2	40.71	6.83	52.46	15.47

Table 4.6: A summary of each components' role in meeting the load in PB control. The SSR_{FCEV} refers to the self-sufficiency ratio in equation 3.4, without the PV component.

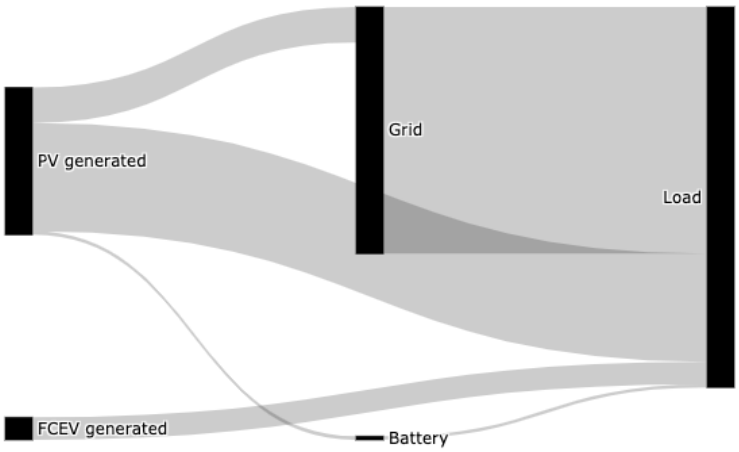

(a) Power flow analysis for the sizing S1 for PB control.

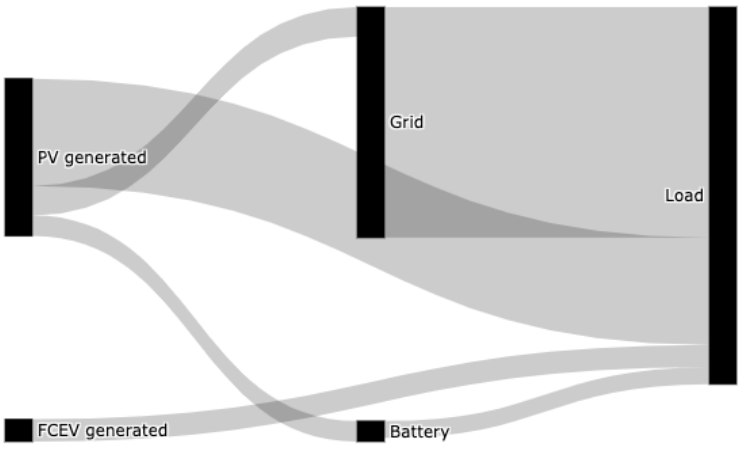

(b) Power flow analysis within the system for the sizing S2 for PB control.

Figure 4.7: Sankey diagrams for PB scenario depicting all the power flows into and out of the system. All values are in MWh/year.

This control is best utilised if there is high price volatility, or higher grid electricity prices at night time. Though the goal of this control was to decrease costs from the grid while also increasing self-sufficiency, decreasing costs was not successful. This is further discussed in the following section where the economic aspect of the project is analysed. A drawback of this control is its higher grid dependence, which can be decreased by adding an extra layer of control, where in addition to the price-based time shifting, another criteria can be volume-based grid reliance as well. This is further discussed in the future work section of the next chapter.

4.4 Comparison of power flows between controls

4.4.1 PV integration

The PV on-site generation has a relatively low direct utilisation by the load, at approximately 32.95% for both control strategies. This can be mainly attributed to the large consumption that occurs during months of low irradiance and the inability to store the excesses generated during high production for months at a time. As to be expected, the BB utilises a smaller fraction of the PV energy to charge in the PB as opposed to the SSB. This is due to the sporadic utilisation of the BB in the PB that doesn't allow the BB to fully discharge at all times. This also causes a larger sum of PV energy to be sold to the grid. In hindsight a smaller BB size could have been utilised for the PB scenario, but in order to make a realistic comparison between the two controls the same sizing was chosen. This oversizing causes an increase in the Levelised Cost of Storage (LCOS) of the BB in the PB. In the figure 4.8, if there is a difference in PV utilisation it is depicted, else there is not indication made. The excess energy that is not accounted for by the direct feed-in, BB charge and amount sold, is lost due to transmission losses, BB efficiency and curtailment.

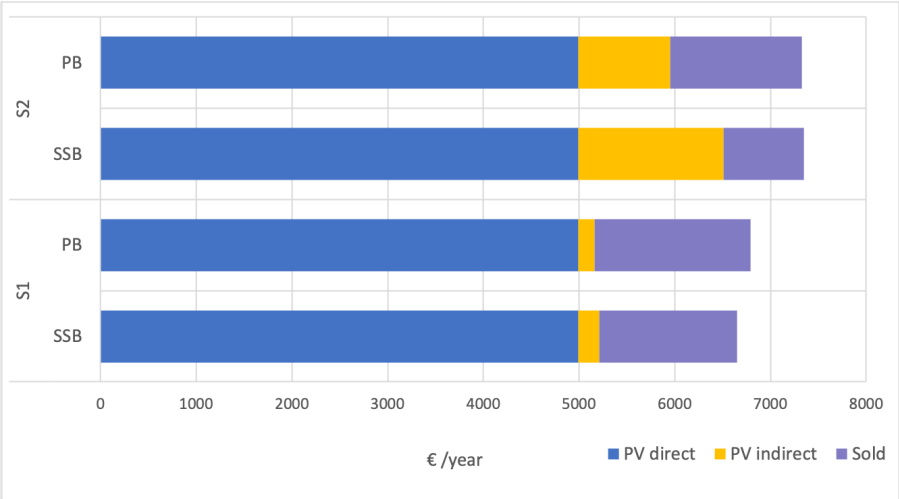

Figure 4.8: Comparing the total PV generation in one year and where all the energy flows based on each control strategy. Here, sold refers the the PV output that is sold to the grid via Equigy.

4.4.2 Analysis of seasonal BB utilisation

The total number of hours the BB is utilised through the year varies based on sizing and the method it is charged and discharged. Increasing the number of hours the BB is used in the year implies that the levelised cost of storage will decrease in that case. Simultaneously, over sizing the battery based on the SSR and TSCoE would lead to inefficient capacity utilisation through the year. As mentioned in sub-section 4.1.2, two approaches were

followed to analyse the best method to size the BB. One based on how the battery charges through the year,S1, and the other based on the point on the SSR curves after which minimal returns are seen, S2.

In figure 4.9, one may note that based on the S1 sizing, the BB for both controls is utilised for less than 57% of the year (i.e.) less than 5000 hours. Correspondingly, in the S1 approach the BB utilisation goes down by 26.6% approximately, while in the S2 sizing approach a decrease of almost 37% is seen between the SSB and PB controls. It is beneficial economically to employ the BB for more number of hours (especially if it is a large battery), as this is an indication of utilising the investment made while it also decreases the LCOE of the BB. As the PV system's output does not change, more hours of BB utilisation also signifies that larger quantities of excess from the PV system was utilised within the UCM, thereby increasing SSR. Furthermore, between the two sizing approaches S2 sees larger number of hours of utilisation. This can be attributed to the larger size of the batteries allowing for a larger capacity to be put into and removed from the battery at any given time. In other words, the larger BB size allows for better PV system utilisation despite the inefficient BB capacity utilisation, and inadvertently allows for the BB to be used at a higher frequency.

An interesting observation that was made, can be seen when comparing the winter utilisation for the S2 sizing in the figure 4.9. The BB is being used for higher number of hours in the PB than in the SSB, this can be attributed to the fact that in the PB control the BB is not allowed to discharge completely at all times. This partial capacity that is left in the system increments whenever there is excess PV generation, this increases the capacity and allows the BB to be used for many short period durations through the winter months. This phenomenon does not extend into the summer months, as the the BB in the SSB control is allowed to fully discharge and charge each, there by providing more number of hours of utility.

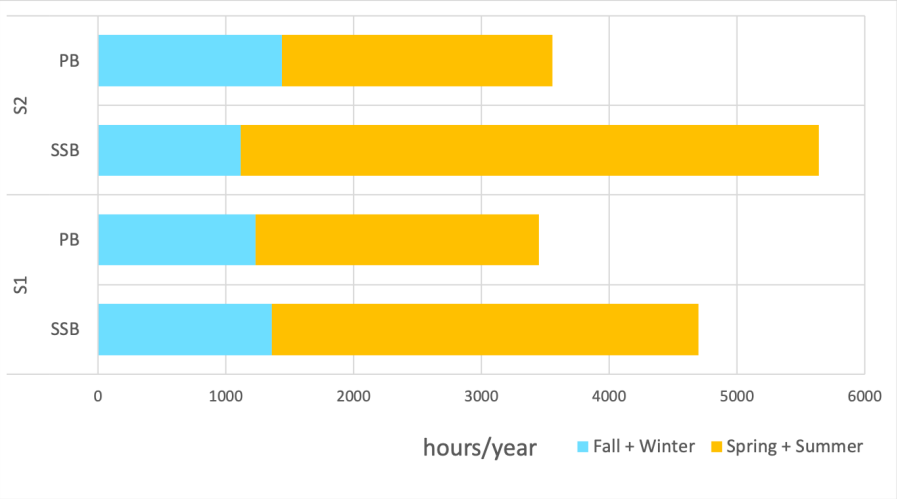

Figure 4.9: Comparing the number of hours of utilisation of the BB for both controls. The two sizing methods are compared to understand the consequences of each sizing approach for each control.

4.4.3 Varying resource usage

The primary goal of the SSB control was to increase self-sufficiency of at the location of implementation of this system, while that of the PB control was to decrease costs. Based on the two sizing approaches implemented, it is evident from figure 4.10, that the maximum self-sufficiency is achieved by the SSB control when it is sized based on S2. It can also be noted that the PB control is about 2% less self-sufficient than SSB control for the same sizing approach, despite having a larger BB size to store more excess generation. This indicates that the

combination of large capacity and sporadic BB usage have a drawback of decreasing self-sufficiency.

In the figure, an additional detail is that it only the indirect PV contribution changes across the four bar lines depicted. This is due to only the BB size varying, while the PV system size and the number of V2G terminals are kept constant at their respective sizes as discussed in section 4.1.

A possible method to increase the SSR of the system would be to utilise the PV energy that is sold to the grid. This could be done by either converting it to hydrogen on-site employing an electrolyser or introducing another generation unit that will run during the winter. The primary reason is due to the large load that is unable to be met by the PV system during the winter months. The demand is relatively large in those months, that increasing the BB size beyond this degree will only result in increased costs and comparatively low returns on the investment made.

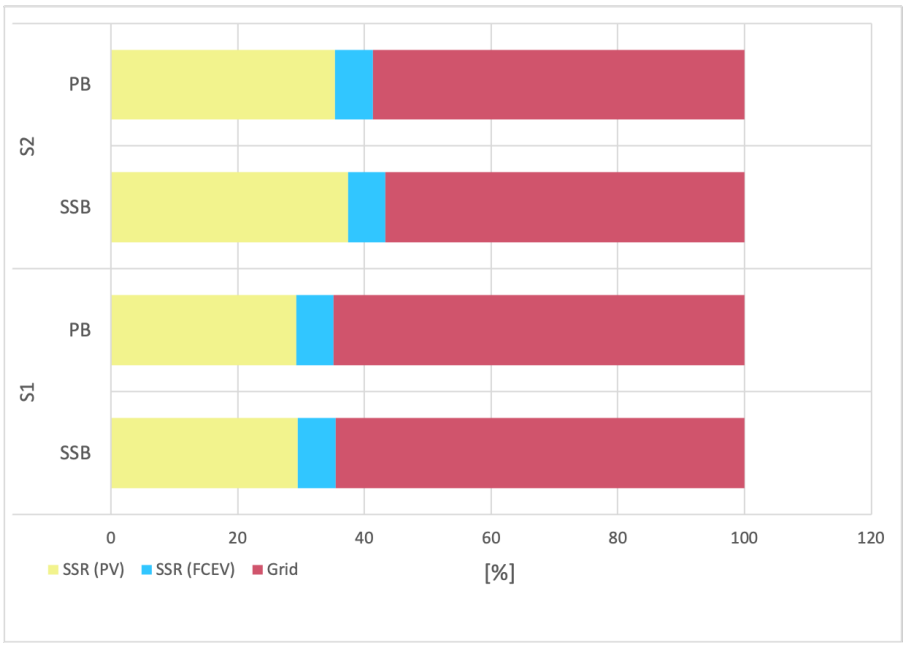

Figure 4.10: Comparing the contributions of the UCM components based on the sizing choices made. SSR (PV) includes the direct and in-direct PV contribution to the load while the SSR (FCEV) includes the FCEV fleet's contribution to the load.

4.5 Economic comparison of the controls

This section discusses the economic aspects of the proposed system. First the system levelised cost of electricity, along with each individual component's contribution to the SLCOE are also discussed. Followed by a comparison of the baseline scenario with the costs for the UCM proposed. All cost projections are made for the year 2030.

4.5.1 System levelised cost of Energy

A major cost of this system belongs to the FCEVs and the BB. The SLCOE formulation was used to identify the total system cost, including relying on the grid. The LCOE on the other hand provides insights into the

individual role each component plays in the total SLCOE. In figure 4.11, a summary of the system levelised cost of electricity along with a breakdown of the individual contributions can be found.

Figure 4.11 encompasses all the levelised costs in one graphical representation. The LCOE varies between scenarios, as it is a ratio of the cost over the consumed electricity. Higher the utilisation, lower the levelised cost. This is clearly seen in the large LCOE seen for the S1 sizing of the BB. The cost of the BB does not match the utilisation it is put to, despite its sufficient Depth of Discharge (DoD) variation through the year. The BB LCOE varies from 80-117€/MWh depending on the scenario. Meanwhile, the PV system has an average LCOE of about 30€/MWh, which is in the range of projections made in [59] for 2030.

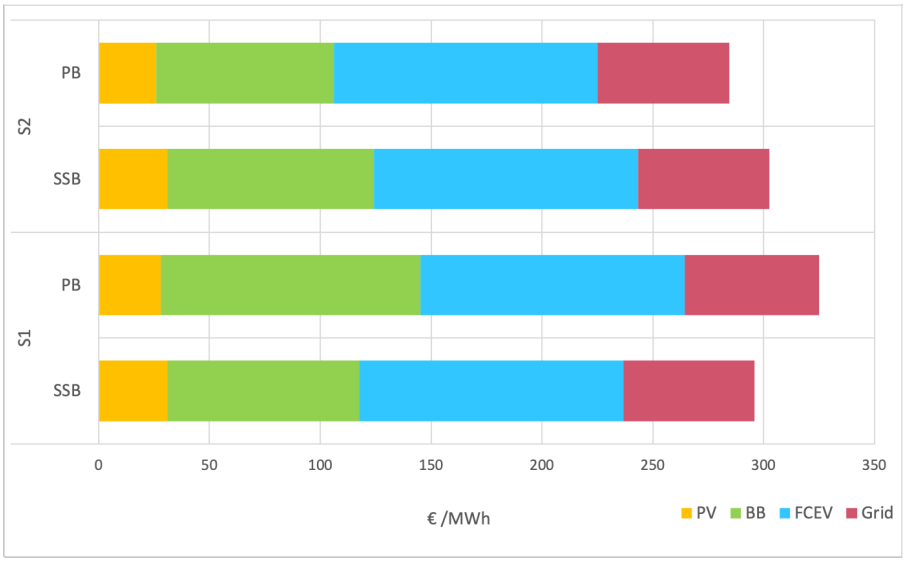

Figure 4.11: A comparison of the levelised cost of storage and electricity from the BB system and the PV system for both sizing approaches.

If the goal of the system is to decrease costs, then a trade-off would need to be made to understand whether decreasing emissions and increasing self-sufficiency hold a higher degree of importance rather than decreasing costs. Due to the expensive nature of the this system, it is important to understand the factors that contribute the highest and why they do so. The ZBFB on average accounts for nearly 31% of the SLCOE. While the price paid for the hydrogen fuel alone accounts for nearly 39% of the total SLCOE on average. The least contribution is made by the PV system, at 19.5% approximately. In hindsight the combination of using two technologies still in the experimental phase with no economies of scale, and with high costs could have been avoided. While instead utilising a cheaper more mature battery storage technology, like the Li-ion batteries. Finally, for secondary generation alternatives that are cheaper can be looked into and analysed in such a system.

4.5.2 Total cost of system

The annual energy cost is the sum of the price paid to the distribution grid and the TSCoE of the UCM. Both controls have a similar TSCoE due to the same system sizing implemented. They vary in their BB costs and costs paid to the grid. In figure 4.12, one may note the annual cost of grid dependence clearly. This large share is seen due to the winter months, where there is low PV, but consumption is at its highest.

[27]Here a distinction is made due to the high cost of V2G terminal costs, to signify to the reader the implications on the SLCOE if the installation and maintenance costs were not included.

In figure 4.12, the baseline scenario has the highest cost, this is the scenario with 100% grid dependence. It is almost counter intuitive that in the SLCOE disambiguation the UCM components hold the majority of the costs, while in the figure below annually the costs paid to the grid are much larger. One explanation for the costs to the grid being so high in the SSB and PB controls could be that, the distribution grid is utilised mostly during times of high prices. Despite the PB control's primary goal to decrease costs from the grid, there are numerous instances during the colder months of the year where the BB was not sufficiently charged. From figure 2.12, it was evident that the price of electricity during the winter months was relatively higher on average to the colder months of the year. While another explanation is that the TSCoE is inherently dependent on the assumptions made by the author, where if the sizes of the BB or FCEV fleet were to be increased, the TSCoE would correspondingly increase and might even exceed the baseline scenario costs to grid.

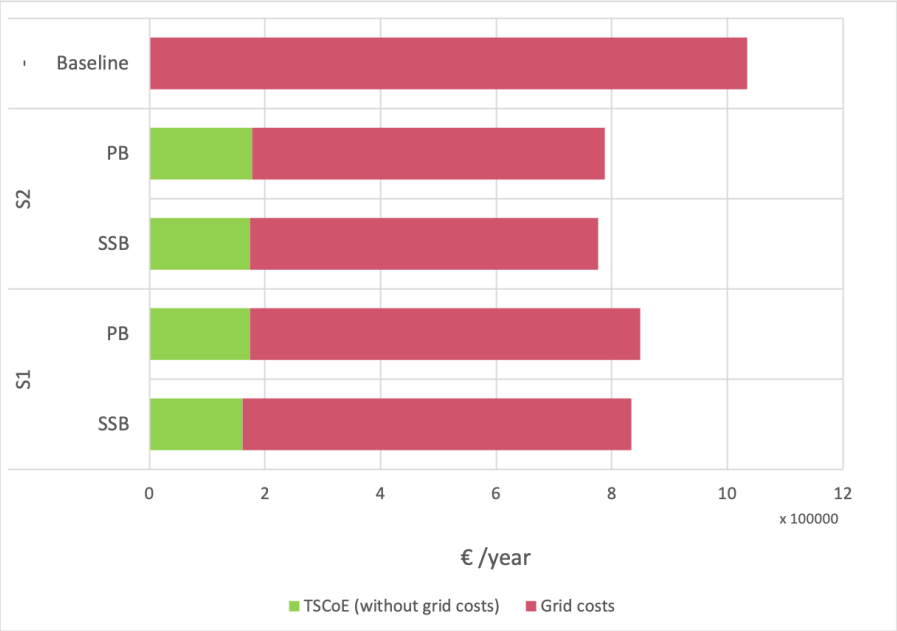

Figure 4.12: The TSCoE of the two controls vs the total cost of energy for both scenarios. The annual energy cost is the TSCoE with the annual price paid to the distribution grid included.

Some factors that were not considered might indeed play larger roles by 2030, like increased network connection costs and increasing capacity connection to the grid due to larger energy demands. Another point is the influence of renewables on the price of grid electricity, as a simplification was made there might be a possibility that during periods of low on-site generation might coincide with periods of low renewable generation of the grid. Implying that the university relies on the grid during times of higher prices in the future.

While it is still uncertain what the actual price of hydrogen will be, as it is dependent on many factors like whether or not the EU will meet its hydrogen road map goals and how cost competitive FCEVs will become in the future.

5 — Conclusion and future work

In this chapter a detailed summary of the objective and findings in this report are recapitulated followed by the future work that could be researched in this direction. The main goal of the report was to understand whether a self-sufficiency based control strategy was better than a price-based time-shifting control strategy when utilising a ZBFB and FCEVs with V2G capabilities in a UCM with on-site PV generation. The focus was to analyse the repercussions of heating electrification on the energy costs, and if increased self-sufficiency alone would provide a more economical solution than grid reliance by the year 2030.

5.1 Conclusion

The following questions were to be answered by the research conducted in this report, they are presented along with the discussions made in chapter 4:

How does a self-sufficiency based control strategy compare economically (over project lifetime) to a price-based time-shifting control strategy when utilising an electricity storage system and FCEVs with V2G capabilities in a UCM with on-site PV generation?

- It was found that economically and with regards to self-sufficiency, the SSB control performed better than the PB control. Economically, it was cheaper than the PB control, while with respect to the SSR it showed the highest self-sufficiency between the two controls. A maximum SSR of 43.34% SSR was achieved in the SSB scenario, while in the PB it was naturally lower at a value of 41.31%. This decrease in the PB scenario can be attributed to the sporadic utilisation of the BB, where it was not allowed to fully discharge at all times. If the wholesale market price was below the daily threshold, the EMS would use the distribution grid to meet the load, thereby not prioritising using the energy that was already stored in the BB.
- The SSR in both PB and SSB control scenarios can be increased by relying on additional, technologically mature microsources (when compared to the FCEV fleet as backup generation). The drawback of using PV generation in a system with electrified heating is that typically this consumption occurs during times of low or no irrandiance. Thus, either adding an extra microsource or implementing a longer term storage option, like hydrogen, can increase the SSR.
- There is approximately 2% higher grid dependence for the S2 sizing approach in the PB scenario compared to the SSB scenario, this sizing is of interest as this was the highest self-sufficiency achieved in this report. This fraction is highly dependent on the assumptions made by the author in this report. Some of the factors playing a role in such a regard are the system sizing, type of DER used and the price profile generated.
- Between the baseline and the PB, SSB control scenarios, the system levelised cost of electricity is is higher in the proposed system. A summary of the numbers can be found in table 5.1 Concluding that the UCM is slightly more cost-effective than 100% grid dependence. But it must be noted that if the number of V2G terminals were increased past 60, grid dependence and the UCM would share a similar TSCoE, thereby increasing the SLCOE as well. Factors such as increasing network costs, payments needed to access additional grid capacity (due to increased electricity demand), the effect of renewables on electricity prices, the influence of cross-border effects on local electricity prices and subsidies for sustainably generated electricity were not considered.

	Cost of electricity [€/MWh]
Basline	58.95
SSB(average)	299.32
PB(average)	304.6

Table 5.1: Summary of cost of wholesale electricity projected for 2030 and the SLCOE of the proposed system's electricity.

- The FCEVs with V2G capability contributed to the largest fraction of the TSCoE of the proposed UCM. An immediate cause of this is the high prices projected for hydrogen as a fuel. This cost of hydrogen is then transferred to the university to pay to the FCEV owners via the contracts. A longer term aspect to be considered is the combination of the immaturity of the V2G technology, lack of economies of scale and lack of public interest or knowledge on the FCEVs as power plants. Though this might change in the future, given the EU's interest in hydrogen. Thus, in hindsight relying on FCEVs for backup generation to meet large demand in the winter months is not the most economical. As the cost of hydrogen is approximately 0.119€/kWh, and the average cost of the grid electricity is approximately 0.57€/kWh.
- Though the system total costs are quite high, another goal of this report was to shed light on the impact of the electrification of heating and what exactly that means for large scale energy consumers that want to be self-reliant. It is evident that if heating is 100% electrified by 2030, energy demand is likely to increase. While moving towards a more decentralised form of energy production it is relevant to identify varying value propositions for the existing DERs and the best combinations for varying locations.

How does the total cost of electricity compare in each control strategy when sizing the battery system based on the ideal sizing versus sizing based highest highest economically optimum SSR (S2 sizing) and best battery utilisation (S1 sizing)?

- The SLCOE is in fact lower for the S2 sizing approach than for S1, this is due to the higher utilisation of an battery storage system that has relatively high investment costs. Implying that the smaller BB size, in fact was a drawback, as its costs could not be recovered through usage. The energy throughput in the BB can be considered as a revenue, when the investment is high and the revenue is low automatically this causes the LCOE and thereby the SLCOE to go up. An alternative flow battery to ZBFB are vanadium redox-flow batteries, which
- Due to sporadic utilisation of the BB, it might be more beneficial to decrease the size of the BB if the PB control is to be used. This has the added benefit of increasing the capacity factor of the BB, decreasing costs drastically while also preserving its lifetime. One major drawback of the PB control is the lack of deep discharges that are required for the ZBFB. An alternative would be to use a different technology altogether, that is more cost-effective and does not need as deep discharges, like the Li-ion battery for example.

How do the two control strategies compare based on self-sufficiency and own-consumption of on-site PV generation?

- The PB control is effective in providing a lower cost option, while also being dependent on the distribution grid. This allows the possibility and flexibility to not invest in a large ESS if need be. But if the goal is to increase self-consumption this control might not be the best option with respect to the SSB.
- In the PB scenario, grid dependence increased by almost 2.7% higher than in the SSB, yet only 1% difference in costs is seen. Indicating that the PB control works sufficiently, but more work needs to go

into fine tuning its ability to decrease costs, while still relying on the grid.

- The SSB control on the other hand reached an SSR of 43.3%, though it has already been mentioned how this can be optimised. If increased self-sufficiency is the only end goal, this control is a good starting point to build on.

5.2 Future work

A list of future work ideas are summarised in the list below. These are based on the author's study of the relevant literature so far.

1. This study shows the importance of understanding the impacts of heating electrification, how even when over sizing the BB, only 43% self-sufficiency was reached. It is important to understand in a future where heating is electrified, for large consumers, what the best combination of DERs would increase self-reliance but decrease costs as well.
2. An addition can be made to the PB control where, the EMS can optimize whether to charge the BB using the utility grid in times of low PV production. In this case then the self-consumption would decrease even further.
3. A volume-based shifting of the BB could be added as an additional layer of control to the existing price-based shifting in the PB control. Where, at night time, based on the volume being consumed and the price of electricity, the EMS decides to meet a portion of the load using the grid and the remaining with the BB.
4. Both controls can be upgraded using model predictive control that optimizes the production from the PV system, charging of the BB and utilisation of the grid. Weather forecasting and demand forecasting can be implemented to coordinate with the predictive control.
5. The EMS could behave as a market participant where it sells or buys electricity, and uses the BB as energy arbitrage to create positive cash flows for the university.
6. Demand response can be implemented to shift the load that can be shifted to times of higher production or lower grid prices; though a study needs to be done to understand how much of the university load during the day can actually be shifted.
7. A new method of BB sizing could be implemented, wherein the BB is only used during times of high grid prices during the early evening and morning hour. An optimization problem can be formulated where the BB rated energy and grid utilisation energy could be constraints and parameters to be optimized while the objective function could be the minimisation of TSCoE or maximisation of Self-consumption Ratio (SCR).
8. Studies can be carried out to understand how the electricity prices are likely to vary in the future, especially for night time, based on the current RES dependence projected in the Netherlands.

A — Battery discharge curves

All curves displayed in this section were obtained from Redflow's ZBM2 flow battery datasheet.

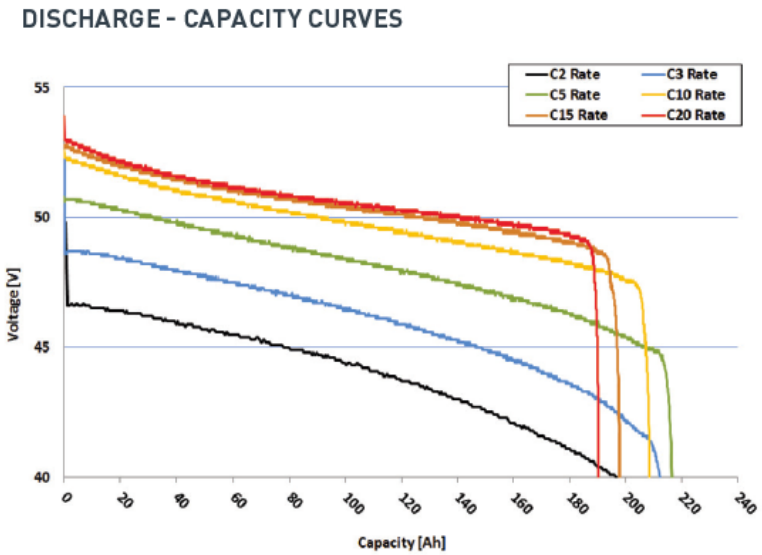

Figure A.1: Discharge voltage versus capacity for Redflow's ZBFB.

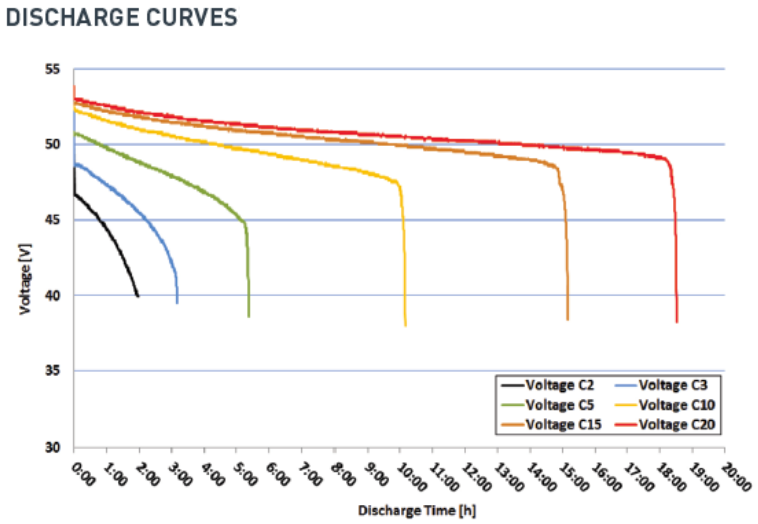

Figure A.2: Discharge voltage versus time for Redflow's ZBFB.

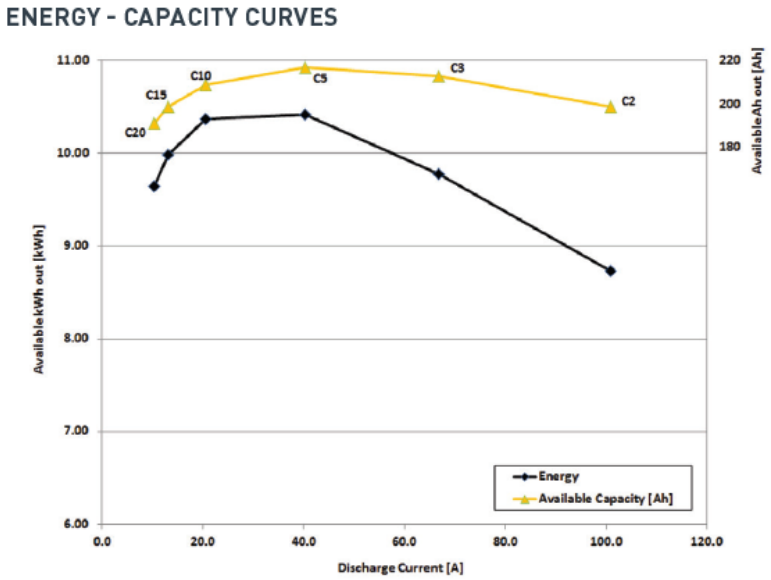

Figure A.3: Energy versus discharge current for Redflow's ZBFB.

Table A.1: Voltage values taken as inputs into the KiBaM. All values are in volts.

C20	52.2	51.7	51.1	50.9	50.7	50.5	50.0	49.8	49.3	40
C15	52.1	51.5	51.0	50.8	50.5	50.0	49.8	49.2	49	40
C10	51.9	51	50.8	50.2	49.8	49.5	49	48.8	48.2	47.8
C5	50.5	49.8	49.1	48.9	48.1	47.5	47	46.5	46.5	45.9
C2	46.8	46	45.7	45	44.2	43.7	43	42.1	41.2	40

B — KiBaM constants

The constants needed in order to simulate the reponse of the BB are tabulated below followed by the summary of the values of each parameter.

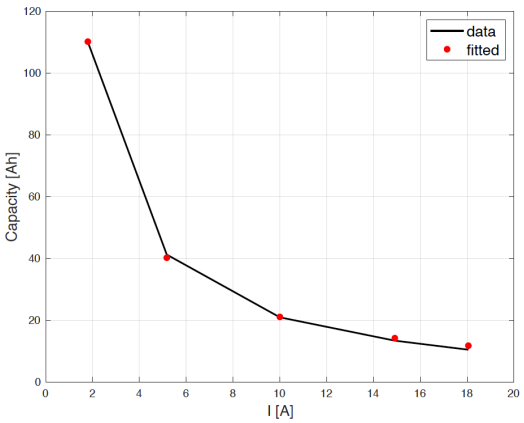

(a) Curve fitting.

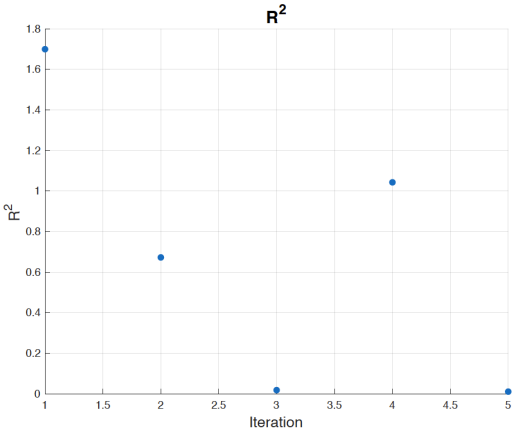

(b) R^2 of the curve fitting performed.

Figure B.1: The capacity constants for the KiBaM are found using the Levenberg-Marquardt algorithm.

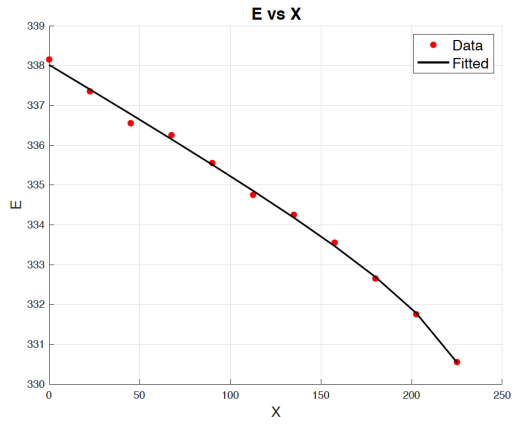

(a) Curve fitting.

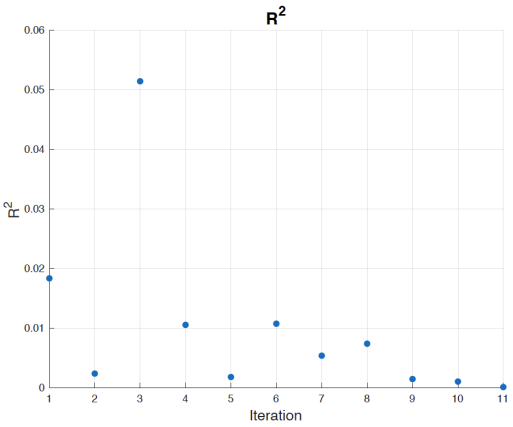

(b) R^2 of the curve fitting performed.

Figure B.2: The voltage constants are found using the Levenberg-Marquardt algorithm.

The results of the curve fitting are summarised below:

Constant	Value	Description
Voltage constants		
A	-0.0262	Parameter reflecting the initial linear variation of internal battery voltage with state of charge
C	-0.3011	Parameter reflecting the decrease of battery voltage during progressive discharge
D	267.68	Parameter reflecting the decrease of battery voltage with discharge and is usually approximately equal to the maximum discharge capacity
E0	338.02	Fully charged internal battery voltage
Capacity constants		
k	5.8662	Rate constant
Qmax	213.21	Maximum capacity
c	0.5554	Immediately available charge

Table B.1: Summary of KiBaM capacity and voltage constant values used to simulate the response of the ZBFB.

C — PV model validation

Validation of the PV model was done comparing it with the output of NREL's PV Watts calculator. Minimal deviation was seen between model built and NREL's calculator.

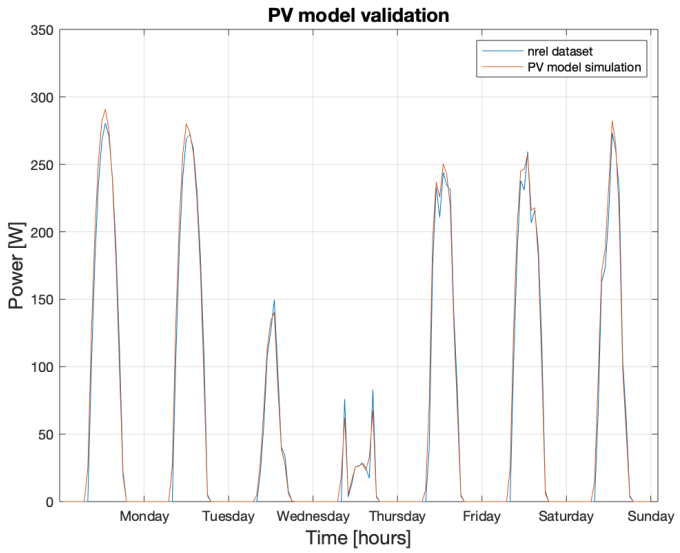

Figure C.1: One week of PV output comparison between simulated output and NREL PV Watts data.

D — Working of hydrogen pool

In figure D.1, one day's working of the model is depicted. As can be seen, the number of cars is constant for 4 hours consecutively before it changes. The change is randomized and is only dependent on the percentage that is 'allowed' based on the time of day. A point to note, is that in the figures depicted at times it seems like the H_2 goes higher than the previous time-step despite the decrease in available cars. This can be attributed to the cars arriving having a higher SOX than the cars that just left.

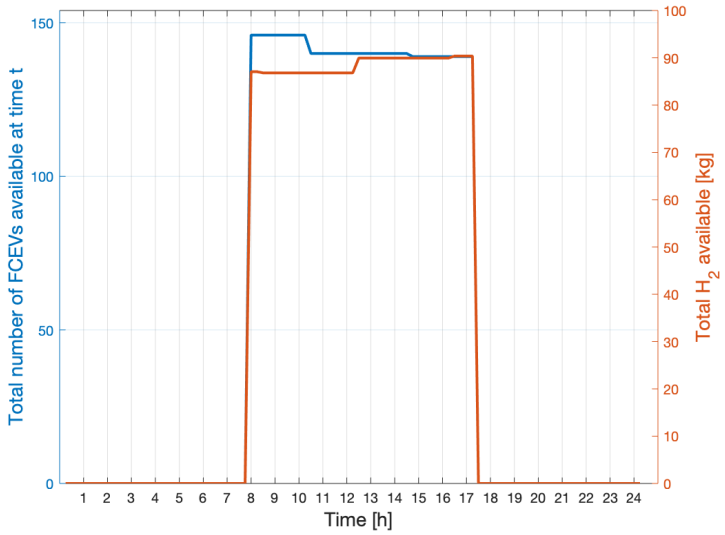

Figure D.1: On a typical workday day number of cars that could probably be available at the university if 5% of the university employees own FCEVs vs the amount of H_2 available in their tanks cumulatively.

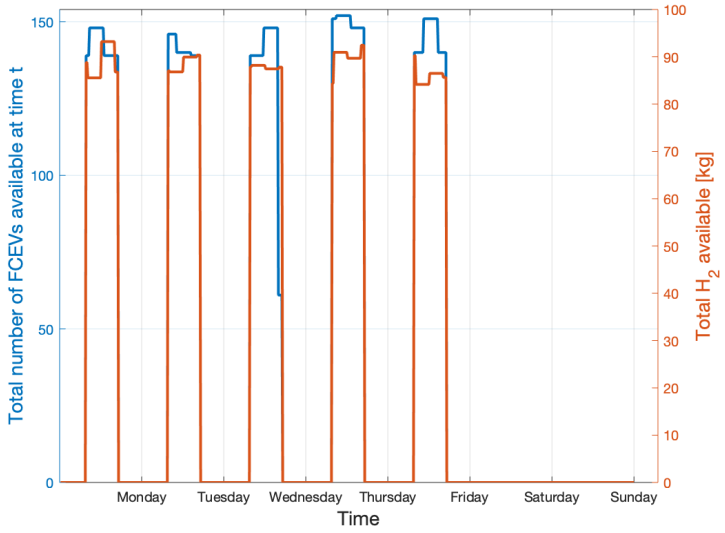

Figure D.2: A typical week of total FCEVs available vs the total amount of H_2 available in the their tanks cumulatively. Saturday and Sunday were assumed to have zero FCEVs available, hence the lack of activity on those two days.

E — TSCoE disambiguation

DER	Q [unit of installed capacity]	IC [€/unit specific to component]	CC [€/year]	OM [%]	OMC [€/year]	CC [€/year])	TC [€/year]
PV [kWp]	2063.6	239.49	0.051	0.02	9855	102994.964	138864.29
BB [kWh]	50	338	0.111	0.02	338	3962.39112	4638.39
HP [kWth]	3	0.53	0.0611	0.01	28.30	190.233896	218.54

Table E.1: TScoE inputs for both scenarios remain the same due to the common sizing approach.

F — Annual energy demand

A summary of the annual energy demanded from 2014-2019 is depicted below. This includes electricity, gas and district heat consumption.

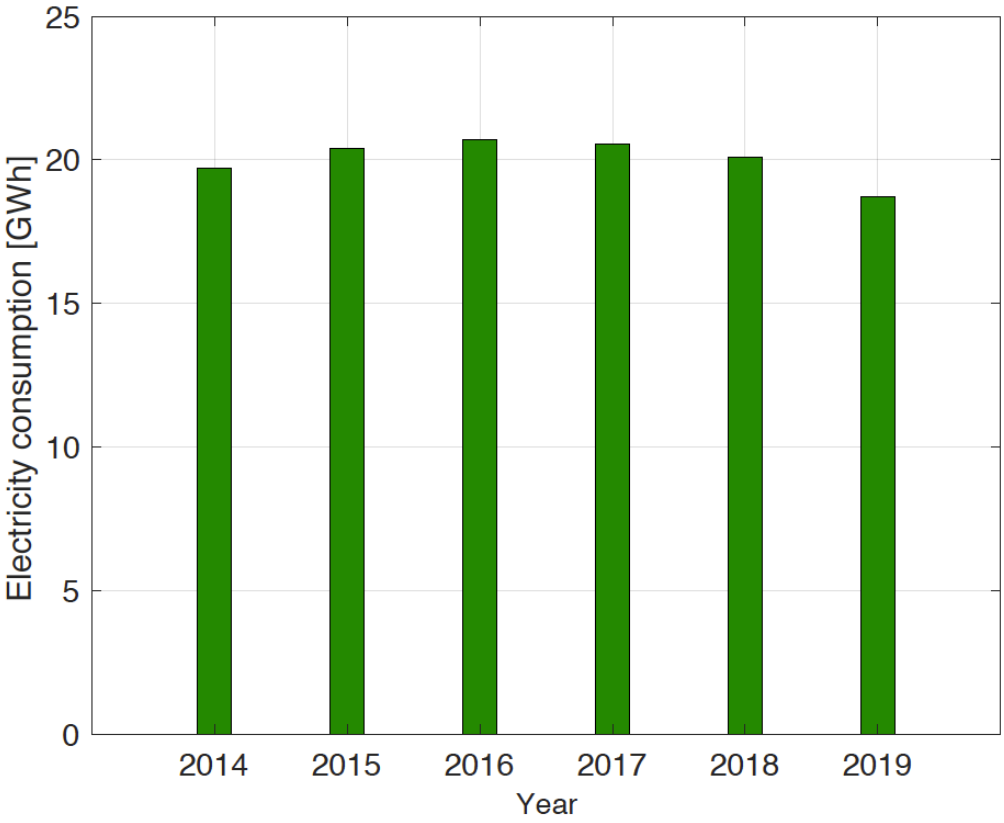

Figure F.1: End usage of electricity obtained from the district heater in the University of Twente [2]. This data includes the entire campus's electricity to offer the reader a comprehensive overview of the annual consumption patterns.

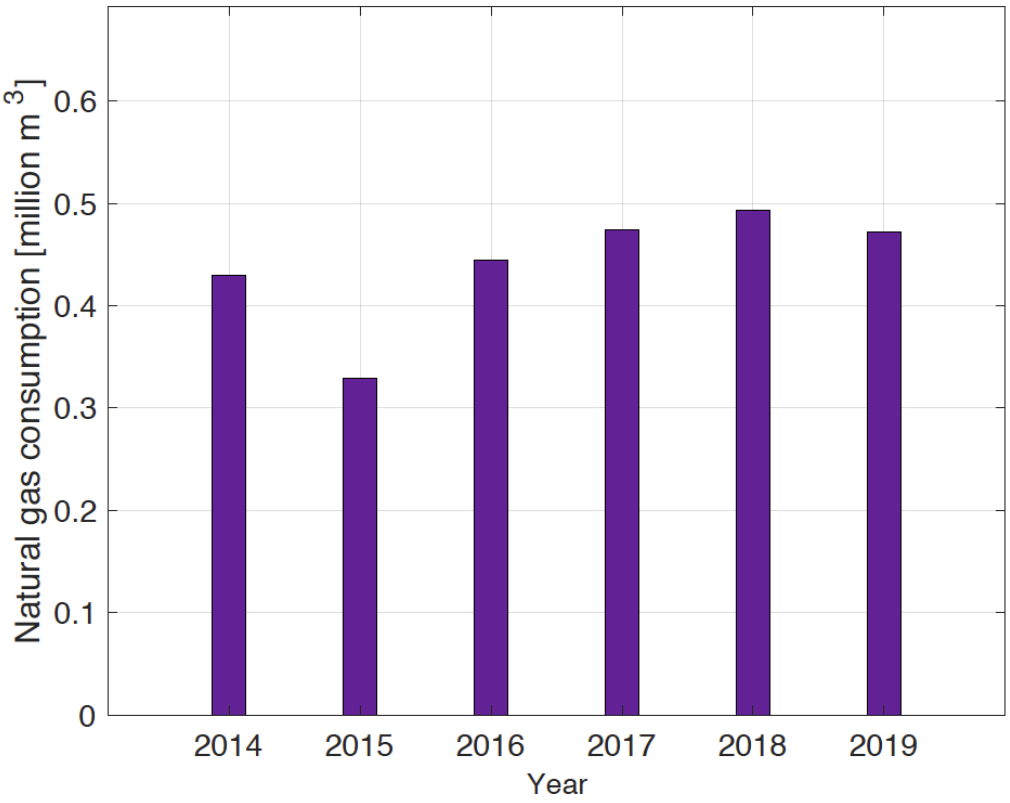

Figure F.2: End usage of natural gas obtained from the district heater in the University of Twente [2]. This data includes the entire campus's gas consumption, to offer the reader a comprehensive overview of the annual consumption patterns.

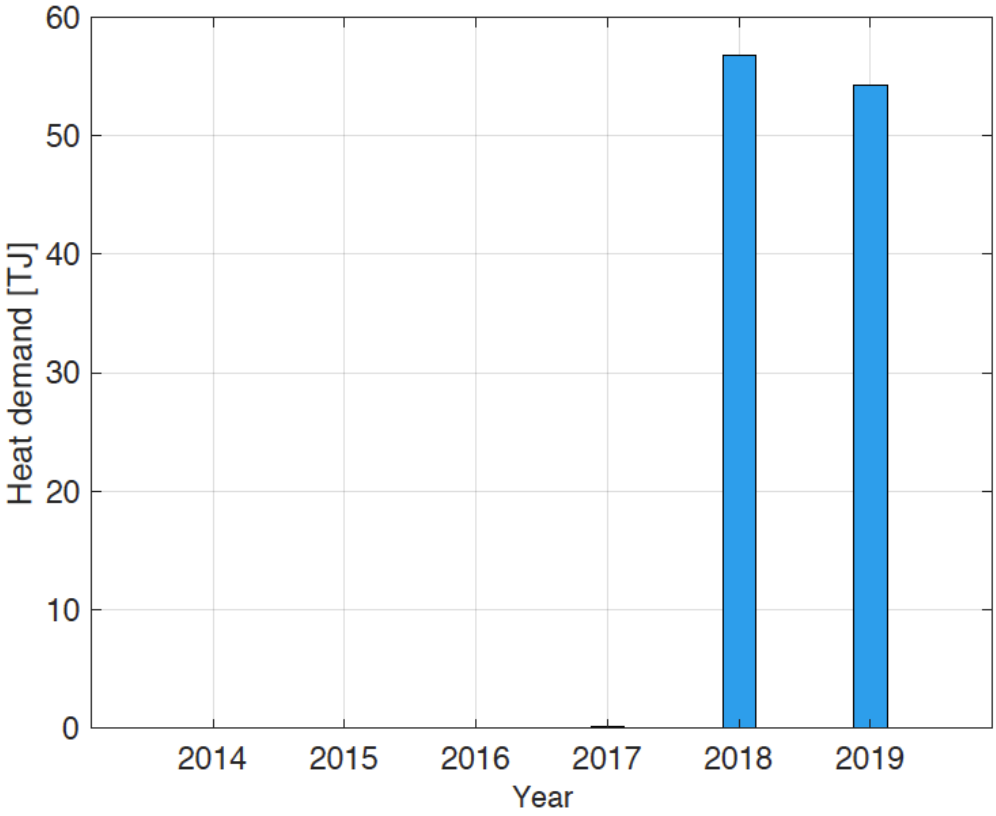

Figure F.3: Annual heat obtained from the district heater in the University of Twente [2]. This data includes the entire campus's electricity and gas consumption, to offer the reader a comprehensive overview of the annual consumption patterns.

G — Inputs for Sandia Inverter model

Parameter	Value	Description
Ps0	2503.626	DC power required to start the inversion process [W]
Pac0	610000	maximum AC power rating for the inverter at reference conditions [W]
Pdc0	630093.8	DC power level at which the AC power rating is achieved at reference operating conditions [W]
Vdc0	590	DC power level at which the AC power rating is achieved at reference operating conditions [W]
C0	-4.97E-08	Parameter defining the curvature of the relationship between AC output power and DC input power
C1	19E-6	empirical coefficient allowing P_{DC0} to vary linearly with DC-voltage input, default value [1/V],
C2	19.19E-4	empirical coefficient allowing P_{S0} to vary linearly with DC-voltage input, default value is zero [1/V]
C3	88.1E-6	empirical coefficient allowing C_0 to vary linearly with dc-voltage input, default value is zero [1/V]

Table G.1: Input parameters for the Sandia National Laboratory's inverter model.

Bibliography

[1] E Source. Business Energy Advisor | Colleges and Universities. https://esource.bizenergyadvisor.com/article/colleges-and-universities.

[2] University of Twente. Energy Data University of Twente. https://energydata.utwente.nl/.

[3] Hussein Ibrahim and Adrian Ilinca. Techno-Economic Analysis of Different Energy Storage Technologies. *Energy Storage: Technologies and Applications*, 2013.

[4] James Manwell and Jon Mcgowan. Extension of the Kinetic Battery Model for Wind/Hybrid Power Systems. *European Wind Energy Conference, Thesaloniki*, 1994.

[5] David Parra and Martin K. Patel. Techno-economic implications of the electrolyser technology and size for power-to-gas systems. *International Journal of Hydrogen Energy*, 41(6):3748–3761, February 2016.

[6] European Commission. Joint Research Centre. Institute for Energy and Transport. and SERTIS. *Energy Technology Reference Indicator (ETRI) projections for 2010-2050.* Publications Office, LU, 2014.

[7] Q&A: A Hydrogen Strategy. https://ec.europa.eu/commission/presscorner/detail/en/QANDA_20_1257.

[8] UNFCC. The Paris Agreement — UNFCCC. https://unfccc.int/process-and-meetings/the-paris-agreement/the-paris-agreement, 2015.

[9] Ministerie van Economische Zaken en Klimaat. Climate Agreement - Report - Government.nl. https://www.government.nl/documents/reports/2019/06/28/climate-agreement, June 2019. Last Modified: 2019-09-18T10:37 Publisher: Ministerie van Algemene Zaken.

[10] RVO. Subsidies and programmes | RVO.nl. https://english.rvo.nl/subsidies-programmes.

[11] ECN. Dutch Renewable Energy Support Scheme (SDE+). https://www.ecn.nl/collaboration/sde/.

[12] Autovista Group. Netherlands introduces BEV incentives. https://autovistagroup.com/news-and-insights/netherlands-introduces-bev-incentives, June 2020.

[13] CBS. Transport and mobility 2016. https://www.cbs.nl/-/media/{_}pdf/2016/38/2016-transport-and-mobility.pdf, 2016.

[14] José Moraga González and Machiel Mulder. *Electrification of heating and transport: a scenario analysis up to 2050.* Centre for Energy Economics Research, University of Groningen, 2018. OCLC: 8086804124.

[15] Michael Blonsky, Adarsh Nagarajan, Shibani Ghosh, Killian McKenna, Santosh Veda, and Benjamin Kroposki. Potential Impacts of Transportation and Building Electrification on the Grid: A Review of Electrification Projections and Their Effects on Grid Infrastructure, Operation, and Planning. *Curr Sustainable Renewable Energy Rep*, 6(4):169–176, December 2019.

[16] O. Alsayegh, S. Alhajraf, and H. Albusairi. Grid-connected renewable energy source systems: Challenges and proposed management schemes. *Energy Conversion and Management*, 51(8):1690–1693, aug 2010.

[17] Nikos Hatziargyriou. *Microgrids: Architectures and Control.* Wiley-IEEE Press, 2013.

[18] Byron Washom, John Dilliot, David Weil, Jan Kleissl, Natasha Balac, William Torre, and Chuck Richter. Ivory Tower of Power: Microgrid Implementation at the University of California, San Diego. *IEEE Power and Energy Magazine*, 11(4):28–32, July 2013. Conference Name: IEEE Power and Energy Magazine.

[19] A. Bonfiglio, F. Delfino, F. Pampararo, R. Procopio, M. Rossi, and L. Barillari. The Smart Polygeneration Microgrid test-bed facility of Genoa University. In *2012 47th International Universities Power Engineering Conference (UPEC)*, pages 1–6, September 2012.

[20] Kayode T Akindeji, Remy Tiako, and Innocent E Davidson. Use of Renewable Energy Sources in University Campus Microgrid – A Review. *2019 International Conference on the Domestic Use of Energy (DUE)*, pages 76–83, 2019.

[21] Higher electricity prices from 2020. https://insights.abnamro.nl/en/2019/05/higher-electricity-prices-from-2020/, May 2019. Section: Energy.

[22] Agency for the Cooperation of Energy Regulators and Council of European Energy regulators. *ACER/CEER annual report on the results of monitoring the internal electricity and natural gas markets in 2011*. Publications Office, LU, 2012.

[23] L. Hadjidemetriou, L. Zacharia, E. Kyriakides, B. Azzopardi, S. Azzopardi, R. Mikalauskiene, S. Al-Agtash, M. Al-hashem, A. Tsolakis, D. Ioannidis, and D. Tzovaras. Design factors for developing a university campus microgrid. In *2018 IEEE International Energy Conference (ENERGYCON)*, pages 1–6, Limassol, June 2018. IEEE.

[24] Joel Singer. Enabling Tomorrow's Electricity System: Report of the Ontario Smart Grid Forum. http://www.ieso.ca/imoweb/pubs/smart{_}grid/Smart{_}Grid{_}Forum-Report.pdf, 2009.

[25] Robert Lasseter, Abbas Akhil, Chris Marnay, John Stephens, Jeff Dagle, Ross Guttromsom, A. Sakis Meliopoulous, Robert Yinger, and Joe Eto. Integration of distributed energy resources. The CERTS Microgrid Concept. Technical Report LBNL–50829, 799644, CERTS, April 2002.

[26] Mohammad Shahidehpour and Mohammad Khodayar. Cutting Campus Energy Costs with Hierarchical Control: The Economical and Reliable Operation of a Microgrid. *IEEE Electrification Magazine*, 1(1):40–56, September 2013. Conference Name: IEEE Electrification Magazine.

[27] M. Silva, F. Fernandes, H. Morais, S. Ramos, and Z. Vale. Hour-ahead energy resource management in university campus microgrid. In *2015 IEEE Eindhoven PowerTech*, pages 1–6, June 2015.

[28] European Commission. Clean energy for all Europeans package. https://ec.europa.eu/energy/topics/energy-strategy/clean-energy-all-europeans_en, October 2017.

[29] PBL. Climate and Energy Outlook 2019: Summary. https://www.pbl.nl/sites/default/files/downloads/pbl-2019-climate-and-energy-outlook-2019-summary-3825.pdf.

[30] Gerd Tomazic and Maria Skyllas-kazacos. *Redox Flow Batteries*. Elsevier B.V., 2015.

[31] James M. Eyer and Garth P. Corey. Energy storage for the electricity grid : benefits and market potential assessment guide : a study for the DOE Energy Storage Systems Program. Technical Report SAND2010-0815, 1031895, SANDIA, February 2010.

[32] Antonis G. Tsikalakis and Nikos D. Hatziargyriou. Centralized control for optimizing microgrids operation. In *2011 IEEE Power and Energy Society General Meeting*, pages 1–8, San Diego, CA, July 2011. IEEE.

[33] M. Shahbazi and A. Khorsandi. Chapter 10 - Power Electronic Converters in Microgrid Applications. In Magdi S. Mahmoud, editor, *Microgrid*, pages 281–309. Butterworth-Heinemann, January 2017.

[34] Carla B. Robledo, Vincent Oldenbroek, Francesca Abbruzzese, and Ad J.M. van Wijk. Integrating a hydrogen fuel cell electric vehicle with vehicle-to-grid technology, photovoltaic power and a residential building. *Applied Energy*, 215(October 2017):615–629, 2018.

[35] C B Robledo, M J Poorte, H H M Mathijssen, R A C Van Der Veen, and A J M Van Wijk. Intelligent Integrated Energy Systems. *Intelligent Integrated Energy Systems*, 2019.

[36] Vincent Oldenbroek, Victor Hamoen, Samrudh Alva, Carla Robledo, Leendert Verhoef, and Ad van Wijk. Fuel Cell Electric Vehicle-to-Grid: Experimental feasibility and operational performance. page 18, 2017.

[37] Vincent Oldenbroek, Lennart Nordin, and Ad van Wijk. Fuel cell electric vehicle-to-grid: emergency and balancing power for a 100% renewable hospital. *6th European PEFC and Electrolyser Forum*, page 19, 2017.

[38] V. Oldenbroek, V. Hamoen, S. Alva, C. B. Robledo, L. A. Verhoef, and A. J. M. van Wijk. Fuel Cell Electric Vehicle-to-Grid: Experimental Feasibility and Operational Performance as Balancing Power Plant. *Fuel Cells*, 18(5):649–662, October 2018.

[39] Samira S. Farahani, Cliff Bleeker, Ad van Wijk, and Zofia Lukszo. Hydrogen-based integrated energy and mobility system for a real-life office environment. *Applied Energy*, 264:114695, April 2020.

[40] Farid Alavi, Esther Park Lee, Nathan van de Wouw, Bart De Schutter, and Zofia Lukszo. Fuel cell cars in a microgrid for synergies between hydrogen and electricity networks. *Applied Energy*, 192:296–304, April 2017.

[41] Farid Alavi, Esther Park, Nathan Van De Wouw, Bart De Schutter, and Zofia Lukszo. Fuel cell cars in a microgrid for synergies between hydrogen and electricity networks. *Applied Energy*, 2016.

[42] TU Delft. Campus Energy. http://emonitor.tudelft.nl/index.php/campus/, March 2018.

[43] University of Leiden. Energy. https://www.universiteitleiden.nl/en/dossiers/the-sustainable-university/energy.

[44] University of Twente. Buildings and house rules | Buildings | Campus University of Twente. https://www.utwente.nl/en/campus/buildings-rules/buildings/.

[45] Initiatives | Energy | Home CFM. https://www.utwente.nl/en/cfm/discover/sustainability/initiatives/energy/.

[46] Ennaturlijk. Warmtebronnen. https://ennatuurlijk.nl/warmtenetten/over-warmtenetten/warmtebronnen.

[47] Ibrahim Dincer and Marc A. Rosen. Heat Pump Systems. In *Exergy Analysis of Heating, Refrigerating and Air Conditioning*, pages 131–168. Elsevier, 2015.

[48] Paul Denholm and Robert M. Margolis. Evaluating the limits of solar photovoltaics (PV) in traditional electric power systems. *Energy Policy*, 35(5):2852–2861, May 2007.

[49] Anna Joanna Marszal, Per Heiselberg, Rasmus Lund Jensen, and Jesper Nørgaard. On-site or off-site renewable energy supply options? Life cycle cost analysis of a Net Zero Energy Building in Denmark. *Renewable Energy*, 44:154–165, August 2012.

[50] G. R. Chandra Mouli, P. Bauer, and M. Zeman. System design for a solar powered electric vehicle charging station for workplaces. *Applied Energy*, 168:434–443, April 2016.

[51] Ministerie van Algemene Zaken. Stimulating the growth of solar energy - Renewable energy - Government.nl. https://www.government.nl/topics/renewable-energy/stimulating-the-growth-of-solar-energy, July 2017.

[52] JRC Photovoltaic Geographical Information System (PVGIS) - European Commission. https://re.jrc.ec.europa.eu/pvg_tools/en/tools.html#TMY.

[53] Klaus-Dieter Jäger, Olindo Isabella, Arno HM Smets, René ACMM van Swaaij, and Miro Zeman. *Solar energy: fundamentals, technology and systems*. UIT Cambridge, 2016.

[54] Valk Pro. Solar mounting Landscape South 10 degrees – ValkPro+ L10 South - Van der Valk Solar Systems. https://www.valksolarsystems.com/en/solar-mounting-systems/flat-roofs/landscape/south/valkpro-l10-south.

[55] Lado Kurdgelashvili, Junli Li, Cheng-Hao Shih, and Benjamin Attia. Estimating technical potential for rooftop photovoltaics in California, Arizona and New Jersey. *Renewable Energy*, 95:286–302, September 2016.

[56] Fraunhofer ISE. Annual report. https://www.ise.fraunhofer.de/content/dam/ise/en/documents/annual_reports/Fraunhofer_ISE_Annual_Report_2014_web_final.pdf.

[57] Christian Breyer Eero Vartiainen, Gaetan MAsson. Pv lcoe in europe 2015-2050. *31st European Photovoltaic Solar Energy Conference and Exhibition*, page 15, 06 2015.

[58] Marcel Werther, Wijnand van Hooff, Kenneth Colijn, Rogier Blokdijk. Next-generation solar power Dutch technology for the solar energy revolution. Technical report, 2018.

[59] Eero Vartiainen, Gaëtan Masson, Christian Breyer, David Moser, and Eduardo Román Medina. Impact of weighted average cost of capital, capital expenditure, and other parameters on future utility-scale PV levelised cost of electricity. *Prog Photovolt Res Appl*, 28(6):439–453, June 2020.

[60] DNV GL. Solar PV powering through to 2030. https://www.dnvgl.com/to2030/technology/solar-pv-powering-through-to-2030.html.

[61] NREL. Best Research-Cell Efficiency Chart. https://www.nrel.gov/pv/cell-efficiency.html.

[62] Dr Simon Philipps, Fraunhofer Ise, Werner Warmuth, and PSE Projects GmbH. Photovoltaics Report. https://www.ise.fraunhofer.de/content/dam/ise/de/documents/publications/studies/Photovoltaics-Report.pdf, 2020.

[63] Canadian solar. Kumax high efficiency polymodule cs3u-375. https://www.canadiansolar.com/.

[64] J. Paidipati, L. Frantzis, H. Sawyer, and A. Kurrasch. Rooftop Photovoltaics Market Penetration Scenarios. Technical Report NREL/SR-581-42306, 924645, NREL, February 2008.

[65] National Laboratory Sandia. PV Performance Modeling Collaborative | Sandia Inverter Model. https://pvpmc.sandia.gov/modeling-steps/dc-to-ac-conversion/sandia-inverter-model/.

[66] Mohammed A. Abdulgalil, Mohamad N. Khater, Muhammad Khalid, and Fahad Alisamail. Sizing of energy storage systems to enhance microgrid reliability. In *2018 IEEE International Conference on Industrial Technology (ICIT)*, pages 1302–1307, Lyon, February 2018. IEEE.

[67] Sheldon S. Williamson, Pablo A. Cassani, Srdjan Lukic, and Benjamin Blunier. Energy Storage. In *Power Electronics Handbook*, pages 1331–1356. Elsevier, 2011.

[68] Sam Lamboo. Zinc-bromine battery for large-scale electricity storage. https://energy.nl/wp-content/uploads/2019/06/Technology-Factsheet-Large-Scale-Temporal-Electricity-Storage-ZnBr-Battery.pdf.

[69] Paul C Butler, Phillip A Eidler, Patrick G Grimes, E Klassen, and Ronald C Miles. ZINC/BROMINE BATTERIES. page 16.

[70] Daler Rakhmatov and Sarma Vrudhula. An analytical high-level battery model for use in energy management of portable electronic systems. *IEEE/ACM International Conference on Computer-Aided Design, Digest of Technical Papers*, pages 488–493, 02 2001.

[71] M.R. Jongerden and B.R. Haverkort. Which battery model to use? *IET Softw.*, 3(6):445, 2009.

[72] James F. Manwell and Jon G. McGowan. Lead acid battery storage model for hybrid energy systems. *Solar Energy*, 50(5):399–405, 1993.

[73] Redflow – Sustainable Energy Storage. https://redflow.com/.

[74] ISO/DIS 19880-2(en), Gaseous hydrogen — Fueling stations — Part 2: Dispensers. https://www.iso.org/obp/ui/#iso:std:iso:19880:-2:dis:ed-1:v1:en.

[75] Hyundai. Hyundai ix35 fuel cell car datasheet. https://www.hyundai.com/content/dam/hyundai/ww/en/images/footer/downloads/eco/e-brochure/ix35-fuel-cell-ebrochure-2015.pdf.

[76] Delloite. FCEVs to be cheaper to run than BEVs and ICE vehicles within 10 years | Deloitte China | Press release. https://www2.deloitte.com/cn/en/pages/about-deloitte/articles/pr-fcevs-to-be-cheaper-to-run-than-bevs-and-ice-vehicles-within-10-years.html.

[77] Jim Francfort. EV Project Data & Analytic Results. https://www.energy.gov/eere/vehicles/downloads/vehicle-technologies-office-merit-review-2014-ev-project-data-analytic.

[78] Hyundai_drivingrange. Hyundai NEXO - Driving range. https://www.hyundai.co.uk/new-cars/nexo.

[79] Patrick Plötz, Niklas Jakobsson, and Frances Sprei. On the distribution of individual daily driving distances. *Transportation Research Part B: Methodological*, 101:213–227, July 2017.

[80] Sebastian Pfeifle, Christopher Ley, Florian Tauschek, and Philipp Enderle. Fleet management in Europe. https://www2.deloitte.com/content/dam/Deloitte/cz/Documents/consumer-and-industrial/cz-fleet-management-in-europe.pdf.

[81] Esther H. Park Lee, Zofia Lukszo, and Paulien Herder. Conceptualization of Vehicle-to-Grid Contract Types and Their Formalization in Agent-Based Models. *Complexity*, 2018:1–11, 2018.

[82] Neha Rustagi Krishna Reddi, Amgad Elgowain and Erika Gupta. Impact of hydrogen sae j2601 fueling methods on fueling time of light-duty fuel cell electric vehicles. https://www.osti.gov/pages/servlets/purl/1389635.

[83] Machiel Mulder and Bert Scholtens. The impact of renewable energy on electricity prices in the Netherlands. *Renewable Energy*, 57:94–100, September 2013.

[84] Tennet. Annual market update 2019: electricity market insights. Technical report, Tennet, March 2020.

[85] IEA. Electricity information overview. Technical report, IEA, 2019.

[86] Tuomas Rintamäki, Afzal S. Siddiqui, and Ahti Salo. Does renewable energy generation decrease the volatility of electricity prices? An analysis of Denmark and Germany. *Energy Economics*, 62:270–282, February 2017.

[87] Thierry CABUZEL. ETS Market Stability Reserve to reduce auction volume by over 330 million allowances between September 2020 and August 2021. https://ec.europa.eu/clima/news/ets-market-stability-reserve-reduce-auction-volume-over-330-million-allowances-between_en, May 2020.

[88] European Commission. Market Stability Reserve. https://ec.europa.eu/clima/policies/ets/reform_en, November 2020.

[89] IEA. The Netherlands - Countries & Regions. https://www.iea.org/countries/the-netherlands.

[90] Equigy. How it works. https://equigy.com/how-it-works/.

[91] Tennet. Equigy platform gives European consumers access to tomorrow's sustainable energy market. https://www.tennet.eu/news/detail/equigy-platform-gives-european-consumers-access-to-tomorrows-sustainable-energy-market/.

[92] Katharina Grave, Barbara Breitschopf, Jose Ordonez, Jakob Wachsmuth, Sil Boeve, Matthew Smith, Torben Schubert, Nele Friedrichsen, Andrea Herbst, Katharina Eckartz, Martin Pudlik, Marian Bons, Mario Ragwitz, and Joachim Schleich. Prices and costs of EU Energy. April 2016.

[93] Home. https://www.entsoe.eu/.

[94] PV_education_FF. Fill Factor — PVEducation. https://www.pveducation.org/pvcdrom/solar-cell-operation/fill-factor.

[95] IRENA. Electricity storage and renewables: Costs and markets to 2030. page 132, October 2017.

[96] pvxchange. Price Index. https://www.pvxchange.com/en/price-index.

[97] Markus Mühlbauer, Oliver Bohlen, and Michael A. Danzer. *Analysis of power flow control strategies in heterogeneous battery energy storage systems*, volume 30. Elsevier, 2020.

[98] Joris Dehler, Dogan Keles, Thomas Telsnig, Benjamin Fleischer, Manuel Baumann, David Fraboulet, Aurélie Faure-Schuyer, and Wolf Fichtner. Self-Consumption of Electricity from Renewable Sources. In *Europe's Energy Transition - Insights for Policy Making*, pages 225–236. Elsevier, 2017.

[99] Shi Jie Tong, Adam Same, Mark A. Kootstra, and Jae Wan Park. Off-grid photovoltaic vehicle charge using second life lithium batteries: An experimental and numerical investigation. *Applied Energy*, 104:740–750, April 2013.

[100] Emanuele Taibi, Raul Miranda, Thomas Winkel, Frederic Barth, and Jean-Christophe Lanoix. *Hydrogen from renewable power: Technology outlook for the energy transition.* IRENA.